1 Introduction

Modern military forces demand ever increasing mobility and ride comfort of their vehicles. This is essential to ensure a fast acting military force with battle ready soldiers and equipment arriving at their destination. Advanced suspension systems, including semi-active, active and hydropneumatic suspension systems are increasingly being considered to address this need. This technology also lends itself to commercial implementation, giving the possibility of commercial return on investment. The aim of this study is to provide improved modelling of a specific hydraulic valve used on a current semi-active suspension system developed in South-Africa by Ermetek funded by Armscor and in Brtain by Horstman Defence Systems Limited. The valve in question (or parts thereof) has potential for use in future hydropneumatic systems currently under research or may serve as the basis for future developments [Els & Giliomee 1998].

In this chapter a brief discussion of advanced suspension systems is given. From this, the need for this study is defined and the methodology explained. The physical detail of the system investigated is shown under the heading 'System physical layout and operation'. Chapter 2 deals with fluid power simulation methods and some of the relevant mathematics.

1.1 Advanced suspension systems

Conventional **passive** suspension systems consist of a spring and damper connecting the sprung and unsprung mass (body and wheels) of a vehicle. The damper has a set characteristic and can only dissipate energy in the form of heat. There are several disadvantages to this system including the well-known trade off between ride (comfort) and handling (directional control) . The aim of advanced suspension systems is to improve on passive systems by altering suspension properties according to the prevailing driving and road conditions. This is usually done by an on-board computer or other control system. In what probably represents the best option in terms of performance, **active** suspension replaces the passive spring and damper with a hydraulic cylinder activated by a control valve and driven by a hydraulic pump mounted on the engine. This system is capable of removing and, opposed to passive systems, also inserting energy into the suspension (at the cost of substantial demands on engine power and added complexity). Active suspension can provide such great improvements in suspension performance that it is used in the world's first supersonic car (named the Thrust SSC) and its use in Formula 1 racing was banned to increase competitiveness [Miller 1988]. A **semi-active** suspension, in simple terms, uses a conventional passive damper fitted with a bypass valve. When activated, this bypass valve connects the top and

bottom chamber of the damper (high and low pressure chambers) with a low flow-resistance valve, thereby substantially reducing the damper force. Although energy can still only be dissipated by the damper, this setup can lead to improving the compromise mentioned between handling, ride comfort and the additional energy requirements of active suspension [Nell & Els 1994][Nell & Steyn 1994]. Another possible contender in the future is the use of **electrorheological** fluid in dampers, where a fluid's properties can be changed by the application of an electromagnetic field [Pinkos et al 1993][Petek et al 1995][Hägele et al 1990]. Some design and performance problems currently still hamper wide spread commercial use thereof. **Hydropneumatic** suspension is a further expansion of the idea to have switchable suspension characteristics. Here the damping and stiffness of the system can be adjusted. The damper and spring of passive systems are replaced with a hydraulic strut (cylinder) connected to two gas-charged accumulators. These accumulators provide stiffness (to support the body mass) and damping is provided by an orifice in the piping system. In order to change the stiffness, one of the accumulators can be shut off with a valve and reduced damping can be achieved by bypassing the orifice with another valve. Such a system provides many possibilities with an acceptable power input requirement [Giliomee & Els 1998]. (The power input is the energy needed by the system to change it's properties, i.e. switch the control valves. This should be as low as possible.)

1.2 Origin, Need and Aim

Semi-active suspension systems have been developed worldwide for many years. In South Africa the company Reumech Ermetek started with development in 1990. To date, four military vehicles have been fitted with working semi-active suspension:

- "Mingwe" 4x4 Armoured personnel carrier (12t - Linear Dampers)
- "Ratel" 6x6 Armoured personnel carrier (17t - Linear Dampers)
- "G6" 155mm 6x6 Self propelled gun (46t - Rotary dampers)
- "Olifant" 1B Tracked main battle tank (50t - Linear Dampers)

These vehicles show marked improvement in ride quality (between 4% and 48% - based on the vibration dose value or VDV [BS-6841 1987]). Developments in hardware and control strategies has also been made [Els & Giliomee 1998]. All the Ermetek semi-active systems use the same valve configuration developed by Nell (1993) to bypass the damper flow.

Currently research is being done on a hydropneumatic system. Availablity, reliability and funding prompted the use of the mentioned existing valve in the hydropneumatic system. It is therefore well worth while to fully understand the valve's operation and to obtain design tools to optimize this valve system.

In both semi-active and hydropneumatic suspensions the response time of the valve (i.e. time

taken to open or close) is very important. This determines how quickly a system is capable of reacting to road inputs and changing driving conditions, since the electronic control system can be made to have a much quicker response than any mechanical system. The ideal valve response time depends on many factors for instance the vehicle's body weight and the control objective in mind. Many references regarding the influence of valve response time can be found in the literature. [Nutson 1991] [Els & Holman 1999] [Nell 1993] [Miller 1988] [Tsutsumi et al 1990] [Lemme & Furrer 1990] [Hagele et al 1990] [Guy et al 1988] [Els & Giliomee 1998] [Nell & Steyn 1994]

It is important to establish convention concerning valve response time. In most cases where the valve is part of a damper system, the time taken from the valve actuation signal to a 95% reduction or increase in damper force is taken as the final delay time. During this change a short period exists after triggering the actuation signal during which the damper force does not change. This is mainly due to electro-magnetic transients in the solenoid and is measured by taking the time for the damper system to achieve a 5% change in damper force. In this study, the damper force is not a suitable trend for calculating time delay, and two other characteristics are used for determination of the valve time delay. These are the pressure drop across the valve and the displacement of the main valve poppet (where available).

From the literature it was found that typical valves have a delay time of anything between 4 and 400ms. This response time of the valve is determined by a multitude of parameters. These include the physical layout, the electrical coil driving signal, the valve state before switching and the hydraulic pressure in the system. The hydraulic pressure is a function of the terrain being crossed, since it is proportional to the damper force induced by the damper compression or rebound speed. (Simply referred to as damper speed.) From literature it is seen that this important fact is generally ignored in studies on suspension systems and very simple constant time delay trends or instantaneous damper characteristic changeovers substitute proper valve models in simulations. Furthermore, simulations are usually conducted with quarter-car linearised models which is a severe simplification of reality. The research at Ermetek included full vehicle, three dimensional, fully non-linear models. With this class of model it is clear that the effect of varying valve response times and proper prediction thereof become a necessary, logic and valuable extension in the endeavour to improve modelling and development capabilities.

---

*The **aim** of this study is to investigate the feasibility of predicting valve response times, using a dynamic mathematical valve model, verified against experimental data. The mathematical model is intended to allow refinement of current and future suspension system simulation and development work should the valve model prove accurate.*

1.3 Methodology

General background on suspension systems was obtained from consultations with Els, Giliomee, Nell and Steyn on previous work conducted. A literature study was conducted on the broader field of hydraulics and the modelling of hydraulic circuits. Two suitable modelling environments were selected to create mathematical models in (MATLAB and AMESim as final choices - refer to paragraph 1.4) The general modelling of hydraulics was investigated with simple models constructed on MATLAB and AMESim to establish the technique and confidence in the methods used.

Experimental work was conducted to acquire physical constants used in the models and to obtain dynamic performance data with which to compare the MATLAB and AMESim models. For this purpose a hydraulic test bench at the University of Pretoria was repaired and upgraded. (Test bench capability: 90 LPM at 300 Bar)

The governing equations for the valve system in question were deducted in a Newtonian form (to allow for possible sensitivity studies). These stiff, nonlinear and discontinuous differential equations were programmed in several MATLAB models with varying levels of assumptions and model complexity. Similar models of varying complexity were programmed in AMESim.

The model (MATLAB and AMESim) efficiency and suitability for future use were evaluated on the basis of sensitivity to parameters, complexity required, numerical stability, solving efficiency and the skills and knowledge level required for the creation thereof. The effort and time required to create practical models was also discussed.

Finally, suggestions are made for future research and work necessary to refine the results of this study.

1.4 Solver environment choice

Several integrator schemes were investigated for use. Since the final model is intended to be incorporated into a DADS full vehicle model (3D), it makes sense to use the available DADS hydraulic components. Although the most current version of DADS was not available at the time of investigation, it was found to be totally insufficient for the problem at hand, both in terms of solver efficiency and possible model complexity.

The DADS ability to interface with external software was also investigated, but this results in a dynamics system solver left to solve fluid power equations, and is a situation generally avoided by simulation experts.

Fortran and MATLAB are predominantly scientific oriented programming languages with advanced built-in mathematical capabilities. These features drastically reduce the amount of work required to construct a new model. MATLAB was selected for the creation of a first principles model because of several advantages:

- MATLAB is readily available and widely used in the engineering community.
- DADS is able to interface with MATLAB (Should the full vehicle model realise).
- MATLAB has several solver algorithms preprogrammed, tested and built in, with some of them specifically developed for stiff systems.
- SIMULINK is a powerful non-linear modeling environment and graphical interface for MATLAB that was evaluated and used to construct several test-models (also in [Book & Goering 1996]). SIMULINK proved to be too slow for use in complicated models.

After initial trials (refer to paragraph 2.4.3) the MATLAB solvers seemed adequate for the type of problem at hand. With the knowledge gained in this study, MATLAB proved too inefficient for the complexity required from the models. This observation refers to the pre-programmed solver algorithms. With a custom designed and optimized solver, the model should pose no problem. The development of a custom solver was deemed to be a substantial additional task falling outside the scope of this study.

Several commercial simulation packages have been developed internationally specifically for the fluid power industry. A complete and updated list of such programs (24 names to date) are obtainable from http://matwww.ee.tut.fi/~piche/fluidpower/softwarelist.html. From literature obtained, Bathfp and AMESim seem to be two market leaders. With kind permission from the AMESim developers a fully functional evaluation license was obtained for use by the University of Pretoria.

AMESim (**A**daptive **M**odeling **E**nvironment for **SIM**ulation) is an user friendly simulation program that can be used to model (mainly) complex hydraulic systems. AMESim has been under development since 1986 (over 150 man-years of experience involved) and has been used on more than 300 industrial and military projects to date. Several world leaders in the hydraulic simulation field are employed at Imagine. (Imagine is a software developer of French origin with its head-office in Roanne, France and offices around the world - See http://www.amesim.com) [AMESim 1998(b)]. Since AMESim provides an easy and fast user interface only requiring the dragging and dropping of fluid power icons to create a model with substantial detail, it was considered to be an appropriate verification tool and simulation environment for future work. The models developed in MATLAB and AMESim are discussed in chapter 3.

1.5 System physical layout and operation

The system layout and operation is discussed to establish terms and definitions. Effort is made to keep the terms and units consistent throughout the study as far as is practical. This section contains a detailed explanation of the system and the operation thereof. For the reader familiar with hydraulic components and their operation, paragraph 1.5.3 is not essential.

1.5.1 Terms used

The term valve system will be used to describe all the components assembled in a single package and in the configuration as used on the vehicle. This consists of a logic element (LC 25), a solenoid pilot valve (WSE 3D), four check valves (CP108) and a combination of valve blocks (or manifold blocks). The valve blocks consist of aluminium or steel blocks machined with connecting ports, cavities for the valves, drillings and plugs to connect the cavities and ports. Three valve blocks are relevant to this study. The original vehicle mounted valve system consists of an aluminium block housing the logic element and check valves. Another aluminium block houses the solenoid pilot valve. The two blocks are bolted together and a seal is obtained with "o"-rings. (These two blocks are shown in photograph 4) For the purpose of this study a replacement steel block (designated manifold CSS) is used which houses the solenoid valve and a displacement transducer to measure the logic element movement (Visible in photograph 6, with detailed drawings in annexure A4.3). Another component used is the damper pack. This refers to damping valves, obtained from a damper of the type for which the valve system was developed, fitted in a steel cylinder with hydraulic connection ports. It's use will be explained in chapter 4 (visible in photograph 5).

1.5.2 Layout

The system layout is given schematically in figure 1.1. All port names used throughout the rest of this study refer to figure 1.1. When the damper rotates (in the case of the rotary damper) a pressure is set up in one chamber and oil is passed to the other by the damper valves thus creating a speed dependant force in the damper. As explained, the purpose of the bypass valve is to allow oil to flow between these two chambers with a low flow resistance, thereby reducing the force created by the damper. The oil flow generated between these two chambers can be very high (Approximately 1000 LPM in extreme cases for the rotary damper). In order to effectively (in terms of energy requirements and component sizes) switch this large flow rate, a two stage system is needed. This entails a small solenoid pilot valve that uses some of the hydraulic energy available to actuate a large control valve (Logic element).

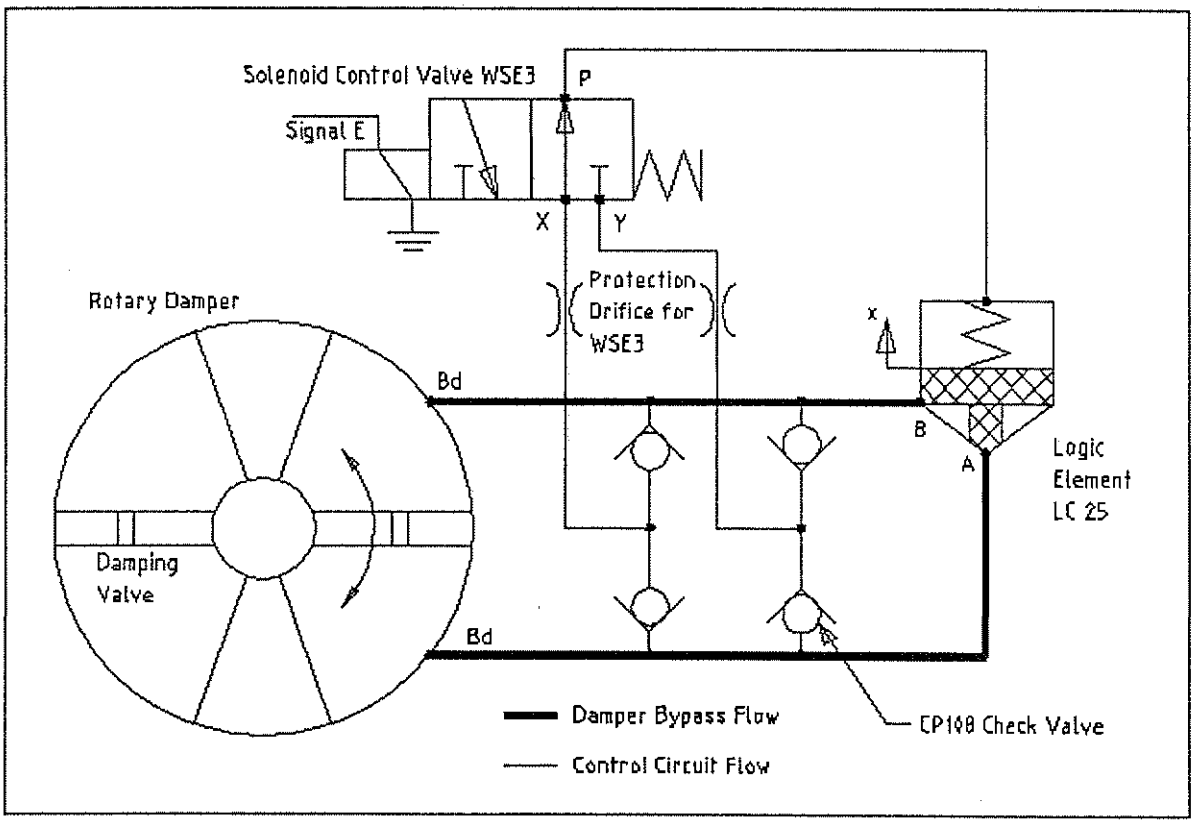

Figure 1.1 System layout and master port name reference

1.5.3 Components

Individual components will be described before an explanation of the system operation is given in paragraph 1.5.4.

Logic elements are devices used to switch large flow rates. Most designs only have a open or closed state and therefore the name logic element derived from binary logic (1 or 0 for 'on' or 'off'). The valve contains a poppet controlled by externally applied hydraulic pressure. With hydraulic pressure applied to port X (poppet chamber, referred to as port X by the manufacturer in figure 1.2 and as port P in this study), the poppet is in the closed position and flow cannot pass from port A to B or vice versa (figure 1.2). Similarly, with the control pressure relieved, the poppet is free to move and flow can pass freely between ports A and B. The poppet used in this study has a diameter of 25mm and a maximum poppet travel of 8mm. Note the spring acting to close the poppet assisting any pressure in the poppet chamber [Catalog (b)]. Forces acting on the poppet result from the control pressure P and spring acting to close the poppet. Both pressures A and B act on their respective areas to open the poppet and contribute a drag force on the poppet related to the flowrate (referred to as flowforce). Different poppet types are available with different area ratios (A_A:A_B). Special logic elements with damping noses and orifices are used to perform specific tasks like pressure or flow regulation. The Rexroth logic element trainer [Schmitt & Lang 1998] gives a detailed description on the operation and use of logic elements in hydraulic circuits. A simple equation can be used to calculate the external forces acting on the logic element in steady state:

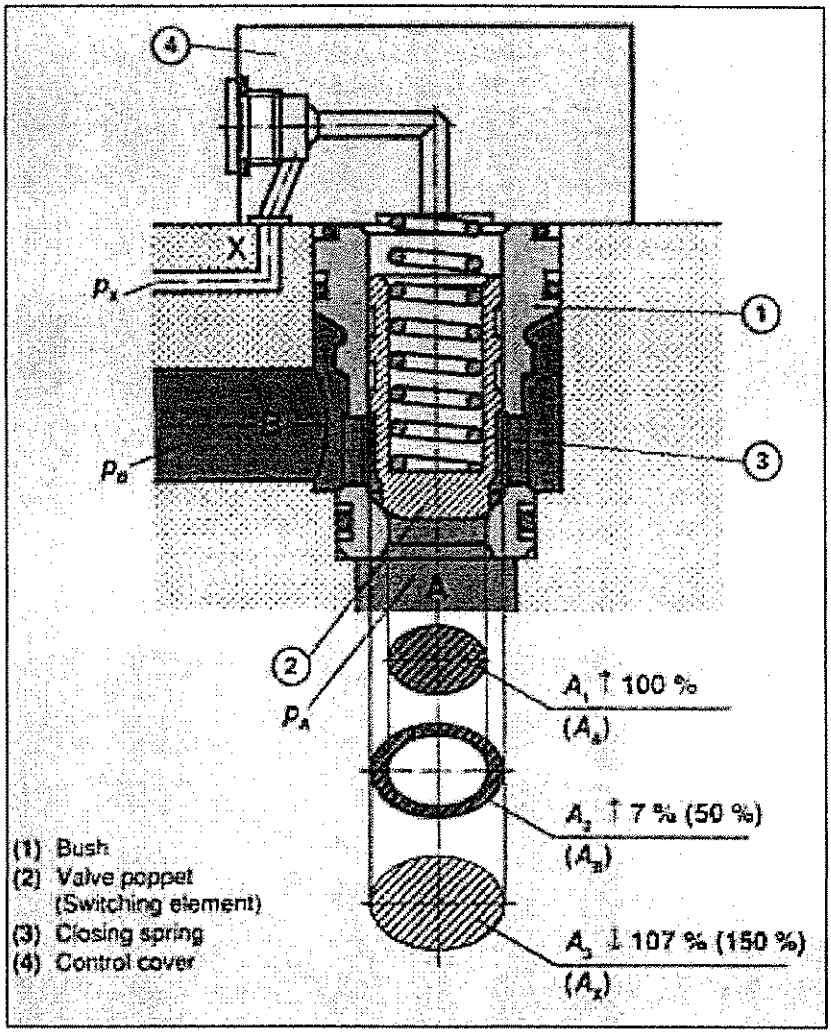

Figure 1.2 Cutaway look of the LC25 logic element

(eq1.1) $$P_A \cdot A_A + P_B \cdot A_B = P_X \cdot A_X + \text{SpringForce} + \text{FlowForce}$$

(Px from figure 1.2 is equivalent to Pp in this study)

The **solenoid pilot valve** (figure 1.3 and 1.4) is used to control the pressure at port P (the pressure in the logic element poppet chamber). An electric signal (24 V, 1.1 A) is used to toggle a solenoid that forces a ball poppet onto its seat thereby halting oil flow from port X to P (figure 1.4) and allowing flow from port P to Y. With no electrical signal applied, oil is free to flow from port X to P. [Catalog (c)] This valve has a small flow rating (12 LPM) and is protected by 1mm orifices in the X and Y lines in order to limit the maximum flowrate through the valve. The need for these orifices (as prescribed by the catalog) is, however, debatable. A WSE3 valve was opened to examine the operation thereof and to measure some physical parameters. Notice the pressure compensating chamber that applies pressure Px from both sides on the poppet in order to reduce the maximum solenoid force needed.

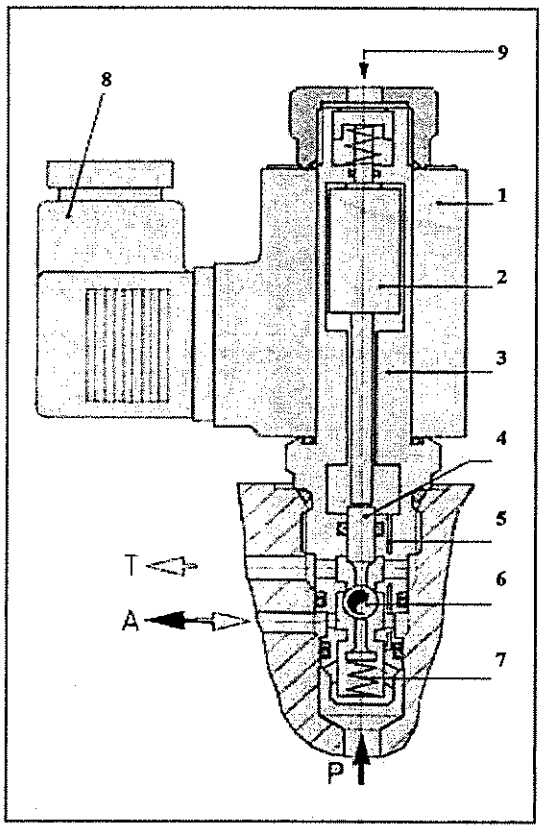

Figure 1.3 Pilot valve schematic (Component description below)

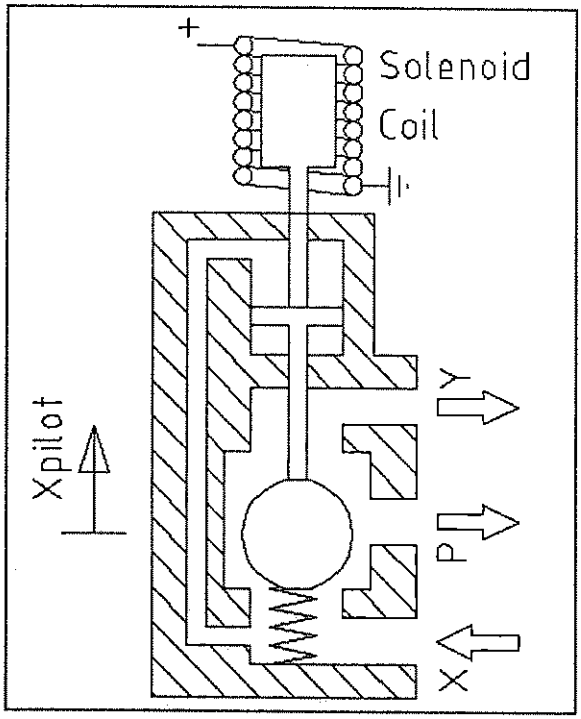

Figure 1.4 Pilot valve schematic layout used for deduction of the governing equations

Components in figure 1.3:

1 - Solenoid coil

2 - Solenoid armature

3 - Solenoid valve housing
4 - Pressure compensating piston
5 - Pressure compensating bore
6 - Closing element
7 - Spring
8 - Electrical plug
9 - Hand emergency button

When the valve system is used in the semi-active system configuration, the damper creates a alternating pressure at the valve system ports, depending on the damper travel direction. Because this alternating pressure cannot be used in the control circuit it must be rectified in the same way alternating current electricity is rectified to direct current. This is done with a bridge rectifier made up of four **check valves** [Catalog (a)]. To simplify installation, two types of check valves are used which allows flow in opposite directions (CP 108-1 and CP108-2). The check valves can be represented schematically as in figure 1.7.

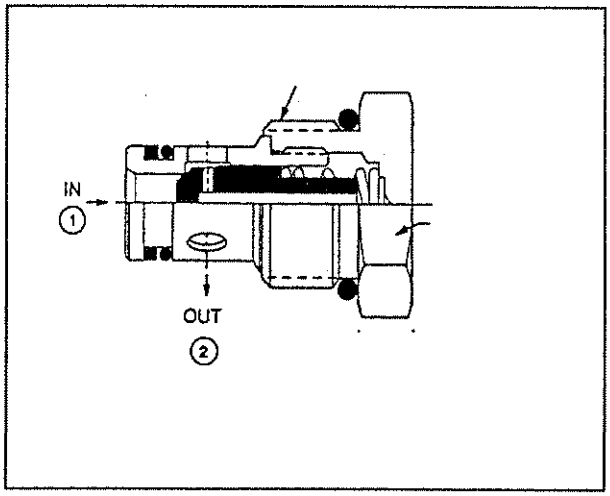

Figure 1.5 CP108-1 Check valve cutaway view

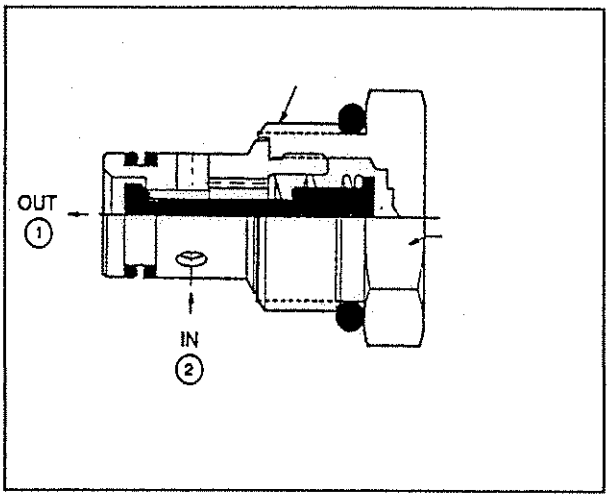

Figure 1.6 CP108-2 Check valve cutaway view

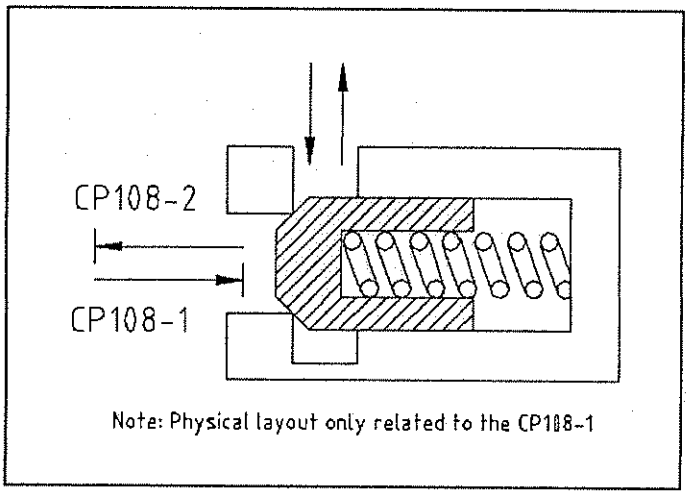

Figure 1.7 Schematic layout of the CP108 check valves. (arrows indicate function only)

1.5.4 System operation

Refer to figure 1.1 for the system layout. The pilot valve switches the pressure in the logic element control chamber to a high or low pressure. This allows the logic element state (open or closed) to alter. The high and low pressure supply needed by the pilot valve is taken from the damper chambers. The rectifier circuit containing the four check valves ensures that the alternating damper chamber pressures are separated into high and low pressure sources for use in the control circuit.

A problem with two stage hydraulic circuits in suspension systems, such as the one described in this study, is that the pressure differential across the damper valves drops to zero as the damper speed reaches zero. This leaves the pilot control circuit inoperable. [Nutston 1991] This fact has to be taken into consideration when future design attempts are to be made.

1.6 The following chapters

The chapter layout of the dissertation is as follows:
In chapter 2 a literature survey and a brief overview of the mathematics involved in simulating fluid power systems are given. A simple test case is established and evaluated.

In chapter 3 the AMESim and MATLAB model development procedure are presented. The governing equations used in the MATLAB model and AMESim model layout figures are presented. A sensitivity analysis on the AMESim model gives insight into the accuracy required of model parameters.

Chapter 4 deals with the experimental work conducted and gives a short discussion on some results.

In chapter 5 the experimental and AMESim results are superimposed and evaluated. This is discussed and analysed before a conclusion is drawn in chapter 6. Annexure 5.1 indicates the MATLAB model success.

#

2 Literature Study

In this chapter background is given on modern vehicle suspension system valve requirements. Trends, problems, methods and software of the fluid power simulation industry are surveyed and some of the mathematical theory underlying this field is discussed. Detailed descriptions of the models developed in this study are given in chapter 3.

2.1 Fast valves

Many requirements are set for valves used on semi-active and hydropneumatic suspension systems. Since the models investigated in this study are intended for use in the development of such valves, a clear description of the requirements placed on these valves is necessary. These valves are generally required to switch large flow rates very rapidly. Further requirements according to Nutston (1991) are:

- Valves used on suspension systems must be much cheaper than industrial equivalents
- High-volume production must be possible
- Power consumption must be kept low (typically below 12 watts)
- Very high reliability (99.99%) is required
- Durability must approach 10^7 cycles for use in the vehicle environment

The following can also be added:

- Easy maintenance and/or easy replaceability
- For semi-active systems zero leakage is not necessary
- Valve size and weight should be kept as low as possible - a small size facilitates various mounting options
- As low as possible flow restrictions in the open position are desired
- The effects suspension shock loads and therefore hydraulic shocks should be considered
- The failure mode for the shock absorber assembly should be the hard damper mode (i.e. bypass valve closed).

All the above requirements are, however, overshadowed by the dynamic response requirement. The exact requirement is dependent on the control strategy used, but in general it could be said that instantaneous valves would be ideal. It is much simpler to limit the switching times with a control system, than to be limited by the physical setup. The dynamic response requirements are summarized as follows: [Nutston 1991]

Suspension type	Required response
Discrete selectable	200-500 ms step response
Semi-active	2-10 ms step response
Fully active	-3 db @ 120 Hz

Flow rates through the valve depend on the size of the damper and therefore the size (weight) of the vehicle. The range of required flows could vary between a low 12 and a very large 1000 LPM. (Flow rates larger than 80 LPM can be considered as too large for most direct acting valves.) Since very large electrical signals would be required to switch such large flow rates directly, a popular system is the use of a double acting system (i.e. small pilot valve controlling the main flow control valve). With this system, some of the available hydraulic power is scavenged and used to amplify the low energy electrical signal. The additional pilot system extends the time delay (response time) and increases the cost and risk of failure of the system.

These dynamic requirements could easily be met with servo valves (proportionally actuated spool with feedback control) but they are far too expensive and bulky for use in automobile suspension applications. Several fast-acting valves have been developed. In most cases, however, only very small flow rates are switchable and the valves are complex, bulky and expensive. The current trend towards Pulse Width Modulation (PWM) control in hydraulics also lends it to the development of very fast valves. It should be remembered that in conventional hydraulic application (cranes, earth moving equipment, etc) very short (10ms) valve response times are generally not required. Most of the development work in conventional hydraulics has been towards the maximum transferable power [Burrows 1994][Burrows1996][Tanaka 1994] and in the cases where the system dynamic performance is of importance, servo valves meet the requirements.

Some research has been done to create fast acting valves. These valves are experimental and most of them are delicate, bulky and expensive and not intended for use on suspension systems. It is, however, clear that very fast-acting valves could be a possibility in the near future. From [Cui et al 1991][Sato & Tanaka 1993] and [Tanaka 1994] the following table can be compiled to illustrate the development history of fast acting valves:

Year	Flowrate	Response Time	Developer
1972	< 4 LPM	1 ms	Hesse, Moller
1976	10 LPM	Cut off @ 50 Hz	El Ibiary et al
1978	26 LPM	1.6 ms	Mansfield, Tersteegen

1980	9 LPM	3 ms	Engelsdorf
1980	8 LPM	3.5 ms	Tanaka
1988	8 LPM	2 ms	Tanaka
1988	8.5 LPM	> 3 ms	Luo et al
1988	6 LPM	< 1 ms	Unknown
1991	18 LPM	2-3 ms	Cui, Burton, Ukrainetz
1993	80 LPM	100 ms	Tanaka, Sato

In the case of electrohydraulic valves both the electromagnetic circuit and the hydraulic circuit determine the valve's time delay. Typical solenoids include a high permeability ferromagnetic material inside a coil. When energised, the number of ampere-turns and reluctance of the coil determine the flux generated. The resulting solenoid force is proportional to the flux generated across the air gap in the magnetic circuit. The maximum rate of change of the force is governed by the inductance of the coil and therefore also on the electronic driving circuit design. [Nutston 1991][Nowici & Oliveto 1994] Various other factors influence the overall performance, especially the use of pressure compensating chambers in the valve design.

The Finite Element Method (FEM) is used if detail analysis is required of high performance solenoid magnetic circuits. This indicates the complexity of solenoid design and analysis. The driver circuit (or absence thereof) used to energize the coil can greatly affect the overall valve performance and several sources indicate the gains achieved by such circuits. (Typical example: 30 ms reduced to 10 ms) [Tanaka 1994][Chimielwski et al 1994]

2.2 Hydraulic simulation overview

Fluid power simulation is fraught with problems. Most literature sources make reference to some of the challenges posed by fluid power simulation. The following list obtained from literature serves as a summary of these problems and the work conducted globally:

2.2.1 On an international basis, fluid power simulation is a competitive business because of the high level of research and investment required. Companies and institutions guard their simulation methods and techniques. Most literature only state the existence of a problem and the success of the solution investigated, but hardly ever will the exact solution, equation or algorithm be given.

2.2.2 Hydraulic systems generally consist of large oil volumes in the connecting pipes and relatively small oil volumes in the control valves and other components. These highly different sized fluid volumes in any hydraulic system give rise to a "stiff" numerical problem. This creates a host of complications for the numerical methods used and is probably the biggest problem in solving fluid power systems. The small volumes have a very fast time constant compared to the larger volumes. This causes an undesirable high frequency component in the solution that greatly affects the solver efficiency and stability. [Piche & Ellman 1994][Ellman & Vilenius 1990][Tilley & Burrows 1995][Krus internet (b)][Jansson internet (c)][Richards 1998] Refer to paragraph 2.4.1 for a discussion on integrator algorithms. One of the selling points of commercial software is their ability to deal with numerical stiffness.

2.2.3 The stiffness of a model can be reduced by replacing the small (and generally insignificant) fluid volumes with incompressible ones. This adds differential algebraic equations (DAE's) to the set of differential equations (DEQ's) which necessitate the use of specialized solving techniques and causes further numerical problems. [Ellman & Vilenius 1990][Richards 1998]

2.2.4 Fluid power phenomena are highly nonlinear, placing a further strain on the numerical method used. Some parameters generally have to be obtained from a lookup table, or empirical equation, thus complicating the model (and adding inaccuracies to the model).

2.2.5 Many discontinuities arise. Typical examples include electrical signals, masses with bump stops (end stops) and flow rates.[Ellman & Vilenius 1990][Jansson et al. n.d.] Discontinuities can adversely affect most numerical methods unless special precautions are taken. This requires customised algorithms. The MATLAB solver used in this study makes provision for such discontinuities. (Discussed in paragraph 3.2)

2.2.6 The well-known orifice flow equation (eq 2.1) used in fluid flow calculations has its own problem. Singularities arise in the Jacobian matrix of the integration algorithm when zero flow is reached. This can be solved by altering the equation slightly. A detailed discussion follows in paragraph 2.4.2 [Piche & Ellman 1994]

2.2.7 There are many parameters in the model for which values have to be found from the physical system. Often the physical system cannot be opened to measure these quantities.[Handroos & Vilenius 1991] Some parameters are very difficult to obtain (like fluid bulk modulus, viscous damping on masses or oil air content). [Tilley & Burrows 1995][Xue & Watton 1995][Viersema n.d.][Mock 1981][Book & Goering 1996][Richards 1998][AMESim 1998 (c)] Techniques developed to overcome this

problem include nonlinear empirical models with parameters identified from measured data [Handroos & Vilenius 1991][Vilenius & Simpura n.d.] and dimension less forms of data. [Kruisbrink 1998] The experimental work necessary to obtain any of the parameters is tedious and complicated (chapter 4).

2.2.8 For some phenomena like flow forces (Bernoulli forces) [Ellman & Vilenius 1990], cavitation [Burrows et al 1992][Richards 1998][AMESim 1998 (c)], pipe friction, pipe elasticity [Tilley & Burrows 1995] and shock waves [AMESim 1998 (c)] proper models are complex and difficult to implement, do not exist or are rough approximations. Long pipe runs with wave, friction and momentum phenomena require partial differential equations (PDE's) for which special care must be taken if they are to be included in the system of differential equations. One dimensional finite element models are often used to model long pipes instead of simple lumped pipe models. [Tilley & Burrows 1995][Lida et al 1992][Jansson et al. n.d.][AMESim 1998 (c)]

2.2.9 Thermal effects are important in many hydraulic systems, but are rarely modelled.

2.2.10 Real fluids are condition dependant. The bulk modulus, viscosity, etc. changes with pressure and temperature [Richards 1998]. This is ignored in most simulations.

2.2.11 There are a vast number of different component suppliers across the globe. All of them have their own unique components and product ranges. This causes models to be very application specific and a massive component model library is needed for commercial simulation software. [Watton & Xue 1994] [Handroos & Vilenius 1991][Tilley & Burrows 1995] A basic set of sub-models can be used efficiently to model any larger system, although this leaves one with unknown model parameters. [Lebrun & Richards 1998] Many hydraulic systems are once-off projects that require unique models at a reasonable cost and effort [Tilley & Burrows 1995].

2.2.12 Hydraulic circuits can have a number of layouts that will fulfill its purpose. The final layout depends on the designer's preference and experience. This complicates the automatic design of circuits by computer and the subsequent optimization. [Tilley & Burrows 1995][Donne et al 1995] If, however, the modeling technique is well understood and the basic set of component models are available, the use of computer simulation can greatly aid the system designer to access designs and design changes.

2.2.13 Noise and vibration is also a major problem with hydraulic systems. Work is being done to predict the noise and vibration behavior of a fluid power system.[Tilley & Burrows 1995]

2.2.14 Fluid power circuits are often used to actuate mechanical systems. These systems have to be incorporated into the hydraulic simulation model. This usually requires adding DAE's to the list of fluid power equations [Gassman 1993][Korte 1990][Tomlinson & Tilley 1993][Burrows et al 1992][Richards 1998] It is common practice to use different simulation programs to simulate different sections of a mechanical and control system. However, with hydraulic systems interfacing with mechanical systems in different software environments, the integrator step size demand of the two systems may be conflicting [Richards 1998].

2.2.15 Many techniques are under investigation to aid in fluid power simulation. Neural networks can be used effectively to model hydraulics. [Xue & Watton 1995] Unit Transmission Line Elements is a special method where the system is split into many subsystems and connected by special time-step equations. [Jansson et al. n.d.][Krus internet (b)][Jansson internet (c)] This method can reduce the stiffness demands on the integrator algorithm, but requires very specialized models.

2.2.16 Most of the design work in the fluid power industry is done on the basis of existing hardware and catalog specifications. In many instances, the advantages of dynamic simulation is outweighed by the cost and time involved. Generally it is only the development industry that requires simulation or is able to afford commercial software.

Despite all the above-mentioned problems, good results are obtained by the international fluid power simulation community. (Typical examples in [Burrows et al 1992][Korte 1990][Tomlinson & Tilley 1993][MATLAB 1998 (a)][AMESim 1998 (d)][AMESim 1998 (e)].) Many advantages can be obtained through the use of simulation. With any hydraulic design certain safety factors must be applied. To the usual designer of these systems the maximum pressure and flow values that might occur in a system are only a guess or are based on simple calculations. This has resulted in the component suppliers substantially under specifying the safe operating conditions of hydraulic components and systems. With computer simulation, an accurate indication of the maximum pressures and flowrates can be obtained. This may lead to greatly reducing the component sizes needed (thus saving on hardware costs and space requirements), or in the other extreme, prevention failure of due to underestimated peak values. [Burrows et al. 1991].

2.3 Compressible fluid power assemblies

To model any dynamic, compressible fluid power system in the simplest manner, two governing equations are needed.

The first is the well known orifice equation of the form:

(eq 2.1) $$Q = Cd \cdot A\sqrt{\frac{2 \cdot \Delta P}{\rho}}$$

with: Cd the discharge coefficient [dimensionless],
A the orifice area [m^2],
ΔP the pressure drop across the orifice [Pa],
ρ the fluid density [kg/m^3], and
Q the flow through the orifice [m^3/s].

The second is the fluid compressibility equation:

(eq 2.2) $$\dot{P} = \frac{\beta}{V}\Sigma Q$$

with: β the bulk modulus [Pa]
V the fluid volume [m^3]
ΣQ represents the excess fluid to be compressed [m^3/s], and
$\dot{P}$ is the time derivative of pressure

The ΣQ in the above equation is quite significant in the sense that it applies conservation of mass to the problem. It describes the flow compressed into the available volume. A simple way of thinking about the compressibility is to allow the compressible volume to be isolated. This can be demonstrated with a simple example.

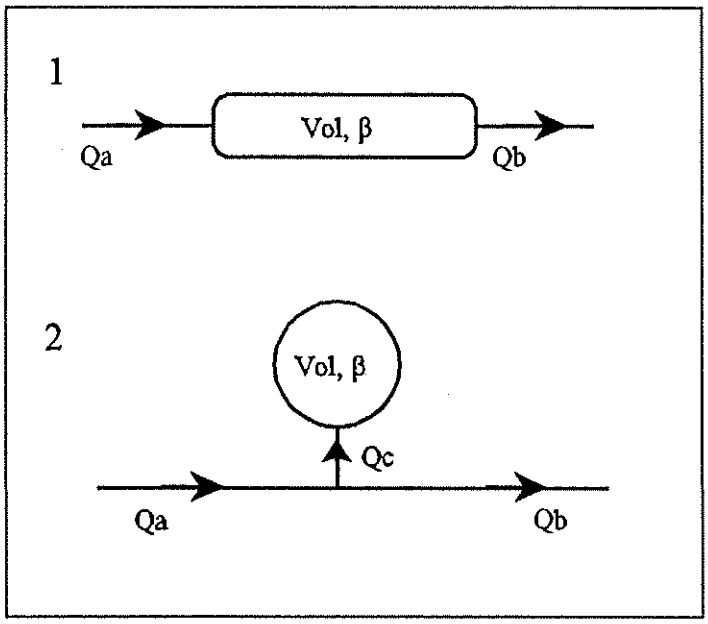

Figure 2.1 Lumped pipe volume

Case 1 in figure 2.1 can be seen as the lumped mass representation of a hydraulic pipe. To simplify deduction of equations and easy programming when several pipes meet at a node, the fluid volume is removed and placed in the form of an accumulator. This is

similar to drawing a control volume around the compressible volume. For the node in case 2 the flow entering the compressible volume can be written as $Qc = +Qa - Qb$ with Qc used in the place of ΣQ of equation 2.2.

2.4 Numerical methods and stiff problems

A stiff method may be defined mathematically as one where the smallest time constant is much less than the simulation time or where a large range of time constants are present. The time constants can be calculated from the eigenvalues of the Jacobian matrix [Richards 1998]. From paragraph 2.2 it is apparent that many demands are placed on the numerical methods used to simulate fluid power systems despite the apparent simplicity of the governing equations shown in paragraph 2.3.

2.4.1 Integrator algorithm

Most of the work done in fluid power system simulation thus far, has gone towards the development of suitable and stable integrator algorithms. Although no detailed mathematical study of integrator algorithms and their mathematical properties were attempted in this study, it is worthwhile to summarize the findings of some authors. No detail relating to these methods was investigated.

In the work of Piche and Ellman (1994) several integrator algorithms are investigated and tested including the method of Gear (a Backward Difference Fitting or BDF member), several semi-implicit Runge Kutta methods, Euler and trapezoid rule methods. Furthermore, several methods specifically suggested for fluid power systems are evaluated (methods of Zhang and Ulrich, the method of Krus, the method of Calahan). Both Burden and Faires (1997) and Piche and Ellman (1994) mention that A-stability of the numerical method (i.e. stable for any positive time increment) is not a sufficient condition to prevent numerical oscillations in very stiff problems. Ellman continues to show that a L-stable method gives better results (The definition of L-stability falls outside the scope of this study). Richards (1998) reports explicit Runge-Kutta methods to be totally unsuitable for stiff problems, and that linear multistep methods (Gear, Adams Moulton, Adams Bashforth and LSODA methods) are difficult to implement, but suitable for use with stiff problems.

The MATLAB ODE suite comprises of several integrator algorithms designed for specific tasks. The ODE23 and ODE15s algorithms are developed specifically for stiff problems. The following table gives a quick and selective summary taken from the MATLAB help file [MATLAB 1998 (b)].

ODE15s	A variable order solver based on the numerical differentiation formulas (NDF's). It is also capable of using backward difference fitting or BDF (Gear's method) and is a multistep solver
ODE113	Variable order Adams-Bashforth-Moulton solver
ODE23s	Modified Rosenbrock formula solver
ODE23t	Implementation of the trapezoid rule

From initial investigations on simple models most solvers provides an answer. The MATLAB solver ODE15s for stiff systems was found to be fastest and gave the least warning messages. After many simulation runs on more challenging models and comparison with AMESim results, all the MATLAB solvers proved unstable (ODE 15s was last to fail).

AMESim has a highly developed integration algorithm that automatically switches integrators depending on the stiffness detected and the discontinuities encountered. This relieves the modeler from a lot of work in the sense that algorithms and step sizes are chosen automatically. Other advantages are that even if the characteristics of the equations change during the simulation, the integration algorithm automatically adjusts. The DASSL algorithm is used for differential algebraic equations and the LSODA algorithm is used for ordinary differential equations. The LSODA algorithm incorporates 17 different methods and switches automatically. These methods are highly adapted for the AMESim environment. Extensive discontinuity handling is built into all the submodels and algorithms and special provision is made for partial differentiation equation incorporation.

2.4.2 Orifice equation

During initial phases of modeling in MATLAB very oscillatory and unstable solutions were found even for trivial test problems. This phenomena is the result of a singular Jacobian matrix ($\partial Q/\partial \Delta P$) used in the numerical method as explained by Ellman (1990) and Richards (1998). The standard orifice flow equation widely accepted for simulation is (similar to eq 2.1):

(eq 2.3)
$$Q = C_d \cdot A \sqrt{\frac{2 \cdot |\Delta P|}{\rho}} \cdot \text{sign}(\Delta P)$$

Where sign(ΔP) facilitates flow in either direction through the orifice. This equation produces an infinite slope for Q as ΔP passes through zero. As mentioned the resulting singular Jacobian causes numerical oscillation. The above equation is further only valid with turbulent flow. Although the turbulency approximation is valid in most hydraulic flow situations, the numerical

problem must still be resolved. To do this Ellman suggests a novel way of modelling the orifice with a transition between laminar and turbulent models at a user specified Reynolds transition number (Re_{tr}). For the laminar region an empirical polynomial approximation is used to model the orifice. This equation (eq 2.4) does not cause the singularity in the Jacobian matrix thereby allowing for efficient solving. Since all orifices differ in their specific flow models, the user has to adjust the C_d and Re_{tr} values for suitable behaviour. This equation is, however, not entirely suited for use in this study and a slightly adapted version was created. The new orifice equation used in this study is given by equation 2.5. A similar scheme for transition between laminar and turbulent conditions is used by AMESim [Alirand 1999].

$$\tau_{tf} = \frac{225 \cdot Re_{tr}^2 \cdot \rho \cdot \upsilon^2}{128 \cdot C_d^2 \cdot D^2}$$

(eq 2.4)
$$Q = \begin{cases} \dfrac{A \cdot \upsilon \cdot Re_{tr}}{64 \cdot D}\left(45 \cdot \left(\dfrac{\Delta P}{\tau_{tf}}\right)^3 - 150 \cdot \left(\dfrac{\Delta P}{\tau_{tf}}\right)^2 + 225\left(\dfrac{\Delta P}{\tau_{tf}}\right)\right) & \text{if } 0 \le \Delta P \le \tau_{tf} \\ C_d \cdot A\sqrt{\dfrac{2 \cdot \Delta P}{\rho}} & \text{if } \Delta P > \tau_{tf} \end{cases}$$

All terms in eq 2.4 and 2.5 have the same definition as for eq 2.1 except:

- ν the kinematic viscosity [m^2/s]
- D the orifice diameter [m]
- Re_{tr} the Reynolds transition number (laminar / turbulent switch) [dimensionless]
- τ_{tf} is a temporary variable

The C_d and Re_{tr} values could be obtained by steady state experiment or possibly by computational fluid dynamics (CFD) analysis [Hayase 1995]. The problem is that the values obtained change with every different valve design, oil properties and even over time as wear sets in (depending on the valve design). Furthermore the Cd and Re_{tr} values might not be a linear function of poppet height, depending on the internal geometry. If the relationship is available, a simple lookup table may then be used or an empirical approximation.

Equation 2.5 has been modified to include the effects of flow direction reversal and different poppet types. To include the effects of a variable poppet height the most basic assumption is to calculate the flow area A as the annular area under the poppet, with a diameter equal to the seat diameter. For this case the area A is replaced with $\pi \cdot D \cdot x$ where D is the poppet seat diameter

and x is the poppet height. The MATLAB implementation of this function is given in annexure A3.3.12.

$$\tau_{tf} = \frac{225 \cdot Re_{tr}^2 \cdot \rho \cdot \upsilon^2}{128 \cdot C_d^2 \cdot D^2}$$

$$Q = \begin{cases} \text{sign}(\Delta P) \cdot \dfrac{\pi \cdot x \cdot \upsilon \cdot Re_{tr}}{64} \left(45 \cdot \left(\dfrac{\Delta P}{\tau_{tf}} \right)^3 - 150 \cdot \left(\dfrac{\Delta P}{\tau_{tf}} \right)^2 + 225 \left(\dfrac{\Delta P}{\tau_{tf}} \right) \right) & \text{if } 0 \le |\Delta P| \le |\tau_{tf}| \\ \text{sign}(\Delta P) \cdot \pi \cdot x \cdot D \cdot C_d \sqrt{\dfrac{2 \cdot \Delta P}{\rho}} & \text{if } |\Delta P| > |\tau_{tf}| \end{cases}$$

(eq 2.5)

Further information required from the orifice equations is that of effective area for the pressure forces to act on the poppet. This area may be assumed constant throughout the poppet travel (as in [Ellman & Vilenius 1990]). A scheme where the area increases or the average of pressure Px and Pp is used was investigated, but did not provide any noticeable improvement. In AMESim a scheme is used where the effective area is determined by a truncated cone drawn from the poppet seat to the poppet.

Since the assumption of an annular flow area (initial MATLAB approximation used) is not completely accurate, the AMESim approximations for effective poppet area was adopted for use in the MATLAB models. [AMESim 1998 (f)]

For sharp seated conical poppets (as used in the logic element model), AMESim determines the flow area and active diameter as in figure 2.2 with equations 2.6 and 2.7.

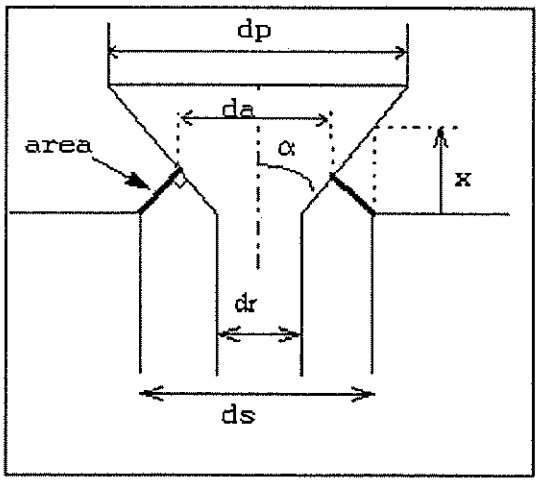

Figure 2.2 Sharp seated conical poppet

$$\text{Area} = \pi \cdot x \cdot \sin(\alpha)(ds - x \cdot \sin(\alpha) \cdot \cos(\alpha))$$

(eq 2.6)

$$da = ds - 2 \cdot x \cdot \sin(\alpha) \cdot \cos(\alpha) \qquad \text{(eq 2.7)}$$

For sharp seated ball poppet variable orifices (as used in the pilot valve model), AMESim uses the following equations to determine the effective flow area. (Figure 2.3, equations 2.8 & 2.9)

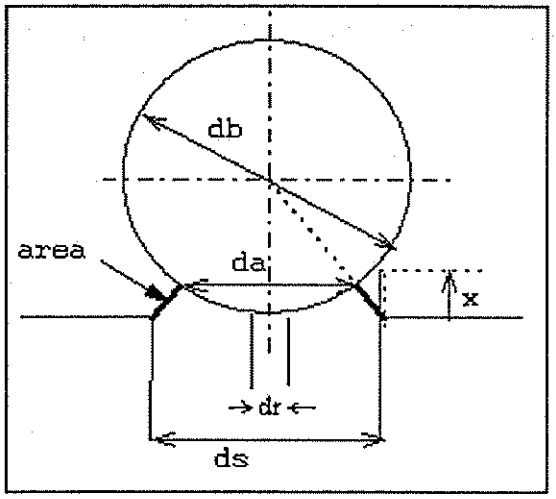

Figure 2.3 Sharp seated ball poppet

$$\text{Area} = \frac{\pi \cdot ds^2}{4}\left\{\frac{\Psi^2 + 1 - \left(\frac{db}{ds}\right)^2}{\sqrt{\Psi^2 + 1}}\right\}$$

with:

$$\Psi = \frac{2 \cdot x}{ds} + \sqrt{\left(\frac{db}{ds}\right)^2 - 1}$$

(eq 2.8)

$$da = \frac{db}{\sqrt{1 + \Psi^2}} \qquad \text{(eq2.9)}$$

These special cases of the orifice equation are implemented in separate MATLAB functions: orificeSC.m for the Sharp seated Conical orifice, and orificeSB.m for the Sharp seated Ball orifice. (Refer to annexure 3.3.10 & 3.3.11) These orifice area assumptions are however substantial simplifications of the real situation where effects like uneven pressure distribution profiles, turbulence and boundary layers, drag and stagnation pressures (fluid momentum changes) will have a marked effect on the force balance for the poppet and its flow coefficients.

2.4.3 Numerical method validation: Test case

To establish the modeling techniques and to gain initial confidence in the solver algorithms the MATLAB and AMESim models were compared to a test case used by Piche and Ellman (1994) to develop and test suitable numerical methods. The strategy followed in developing any of the later models was to start with small manageable elements that could be compiled into larger models. The example by Piche and Ellman proved to be a suitable starting point for this purpose.

The test case consists of a steady state flow source with a step change. The flow passes into a lumped volume at pressure P1, through orifice one into a volume at pressure P2, through a second orifice and drains to atmosphere. Volume 2 is 1000 times larger than volume 1 to establish stiffness. The AMESim model layout is shown in figure 2.4.

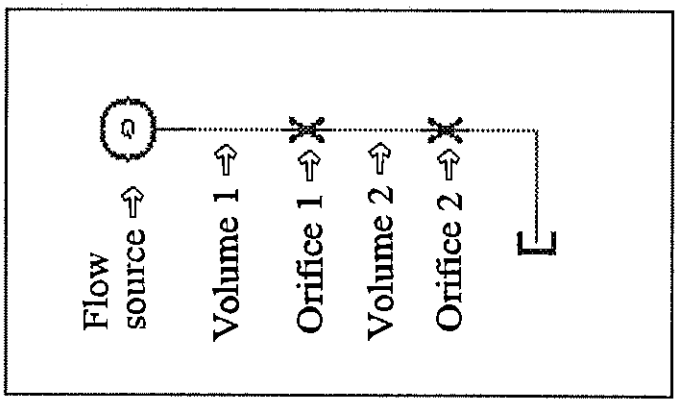

Figure 2.4 Piche and Ellman example model layout in AMESim

It was found that AMESim produced very stable results under any circumstances. In MATLAB a choice of several different solvers was made together with a range of tolerance requirements for the integrator algorithm. The ODE15s algorithm designed for very stiff problems proved accurate and fast. The ODE23 range of algorithms in MATLAB provided solutions only at high tolerance levels and solved several magnitudes slower than the ODE15s.The ODE 45 algorithm (general Runge-Kutta) does not converge at all.

The MATLAB and AMESim results are superimposed in figure 2.5. The results showed exact agreement to the results of Ellman (by visual inspection).

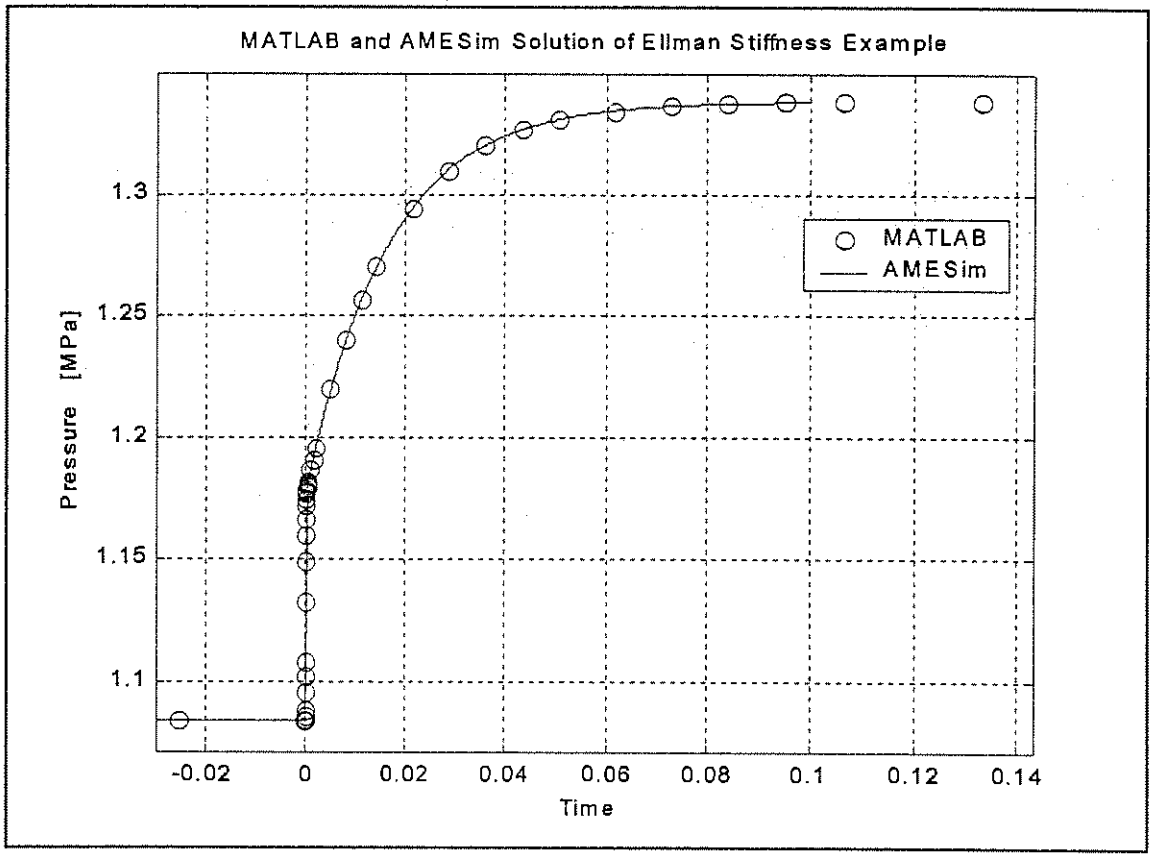

Figure 2.5 MATLAB and AMESim solution of Piche and Ellman example superimposed

The test case raised confidence in the solver environments chosen and indicated that the mathematics used correlated. This sets the field for expansion of the models.

#

3 Mathematical Model

This chapter explains how AMESim and MATLAB models were developed and used. The chapter starts with a brief description of AMESim and the MATLAB ODE (ordinary differential equation) suite that were used to solve the system of DEQ's (differential equations). Thereafter individual models are discussed. On a model by model basis a schematic layout, governing equations and the AMESim block diagram are shown.

Most of the AMESim models were saved as sub-models and can therefore be reused in subsequent projects. Some 15 models were developed using AMESim, and 11 models using MATLAB. Paragraph 3.11 at the end of the chapter gives a table format overview of these models.

Evaluation of the models and presentation of the results obtained is deferred to chapter 5. Source code and parameters of the models are given in annexures A3.2 and A3.3.

3.1 Developing models in AMESim

Background on AMESim and it's developers (Imagine) is given in paragraph 1.4. AMESim is based on a principle called multiport which is comparable to the BondGraph energy technique. Both Multiport and Bondgraph techniques use information flow between models in two directions as opposed to signalport models (SIMULINK) which only allows information flow in one direction (typically used for control system design). Bondgraphs are based on nine elements in terms of physics, whereas the multiport method is generally divided into elements based on engineering sub-systems [Dransfield 1981][Scavarda & Richard n.d.][Lebrun & Richards 1998]. AMESim contains a powerful solver algorithm specifically developed for hydraulic (stiff, non-linear and discontinuous) systems. (Refer to paragraph 2.4.)

The power of AMESim lies in the four easy steps with which models can be constructed or modified and accurately simulated. To create a model on AMESim, the system is firstly drawn by placing (dragging and dropping) standard hydraulic component icons onto the model page. Connecting the hydraulic and signal ports is done with mouse input. A large collection of fundamental building blocks (e.g. a mass with endstops, a poppet or a piston) may also be used to construct models of non-standard equipment (as was necessary in this study). This step is easy, fast and very intuitive.

Secondly, submodels are associated with the placed components. This facilitates the user to specify the complexity and detail that are required from the model. For example, several hydraulic pipe models exist, ranging from a direct connection to very complex wave equation models. [AMESim 1998(c)] AMESim also has the ability to automatically assign submodels to speed up the process. This provides an easy start where upon the model can be refined to its specific purpose.

Thirdly, AMESim builds the model executable file. This means that the mathematical equations, model layout and parameter settings are compiled into a file that describes the system in C or Fortran code. The whole process from drawing the circuit to this point is very easy and depending on the operator's skill, a simple model can be built in a matter of minutes. At this stage the specific model parameters must be set (e.g. masses, frictions, flow coefficients, spring stiffness). As with any model, this requires some modelling experience, experimental work, and assumptions. Fortunately AMESim has default values that can be used directly in many cases.

Finally, AMESim is set to simulation mode, where a complex integration routine solves the equations from the executable file. Fast simulations are possible, depending on the system complexity. From this, graphs can be plotted and analysed. It is easy to change parameters in the model and redo the simulation to see the effect that physical changes will have on the performance of the real system. Additional features include linearisation around a certain point, batch run facilities, and interfacing with other software.

3.2 Differential equation solution strategy in MATLAB

A brief overview of the MATLAB model layout will be helpful to understand the model development and strategy. One of the targets in writing source code for the MATLAB model was to allow future expansion thereof into a system that is able to automatically compile the system equations with a simple user interface. This would require some matrix structure defining the physical nodes and their interfaces with each other. Generic algorithms can be used where every individual hydraulic or mechanical subsystem has a reference number whereby it's parameters and port numbers can be identified. Similar layouts are used (or are suggested) by [Ellman & Vilenius 1990][Lida et al 1992][Ribeiro et al 1986]. This approach enables a single function containing only a few equations to be compiled as a separate entity, simplifying debugging, upgrading and managing of equations. Several other 'support' functions were written to keep the model code neat. This included a function in which all the system parameters could be defined and stored in a structure variable. This greatly reduced the effort to change model parameters since everything is located neatly in a single file.

Figure 3.1 shows the main program flow diagram for the MATLAB programs developed. Three main elements are needed to solve differential equations (DEQ's) in MATLAB (as with most other solver algorithms).

#1. A main program is used to initiate the model and set all the variables needed to solve the DEQ. After completion of the solution it receives the state-variable versus time values from the solver algorithm and plots the desired graphs before terminating.

#2. A solver function makes repeated calls to the DEQ file and numerically integrates the DEQ's. Most mathematical computer languages (MATLAB and FORTRAN) have well developed pre-programmed and optimized algorithms for different types of DEQ problems. These solver algorithms all have the same interface, which enables one to easily use a different solver for the same set of DEQ's. The DEQ function is called repeatedly at different time steps dependent on the method used and the solution tolerance required.

#3. DEQ file. This is a function that receives the previous time-step state-variables and new time value from the solver algorithm and computes the derivative of the state-variables at the new time step. This file can be considered the 'heart' of any new model, since the governing equations are coded here. Second and higher order DEQ's must be written as sets of first order DEQ's. In MATLAB this function is also used to calculate the zerocross variables used for discontinuity checking and analytical Jacobian calculation if it is available.

Numerical solution of the above equations applied to fluid power circuits therefore has the following sequence. The solver algorithm sends a vector of state variables to the DEQ file (e.g. pressure, position and speed). The DEQ file uses the pressures to calculate flow rates through orifices. (The pressure on both sides of an orifice must be known.) These calculated flow rates are used to determine the flow compressed into any volume. This compressed flow is substituted into the compressibility equation and the state variable derivatives (e.g. $\dot{x}$, $\ddot{x}$, $\dot{P}$) are calculated. The positions, velocities and pressures are used to determine a force balance on the masses from which the acceleration is calculated. These state variable derivatives are sent back to the solver algorithm where integration and determination of the next step size takes place.

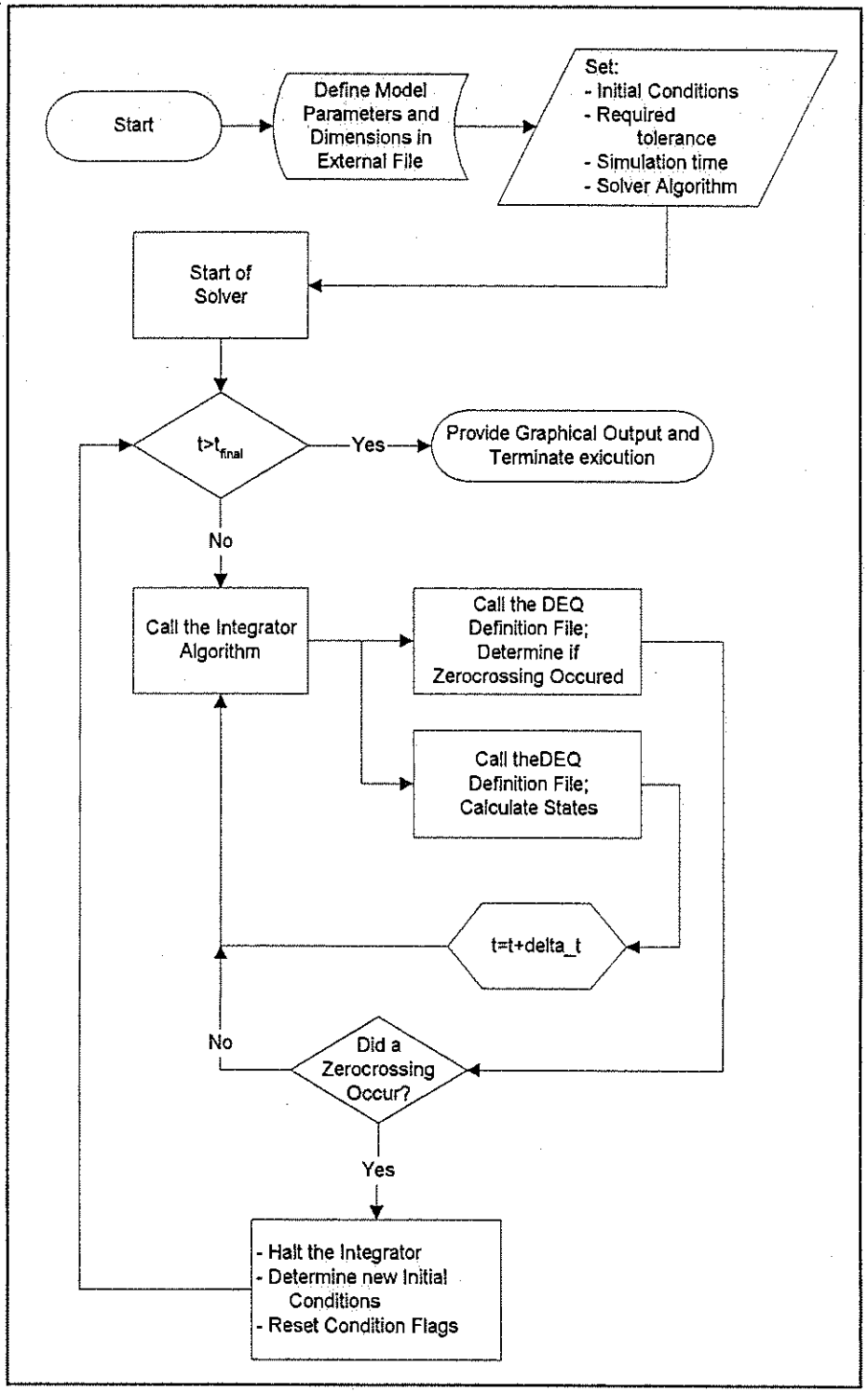

Figure 3.1 Integrator flow diagram as implemented in MATLAB

3.3 Global assumptions

Some assumptions are valid for all models.

- AMESim uses an advanced cavitation model that takes into account oil properties such as viscosity and percentage air content. No cavitation assumptions were included in the MATLAB model and avoided as far as possible in the AMESim models.
- AMESim is able to calculate pressure dependent oil properties. This function was not activated to enhance the correlation with MATLAB models.
- Fluid velocity profiles are always assumed to be uniform. Pressure distributions acting on areas are also taken as uniform. The orifice equations in MATLAB do however take laminar and turbulent flow into account, using the Piche and Ellman model. AMESim uses a comparable technique switch between laminar and turbulent flow models [Alirand 1999].
- Only some of the AMESim models take pipe friction into account. For all the other pipe models, the pressure at both ends are equal.
- With the MATLAB models all nodes are calculated as a compressible volume. This is because no differential algebraic equations were implemented in the MATLAB model. Some of the AMESim models do use incompressible nodes.
- No fluid momentum phenomena are included in the MATLAB models.

3.4 Orifice equation nomenclature

In this study four main possibilities exist for the calculation of flow rate through an orifice. As discussed in chapter 2, the flow rate through a restriction in the flow line may be calculated by equation 2.5, based on certain constants and the pressure drop across the orifice. Other modifications to equation 2.5 allow the calculation of flow rate through a sharp seated ball poppet orifice and through a sharp seated conical poppet orifice (according to equations 2.6 to 2.9). The possibility to use external data matching flow rates to pressure differentials can be treated with a interpolating lookup table. To facilitate easy reading, the following method will be used to indicate the type of orifice equation:

Type of orifice	Representation	Input parameter
circular pipe restriction	Orifice{ΔP,d}	Pressure drop, orifice diameter
sharp seated ball poppet	OrificeSB{ΔP,x}	Pressure drop, poppet height
sharp seated conical poppet	OrificeSC{ΔP,x}	Pressure drop, poppet height
lookup table	Lookup	dP, external data

3.5 Model detail: Isolated logic element (LC25)

It was found that to model the simple LC25 logic element posed no real problems in AMESim, but in MATLAB the bumpstops (or endstops) of the mass proved very challenging. The logic element model consists of a poppet element, a mass with end-stops and a piston. (Refer to figure 1.2 for the true cutaway look and to paragraph 1.5.3 for its operating principle.) To model leakage past the poppet in AMESim, a single additional block can be added as shown in the figure (3.2). This was, however, not used in any of the simulation work for the sake of simplicity. The poppet parameters were adjusted until the model behaved closely to measured data (in steady state). Parameters affecting dynamic behaviour were adjusted once the valve system model was compared to experimental data.

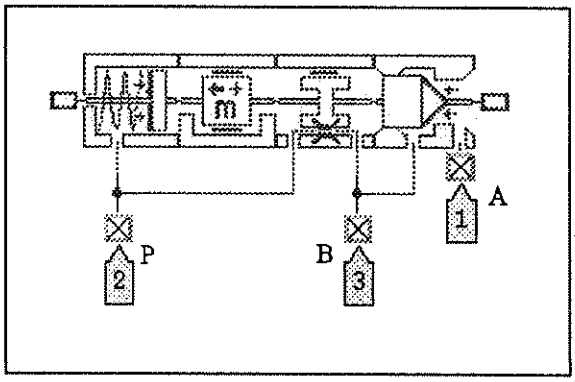

Figure 3.2 LC 25 Submodel in AMESim

The AMESim model was used to create a three-dimensional graph of pressure drop versus flowrate and poppet height. This information was previously unavailable, even from the manufacturers in Germany as confirmed. Since the poppet does not necessarily open fully during operation it is valuable to have this information. (See figure 4.9 & 4.10)

3.5.1 Mass equation and bumpstop implementation

Both the logic element and pilot valve models use similar second order differential equations to model poppet mass movement ($\Sigma F = m \cdot \ddot{x} + c \cdot \dot{x} + k \cdot x$). Separate MATLAB functions were written to calculate the mass acceleration and spring forces that may be reused in any model.

The forces acting on the logic element poppet are:

- *The spring and viscous damping force* - The spring has a linear characteristic and an initial displacement. The damping is assumed to be simple linear viscous damping. Windage (damping force proportional to the velocity squared) was investigated on the AMESim model, and found to be negligible.
- *The pressure Pa* acting on the bottom of the poppet (supply pressure). If the poppet is closed, the pressure acts only on an area determined by the poppet seat diameter. When the poppet is lifted off its seat, some assumption has to be made on the effective area and the pressure distribution across that area. As mentioned in par 2.4.2, two schemes were tested to estimate the effective area.

- *The pressure Pb* acting on the bottom of the poppet - The same reasoning holds as for pressure Pa.
- *The pressure Pp* acting on the poppet control chamber area. This area stays constant throughout the poppet travel.
- *The flow force* resulting from fluid velocity past a stationary object is ignored. Authors Ellman & Vilenius (1990) (amongst others) used several methods of incorporating this force, but many other authors disregard it. The methods commonly used to include this force consist of empirical equations based on the general poppet configuration, factors related to the fluid jet angle through the poppet opening (as is possible with AMESim), and lookup tables containing experimental data. More detailed studies would require CFD investigations.
- *Poppet inertia*: The force associated with accelerating the valve poppet.

The above pressures and forces give the mass acceleration equation and variables:

(Eq 3.1)
$$m \cdot \ddot{x} - k(x + InitD) + C \cdot \dot{x} + P_A \cdot A_A + P_B \cdot A_B - P_P \cdot A_P = 0$$

x = Poppet displacement [m]
m = Poppet mass [kg]
k = Spring stiffness [N/m]
C = Damping coefficient [Ns/m]
InitD = Spring initial displacement [m]
A = Area (relating to it's subscript) [m^2]
P = Pressure (relating to it's subscript) [Pa]

This second order differential equation is split up into a system of two first order differential equations for computer implementation in the MATLAB function Mass_DEQ.m in appendix A3.3.13.

To implement a bumpstop or physical limitation on the logic element and pilot valve poppet movement proved to be one of the biggest challenges in this study. The above mass acceleration equation (eq 3.1) poses no limit on the poppet travel x. The physical limitation on the movement of the poppets is, however, one of the main influences on the valve behaviour. Some authors have implemented a bumpstop system where the metal to metal contact act as very stiff or nonlinear springs. [Korte 1990][Tani et al 1993][Vilenius & Simpura n.d.][AMESim 1988 (f)] This method models the physics well, but has several disadvantages. From investigation large oscillations of very high frequency were observed when the stiff springs engaged, as was expected. This

obscures the dynamics of interest and is computationally intensive. The high frequency oscillations could be damped but this damping greatly affects the poppet dynamics. This requires some scheme where damping is only increased once the mass is past its mathematical limits. This added damping may only work in one direction since the external forces would otherwise not be able to 'pull' the mass away from it's bumpstop position. Implementation of such a scheme proved impractical.

An ideal bumpstop sets the speed of the mass to zero once it hits the travel limit. The differential equation solver is programmed on the assumption of a smooth solution and has trouble finding solutions around such discontinuities. To overcome this, the solver has to be halted and restarted with new initial conditions guiding it in the right direction after the discontinuity.[Jansson et al. n.d.] In terms of the mass equation a discontinuous velocity and therefore an infinite acceleration must be dealt with. Once stopped in position the mass may only move in the direction away from the bumpstop once the force balance reverses direction. [MATLAB 1988 (a)][Jansson et al. n.d.] All these requirements prompted the use of the MATLAB ODE solver 'events' or 'zerocrossing' function whereby any variable can be traced for a crossing through or from zero. When a defined variable crosses zero the integrator can be halted. For detail on the implementation thereof, the source code (annexure A3.3) and solver graphical layout (fig 3.1) may be consulted. It should be noted that many other schemes for implementing the bumpstops were investigated and found to be inadequate or unpractical.

3.5.2 Orifice equations and compressibility in the logic element model

The orifice equation (Eq 2.1) as used in this study (Eq 2.5) was implemented in a MATLAB function. To implement the flow equation the pressure drop across the orifice and the effective gap size has to be provided. The flow is assumed to be uniform through the flow area as calculated. The control chamber fluid volume can be assumed compressible with the equation: (relating to figure 3.2)

$$Q_{Logic} = \text{OrificeSC}\left\{(P_A - P_B), x_{Logic}\right\} \quad \text{(Eq 3.2)}$$

$$QC_P = Q_P + A_P \cdot \dot{x} \quad \text{(Eq 3.3)}$$

$$\dot{P}_P = \frac{\beta}{V_P} QC_P \quad \text{(Eq 3.4)}$$

Thus leaving the state variable vector:

$$\begin{bmatrix} x_{Logic} & \dot{x}_{Logic} & P_P \end{bmatrix} \quad \text{(Eq 3.5)}$$

3.6 Model detail: Test bench

One of the major factors influencing model performance (compared to the experimental results) is the presence of test bench dynamics in the measured data. To improve and refine the models, it became clear that a very well detailed test-bench model is a necessity. As the detail modelling of the test-bench is a massive task some simplifying assumptions had to be made. As explained in paragraph 4.3 the test bench controls the maximum flow and pressure allowable by means of proportional solenoid valves. The dynamics of these valves is not taken into account in the models, but the long test bench supply lines are modelled. Several levels of model complexity were attempted.

Initially the supply line compressibility was modelled as a single fluid volume. The parameter adjustment thereof is difficult and a model representing the real layout of the supply line was constructed (Figure 3.3). In AMESim the longer steel pipes are modelled with fluid inertia, while the short rubber hoses are simply modelled as compressible volumes. AMESim calculates the effective pipe compressibility based on the fluid volume and the pipes' wall thickness and material properties.

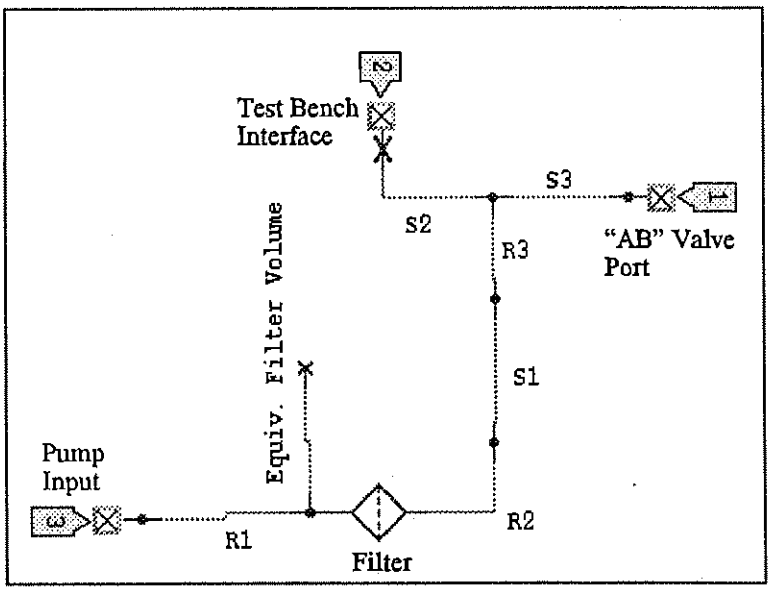

Figure 3.3 Detailed AMESim model of test bench supply line.

In figure 3.3 the pump oil supply is fed to port 3. Port 2 and the orifice right before it, represents the quick-couplers fitted to the front console of the test bench. Port 1 represents the connection to valve "AB", that allows separate or coupled operation of pumps A and B. The high pressure filter fitted to the test bench supply line is modelled as a orifice with a equivalent volume. It would be possible and helpful to construct a model of the test bench that contains detail of the control

valves, PID control system, pump variable flowrate mechanism and detail of the supply line compressibility and flow resistance. However the work involved put that outside the scope of this study. The work involved and related cost would also have to be evaluated against alternative experimental designs with less influence on the system to be tested.

3.6.1 Relief valve

In order to approximate the test bench control system functioning in the models, an ideal flow source was used together with an ideal relief valve at the entrance to the supply line model. This setup effectively limits the maximum flow to the flow source setting and limits the maximum system pressure to the relief valve cracking pressure.

The flow through the relief valve is a linear function of pressure drop (ΔP*Gradient) and it opens once the cracking pressure is exceeded. In the following equation FlowGrad is the linear flow gradient parameter:

$$\Delta P = P_{in} - P_{out} - P_{crack}$$

(Eq 3.6)

$$Q_{relief} = \begin{cases} \Delta P \cdot FlowGrad \mid \Delta P \geq P_{crack} \\ 0 \mid \Delta P < P_{crack} \end{cases}$$

These equations are used in the AMESim and MATLAB models. The MATLAB function implementing these equations is shown in Appendix A3.3.14.

3.7 Model detail: Isolated pilot valve (WSE3)

The WSE3D pilot valve (figure 1.3 and 1.4 for the true cutaway look) proved challenging to model because of the detail required and the sensitivity of the model to certain parameters. The model consists of the following mechanical components:

- Spring
- Ball poppet
- Mass with end-stops
- Pressure compensating chamber piston
- Solenoid model (several possibilities considered)
- Connecting lines
- Test bench approximations needed to correlate the model results with experiments conducted.

The pilot valve specifications quote 12 LPM as the maximum permissible flow. The pressure drop across the valve is approximately 5 MPa (50 Bar) at this flow. Raising the pressure to above 5 MPa therefore necessitate a flow limit setting of 12 LPM on the test bench.

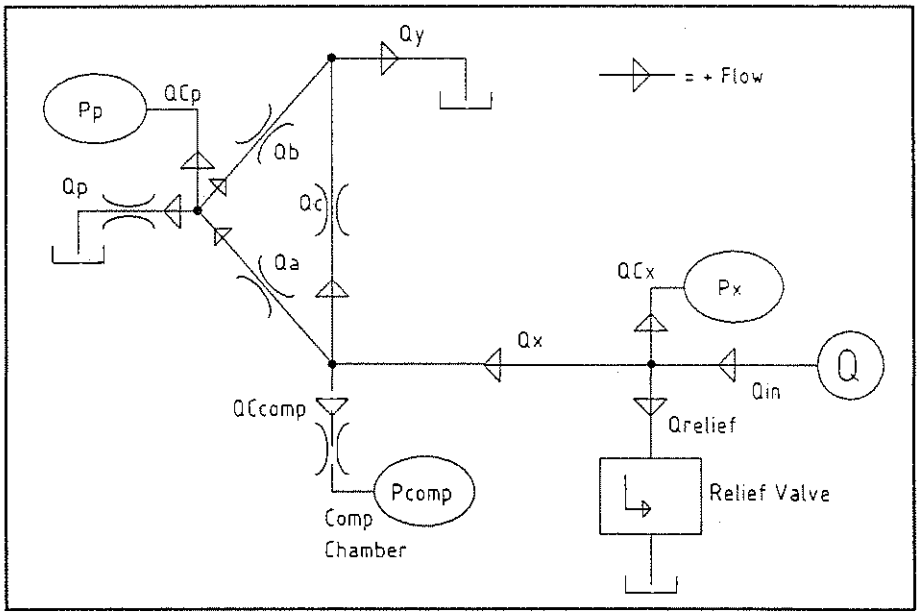

Figure 3.4 Pilot valve model schematic flow layout for MATLAB equation deduction

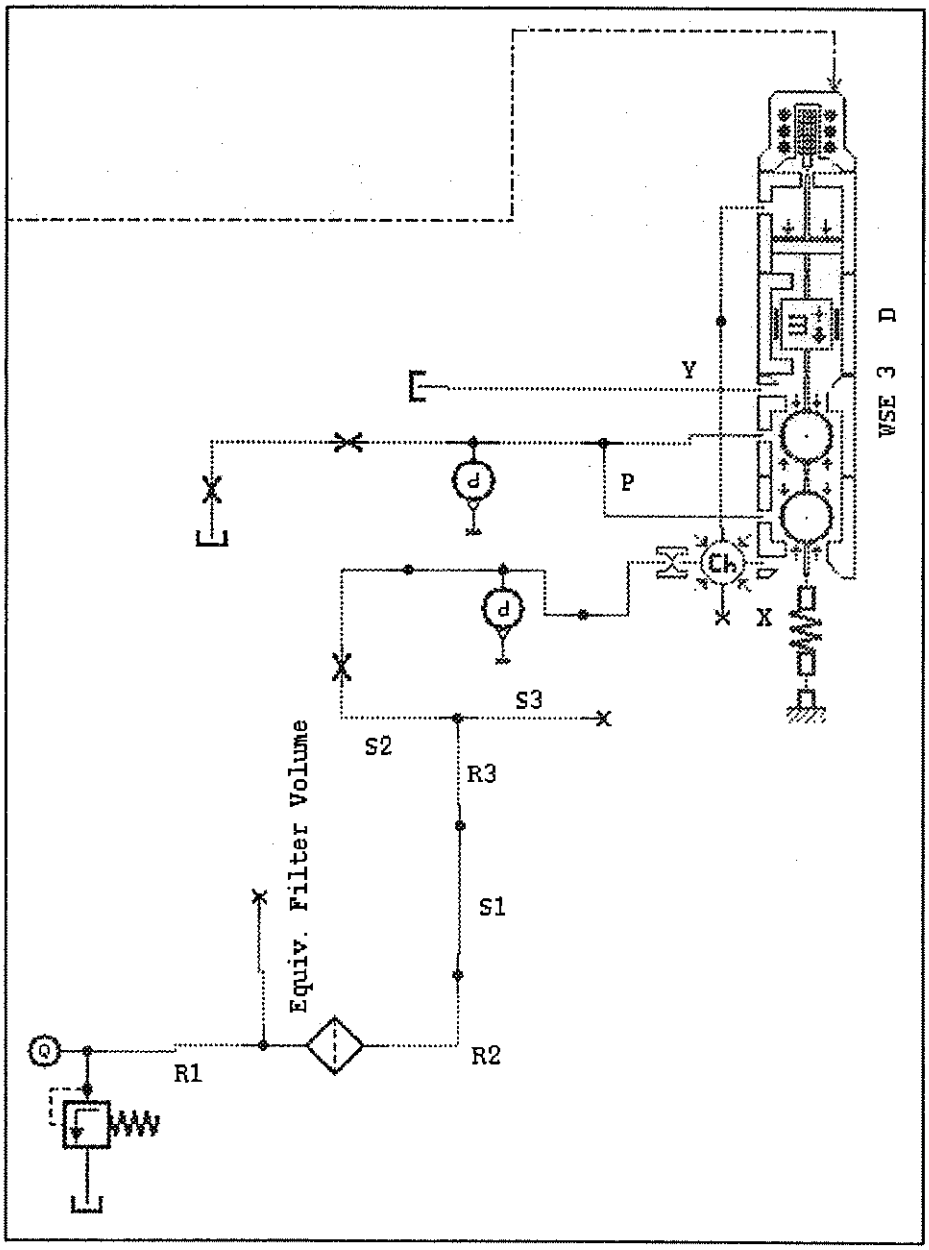

Figure 3.5 Pilot valve model in AMESim with test bench supply line model

3.7.1 Mass equations for the pilot valve model

As explained in paragraph 3.5.1, the pilot valve and logic element models use the same second order differential equation to model poppet movement but only with different external forces.

The forces acting on the pilot valve poppet are:

- *The spring and viscous damping force* - The same assumptions hold as for the logic element as in paragraph 3.5.1.
- *The solenoid force* - The solenoid converts an electrical signal to a force. Several solenoid models were evaluated and are described later due to complexity (annexure A3.1).
- *The pressure Px* acting on the bottom of the poppet (supply pressure). The same assumptions hold as for the logic element in paragraph 3.5.1.
- *The pressure Py* acting on the top of the poppet - The same reasoning holds as for pressure Px, except for the solenoid actuator rod, which reduces the active area. The effective reduction in area is difficult to determine since the poppet is spherical and the connecting rod-end is flat. Theoretically this would imply a point contact with zero reduction in area. Another assumption is that the connecting rod and poppet stay permanently connected. In the physical system the actuator rod may separate as it cannot exert a pulling force on the poppet. This fact is ignored in both the AMESim and MATLAB models because the flow into the valve is introduced in one direction only (i.e. phenomenon need to be modelled, an ideal bumpstop or metal to metal contact surface would be required. A complex surface deformation model might also be considered to calculate the reduction in effective poppet area.
- *The pressure Pp* acts on the remainder of the poppet area. Since Pressure Pp acts on both sides of the poppet, the effective force and its direction is a function of the poppet position. Figure 3.6 shows this effective area as a hatched annular projection (Area P). With the assumptions made, the force would have a zero value if the poppet is half-way between the poppet seats.
- *The pressure compensating chamber* acting to oppose the Px force. The purpose of this chamber is to balance the force resulting from the supply pressure Px. This is necessary to reduce the solenoid force demand. A small diameter tube inside the valve connects the supply pressure Px to the pressure compensating chamber on the other side of the poppet. There the pressure acts on a piston with approximately the same diameter as the poppet seat.
- The flow force resulting from fluid motion past the poppet is ignored. In this regard, the same assumptions hold as for the logic element in paragraph 3.5.1.
- Inertia: The poppet mass includes the solenoid armature mass that is orders of magnitude greater than the mass of the ball poppet.

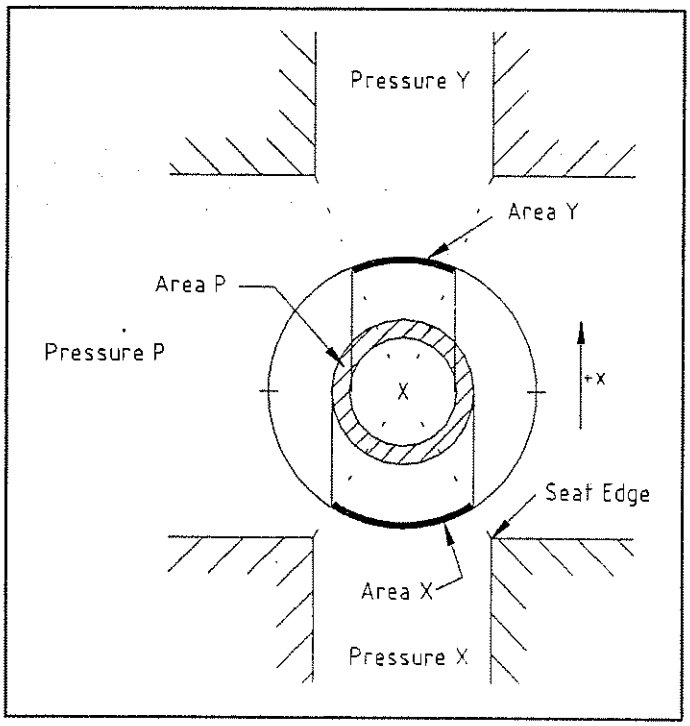

Figure 3.6 Effective area for pressure P to act on

The above pressures and forces give the mass acceleration equation and variables:

(Eq 3.7)
$$m \cdot \ddot{x} - k((X\max - x)) + InitD) + C \cdot \dot{x} - Px \cdot A_x + Px \cdot A_{comp} + Py \cdot A_y + Fsol + Fp = 0$$

(Eq 3.8)
$$Fp = \begin{cases} Pp \cdot Ap & |x < 0.5 \cdot x_{limit} \\ 0 & |x = 0.5 \cdot x_{limit} \\ -Pp \cdot Ap & |x > 0.5 \cdot x_{limit} \end{cases}$$

x = Poppet displacement [m]
x_{limit}=Maximum poppet travel [m]
Xmax = Displacement when fully open [m]
m = Mass [kg]
k = Spring stiffness [N/m]
C = Damping coefficient [Ns/m]
InitD = Spring initial displacement [m]
Fsol = Solenoid force [N] - Refer to annexure A3.1
A = Effective areas [m^2]
P = Pressure acting on the effective area [Pa]

Implementation of this equation and the associated bumpstops is exactly the same as with the logic element poppet of paragraph 3.5.1.

3.7.2 Orifice representation for the pilot valve model

The pilot valve schematic flow layout is shown in figure 3.4. The poppet and seat have been replaced by a triangular network of orifices. This is a common method of modelling hydraulic valves and almost any valve configuration can be represented by a Wheat-Stone bridge type layout of orifices [Vilenius & Simpura n.d.][Viersema n.d.]. Most 4-way spool valves can be represented by a full bridge layout thus incorporating leakage past the spools. The pilot valve in this study only requires a half-bridge layout of orifices to model all possible flow paths in the valve.

Orifice A in the triangular network (figure 3.4) allows flow from port X to P and is closed with the poppet in the bottom position. Orifice B allows flow from port P to Y and is closed with the poppet in the top position. Orifice C represents leakage from the high pressure port X to the drain pressure port Y. It is active only with the poppet not touching any seat. The effect thereof can be seen in simulations and experiment as a small bump in the drain-line pressure when the valve switches. (Not shown because of it's small effect and size) To include these effects, the poppet height is described in term of three variables representing the effective poppet height for each orifice, that can be substituted into the individual orifice equations.

Derived equations for the individual effective poppet openings related to the true poppet height (state variable x) are: ('Top' and 'Bot' describe the valve seat geometry)

(Eq 3.9 a) $$x_a = x$$

(Eq 3.9 a) $$x_b = (Top - Bot - x)$$

(Eq 3.9 c) $$x_c = \frac{(Top - Bot)\cdot(x - Top)\cdot(x - Bot)}{-\frac{1}{4}(Top^2 + Bot^2) + \frac{1}{2}(Top \cdot Bot)}$$

These equations are represented graphically in figure 3.7.

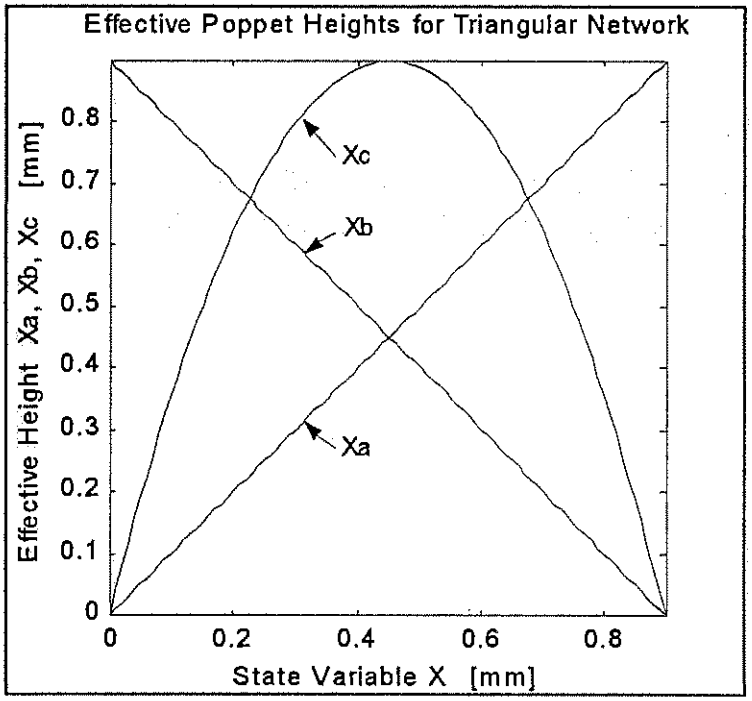

Figure 3.7 Normalised effective poppet heights used in the triangular orifice network for the pilot valve model (rippled line effect due to computer graphics format)

Flows are indicated as Q with positive values in the direction of the arrows in figure 3.4. Flows that represent fluid compression are indicated as QC. Orifice equation nomenclature is discussed in paragraph 3.4.

For the triangular network the flow is defined as:

(Eq 3.10 a) $$Q_a = \text{OrificeSB}\{(P_X - P_P), x_A\}$$

(Eq 3.10 b) $$Q_b = \text{OrificeSB}\{(P_P - P_Y), x_B\}$$

(Eq 3.10 b) $$Q_c = \text{OrificeSB}\{(P_X - P_Y), x_C\}$$

For the drain line resistance (as encountered in the experimental setup) the flow is:

(Eq 3.11) $$Q_P = \text{Orifice}\{(P_P - P_{Atm}), D_P\}$$

(With Dp the drain orifice diameter)

The fluid in the pressure compensating chamber is assumed to be compressible, but with a constant volume (i.e. independent of the poppet position). In the valve it is connected by a drilling of diameter less than 1mm and length in excess of 30mm. To investigate any possible phase lag

between the pressure Px and the pressure in the compensating chamber the flow to and from it passes the orifice:

(Eq 3.12) $$QC_{comp} = \text{Orifice}\{(P_X - P_{comp}), D_{comp}\}$$

(with Dcomp the compensating chamber orifice diameter)

An attempt was made to simplify the model by removing this orifice (thus setting the control chamber pressure directly equal to pressure Px), but instability occurred.

3.7.3 Nodes and compressibility

The flow from these orifice equations can be summed at the nodes (relating to figure 3.4):

(Eq 3.13 a) $$Q_X = Q_a + Q_c \quad (+QC_{comp})$$

(Eq 3.13 b) $$QC_P = +Q_a - Q_b - Q_P$$

(Eq 3.13 c) $$QC_X = +Q_{in} - Q_{relief} - Q_X$$

The pressure compensating chamber flowrate (+QCcomp) is left out from the above MATLAB equation implementation to reduce the overall stiffness (In AMESim the term is included). These node flows are substituted into fluid compressibility equations giving rise to the state variable equations:

(Eq 3.14 a) $$\dot{P}_P = \frac{\beta}{V_P} QC_P$$

(Eq 3.14 b) $$\dot{P}_X = \frac{\beta}{V_X} QC_X$$

(Eq 3.14 c) $$\dot{P}_{comp} = \frac{\beta}{V_{comp}} QC_{comp}$$

To complete the model, the state equations (Eq 3.7 and Eq 3.14) can be assembled into the state variable vector of the form:

(Eq 3.15) $$\begin{bmatrix} x_{WSE} & \dot{x}_{WSE} & P_X & P_P & P_{comp} \end{bmatrix}$$

3.8 Model detail: Rectifier circuit and check valves

The addition of fully dynamic check valves in the model would drastically increase the number of state variables and stiffen the equations because of their fast dynamics, thereby increasing the demands on the integrator system. In attempts to reduce the initial model complexity, the check valve rectifier circuit was excluded from the models. The decision was based on a hypothesis that the check valves have a much faster time constant than other components in the system, and would not drastically affect the overall system dynamics. From simulation this proved true, although the check valve cracking pressure was found to have a significant influence. Therefore the check valves have to be included albeit ideal check valves (no poppet mass dynamics) as used in all the models created.

In all the experiments conducted, flow is only introduced in one direction through the valve system. This effectively halves the functionality needed from the rectifier (only two check valves are needed). The hypothesis was confirmed using AMESim to construct a model with a full rectifier circuit. No difference was noted between the models with four and two check valves.

Since the check valves have a small spring stiffness, it is very difficult to determine the cracking pressure from experiment. No cracking pressure information is supplied in the product catalogue. The sensitivity analysis conducted (paragraph 3.10) indicates the importance of the check valve cracking pressure.

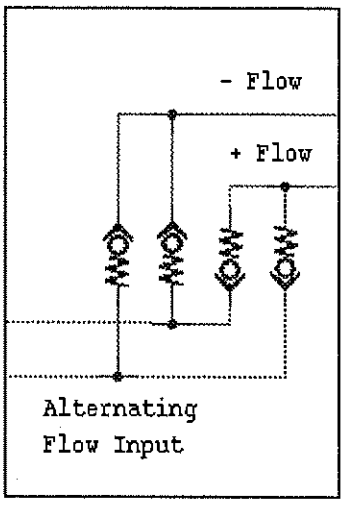

Figure 3.8 Rectifier circuit

3.9 Model Detail: Valve system with parallel damper

The valve system model contains all the pilot valve model elements (mass, triangular network, compensating chamber) added to the logic element and damper models.

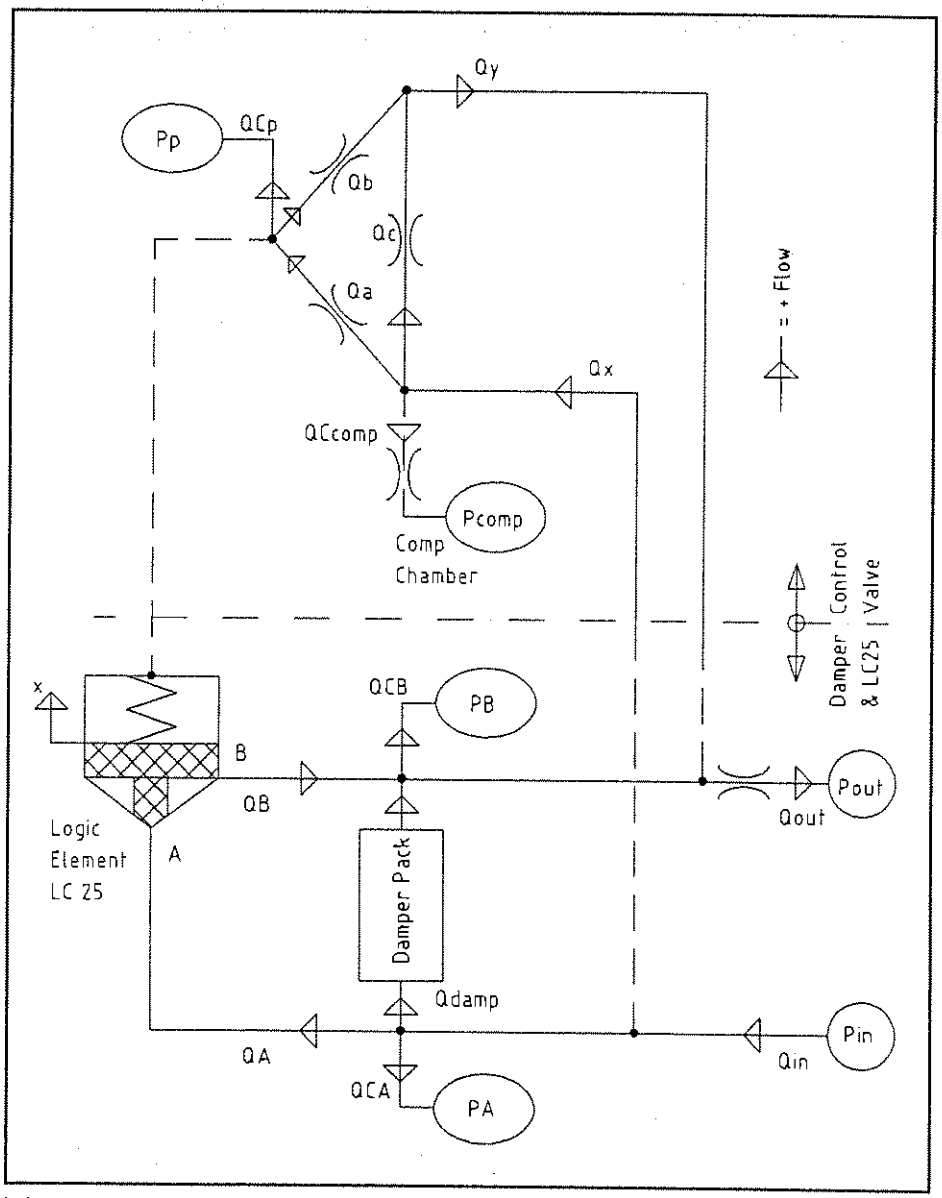

Figure 3.9 System with parallel damper schematic layout for MATLAB equation deduction. Indicated without rectifier check valves.

Figure 3.9 represents the MATLAB model equations and requires some explanation: everything above the horizontal dash line indicates the pilot valve model as constructed in paragraph 3.7 without the test bench assumptions.

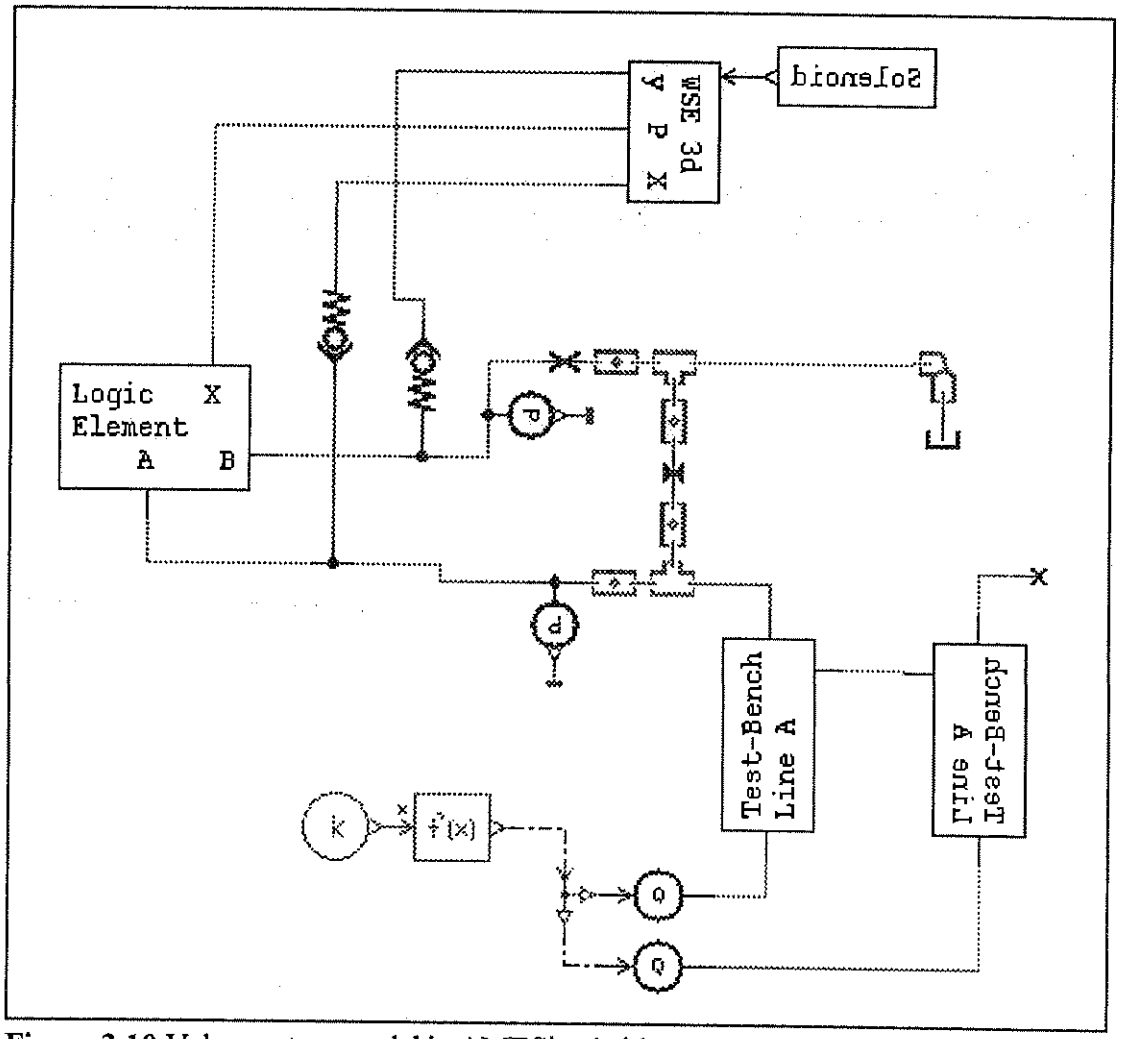

Figure 3.10 Valve system model in AMESim (with two test bench supply line models). (Inverted text due to AMESim graphics format.)

The first assumption made in the MATLAB model to reduce complexity is that of flow summation at nodes. The dashed lines from the pilot valve ports to nodes in the main flow lines represent a connection in terms of pressure but not in terms of flow. The reasoning is that the pilot circuit has much smaller flow rates than the main valve lines and therefore the model complexity can be reduced by disregarding the pilot flow in the node flow summation equations. This statement was tested by adding the flows in a model and superimposing results. A minor change resulted that shows a trend closer to the AMESim model but the effect is still very small. It is not shown in this chapter, but can be viewed in figure A5.1, with a discussion of the results.

The second assumption made in the MATLAB model is that the logic element chamber volume is constant (i.e. does not change as the logic element poppet displaces). The flow generated passes into the WSE Px port, at a flowrate equal to $A \cdot \dot{x}$. Investigation of this assumption shows extreme effects on the results. The MATLAB model is completely unstable with a variable chamber volume.

3.9.1 Damper

The damper characteristics as measured on the test bench (fig 4.12) were used in the AMESim and MATLAB models in the form of a lookup table. The linear interpolation algorithm used in MATLAB cannot extrapolate a curve and since the differential equation solver generates many unrealistic test points to obtain a valid solution, it was necessary to expand the curve to larger flow rates. This was done by linearly extending the limits of the graph by adding two points manually. This corresponds with the AMESim extrapolation method, to allow correlation between AMESim and MATLAB results.

In the true damper configuration (linear and rotary) the volumes of the damper chambers change as the vehicle moves. These changes will affect the total compressible volume and could have an influence on the natural frequency of the system. This effect is ignored in all the models since the damper chamber volumes are assumed constant.

3.9.2 Orifice representation for the valve system with damper model

Orifice equations nomenclature are discussed in paragraph 3.4.

The flows through the pilot valve triangular network can be taken directly from the previous model's equation 3.10 since the same pilot valve model is included (these equations are not shown again). Other orifice equations for the valve system model network are:

(Eq 3.16 a) $$Q_A = \text{OrificeSC}\{(P_A - P_B), x_{Logic}\}$$

(Eq 3.16 b) $$Q_{Damp} = \text{Lookup}\{(P_A - P_B), \text{DamperCurve}\}$$

(Eq 3.16 c) $$Q_{Out} = \text{Orifice}\{(P_B - P_{Out}), D_{Out}\}$$

(With Dout the drain orifice diameter)

3.9.3 Nodes and compressibility

Equation 3.13 is again applied directly for the pilot valve model. Additional equations are:

(Eq 3.17 a) $$QC_A = Q_{in} - Q_A - Q_{damp} \quad (-Q_x)$$

(Eq 3.17 b) $$QC_B = Q_B - Q_{Out} + Q_{damp} \quad (+Q_y)$$

(Eq 3.17 c) $$QC_P = Q_a - Q_b \quad (+\dot{x}_{LC} \cdot A_P \cdot \text{Frac})$$

Note the use of lowercase a and b to indicate flows in the triangular pilot valve circuit and upper-case flows A and B for the main line flow through the damper and logic element. In the above

equations Qx and Qy are the additional pilot valve flow terms not included. The term $\dot{x}_{LC} \cdot A_P \cdot Frac$, not included in the equation, is the variable poppet volume term, with Frac an additional compensation term, evaluated to reduce computational intensity once the MATLAB instability was found. This term served only an experimental purpose and may be considered as unity throughout the rest of this study. The compressible volumes introduce the following state variable derivative equations:

(Eq 3.18 a) $$\dot{P}_A = \frac{\beta}{V_A} \cdot QC_A$$

(Eq 3.18 b) $$\dot{P}_B = \frac{\beta}{V_B} \cdot QC_B$$

(Eq 3.18 c) $$\dot{P}_P = \frac{\beta}{V_P} \cdot QC_P$$

To complete the model, the state equations 3.1, 3.7, 3.14, and 3.18 can be assembled into the state variable vector of the form:

(Eq 3.19) $$\begin{bmatrix} x_{LC} & \dot{x}_{LC} & x_{WSE} & \dot{x}_{WSE} & P_A & P_B & P_P & P_{comp} \end{bmatrix}$$

Several simple checks were done on the AMESim model. These included manual (visual inspection of a short time trend) integration of the flow rates through the check valves and poppet element chamber. Conservation of mass was validated in this experiment. Other checks such as manual addition of forces acting on the logic element in the MATLAB model confirmed the correct determination of resultant forces.

3.10 Sensitivity study on an AMESim model

A sensitivity analysis on the valve system model (paragraph 3.9) was done using the AMESim model. This consisted of an automatic routine to simulate the system over a range of flow settings, each time with one parameter changed with plus 10% and minus 10%. The data obtained was reduced to the final delay times and steady state values in terms of supply pressure and logic element poppet displacement. This was done for 30, 80 and 210 MPa initial pressure cases to obtain a range of values. These extracted data trends are represented graphically in annexure A3.4, with the complete sensitivity analysis in table format. To provide a quick overview of the results and point out some important facts, the minimum, maximum and average change for the pressure or displacement variation was calculated and is given in the following table. Please note that this table is only intended to provide a general overview of the data in annexure A3.4. Several important notes related to the information are given below the table.

Please note the Important Notes at the end of the table.

Ref. Figure	Parameter	Minimum change (%)	Maximum change (%)	Mean change (%)
A3.4.1	Exponential solenoid time constant: ON	0.04	2.49	0.84
A3.4.2	Exponential solenoid time constant: OFF	0.04	1.25	0.67
A3.4.3	Pilot valve pressure compensating chamber diameter	0.02	3.58	1.27
A3.4.4	Pilot valve spring stiffness	0.02	2.13	0.92
A3.4.5	Pilot valve spring initial displacement	0.03	2.41	0.98
A3.4.6	Logic element poppet mass	0.03	1.27	0.43
A3.4.7	Logic element viscous friction	0.36	1.67	0.89
A3.4.8	Logic element spring stiffness	0.21	1.39	0.63
A3.4.9	Logic element spring initial force	1.03	7.01	3.33
A3.4.10	Logic element control chamber diameter *NOTE 1*	13.68	42.54	26.63
A3.4.11	Check valve #1 cracking pressure (flow from X to P) *NOTE 2*	8.46	270.06	77.90
A3.4.12	Check valve #2 cracking pressure (flow from P to Y)	6.57	17.96	13.26
A3.4.13	Damper pressure drop multiplier *NOTE 3*	7.08	20.52	15.62
A3.4.14	Drain elbow diameter	6.37	23.72	14.02

A3.4.15	Test-bench quick coupler diameter	7.07	21.99	13.43
A3.4.16	Test-bench rubber hose stiffness	8.52	22.11	14.48
A3.4.17	OIL: Bulk modulus	2.79	16.00	8.33
A3.4.18	OIL: Kinematic viscosity	1.90	19.42	9.35

Important notes

1 With a 10% reduced control chamber area the valve does not fully close. This effectively lowers the initial pressure and alters the system dynamics.

2 The base value for cracking pressure is 0 Bar. The -10% and +10% value is set equal to the check valve #2 cracking pressures (ie 1.35 Bar and 1.65 Bar).

3 In AMESim, a gain (multiplier) parameter is used to scale values in lookup tables. The damper pressure drop gain parameter effectively alters the damper characteristics. Since the model takes flow rate as an input, the initial pressures must differ since the damper creates a higher pressure drop with a higher gain. The steady-state errors are therefore not physically interpretable and the delay times are calculated based on mismatching initial pressures. The only physically relevant information from this run is obtainable by examining the relevant graph (figure A3.4.13)

Discussion

It should be noted that the percentage change was calculated using an automatic subroutine. From visual inspection of time domain graphs it was observed that some of the small changes may be attributable to machine precision and sampling rate of the modelling results and should therefore be treated with care.

It is further important to note that the parameters with a large influence on the system response are almost exclusively related to the test bench. The only system parameter with a large effect on the system response is the check valve cracking pressure. This parameter is difficult to obtain accurately by experimental work and no manufacturer's data is available. Two other parameters also having an apparently large effect on the system response are the logic element control chamber diameter and the damper pressure drop gain (refer to note 3, end of table). Please note that the percentage change calculated for these values have no physical meaning since equivalent time domain trends are not used in calculating the percentage change. The only relevant information obtainable from these runs is in the delay trend figures (shown in annexure A3.4)

The above information again confirms the major influence that the test bench have on the system. In order to conduct a sensitivity analysis on the valve, with enough detail for use in future design work, one would need a model of the valve system with enough accuracy to have confidence in

isolating the valve and applying ideal flow or pressure sources. Only once the effect of the measurement system is reduced (or completely removed) will the system response not be dominated by the measurement system.

3.11 Overview of models created

The following table shows the extent of the models created and indicates where these models were discussed in this chapter.

✔ indicates that the model was created or is discussed.
✘ indicates that the model was not created or is not discussed.

Model	AMESim	MATLAB	Discussed / not discussed
Single logic element	✔	✔	✔ (§ 3.5)
Ellman example of stiff system	✔	✔	✔ (§ 2.4.3)
Ideal bumpstop for a mass	✔	✔	✔ (§ 3.5.1)
Physical bumpstop using metal to metal contact spring forces	✔	✔	✔ (§ 3.5.1)
Full MMF solenoid sub-model without hysteresis	✔	✘	✔ (§ A3.1.1)
First order lag solenoid approximation	✔	✘	✘
Dual (separate rising and falling) first order lag solenoid approximations	✔	✘	✘
Exponential rise and decay solenoid force model	✘	✔	✔ (§ A3.1.2)
Single dynamic check valve	✔	✔	✘
Ideal check valve rectifier sub-model	✔	✔	✔ (§ 3.8)
Dynamic check valve rectifier sub-model	✘	✔	✘
Complete system with logic and solenoid valve	✔	✔	✘
Complete system with logic, solenoid and rectifier	✔	✘	✘
Experimental model of the non-linear damper in terms of flow and pressure difference	✔	✘	✘
Complete system with: logic, solenoid valve, parallel damper, no check valves. No pilot system flow connected	✘	✔	✔ (§ 3.9)

Complete system with: logic, solenoid valve, parallel damper, no check valves. Pilot system flow is connected	✔	✔	✔ (§ 3.9)
Complete system with: logic, solenoid valve, parallel damper, two check valves. Pilot system flow is connected	✔	✘	✘
Complete system with: logic, solenoid valve, parallel damper, four check valves. Pilot system flow is connected	✔	✘	✘

#

4 Experimental Work

The aim of experimental work in this study is to obtain operational parameters and dynamic response data with which the mathematical model may be verified and refined. This chapter starts with a description of what should ideally be measured. The concepts and final choice of an experimental setup to realize these measurements are discussed thereafter. Finally, detail of the experiments conducted and some results are shown. Where applicable, some analysis of data is made, although the bulk of this work is conducted in chapter 5 where all the data from this study is merged and analysed. Detail of the instrumentation with their calibration is shown in annexure A4.1. Equipment specially manufactured for the experiments is shown in annexure A4.3.

4.1 Experimental needs

As a first step in the experimental planning it is established what needs to be measured and an estimate of the expected results is made. For this reason the following list of ideally required characteristics was compiled. It was not feasible to conduct all of these experiments.

- **Physical parameters,** including poppet masses, orifice diameters, oil properties, etc. Not all the parameters needed are realistically measurable, with several requiring special experimental setups or procedures. For the purposes of this study, the unknown parameters are approximated.

- **Steady state** pressure drop versus flow rate for the solenoid pilot valve (WSE 3), check valve (CP 108) and logic element (LC 25). The pressure drop versus flowrate graphs can be used to determine approximated orifice coefficients needed in mathematical models. Experiments were conducted by adjusting the flow rate through the valve incrementally and measuring the corresponding pressure drop. Results are expected to match the curves given in manufacturers' catalogs. For the logic element a further extension is to repeat the pressure drop / flow rate measurements for different poppet heights. (This was done with the aid of a poppet stroke limiter). The flow rate versus pressure drop experiment should ideally also be conducted for various other items used such as the pipe fittings and test-bench fittings used in experiments and the individual valve block ports connecting the valves. Determination thereof is however impractical, since the very same fittings are needed to conduct the experiments with. It is for instance impractical to mount pressure sensor ports directly next to any given orifice without adding additional fittings, or

modifying the existing fittings. Since these pressure losses are designed to be of a low magnitude, efforts were concentrated on restricting elements, such as the valves.

- **Flow force** is caused by the viscosity of fluid flowing past any stationary object. In the case of any valve poppet, this force could have a marked effect on poppet's external force balance. Some commercial simulation software packages include empirical formulas for the calculation thereof, and suggest fine-tuning with experimental values. [Lebrun & Richards 1998][Ellman & Vilenius 1990] The practicalities involved in measuring such forces and their effects make these values a luxury.

- **Dynamic response** of the solenoid pilot valve. This valve has a complex mathematical model and separate experimentation is required to verify the model in isolation. Experiments conducted are done by adjusting the maximum allowable flow rate and switching the solenoid for different initial pressure conditions. The corresponding pressure drop versus time is measured.

- **Dynamic response** of the check valves. The time constant of this valve is expected to be very fast compared to other valve elements. Conducting these experiments would require a flow or pressure step input, or detail models of the test bench behaviour. It should be possible to introduce a sinusoidal flow or pressure signal and determine a transfer function from the measured response. Similar work has been conducted [Watton & Xue 1994] but the technique requires special measuring equipment. The experiment is not conducted in this study.

- **Dynamic response** of the logic element. As with the check valves, a flow or pressure step-input would be required. Since some other external control element is needed to activate the logic element, both systems would have to be included in a mathematical model.

- **Dynamic response** of the valve block assembly. Since the system is self-contained, no external flow switching is required. The results from these tests would provide the ideal verification tool based on the overall system dynamics.

- **Dynamic response** of the valve assembly parallel to the damper valve. Since the damper valves also include some dynamics, and since the valve is exclusively used in this configuration, this experiment provides some results directly applicable to the suspension development requirement from which this study originated. The results from this experiment would also be comparable to previously conducted work [Els 1997] (dependant on the level of test bench interference with the system operation).

- **Dynamic response** of the damper pack in isolation. The damper pack valves use Belleville springs and are inherently dynamic. Complex dynamic behaviour (e.g. resonance) has been observed in these valves by Els. It was considered outside the scope of this study to model the dynamics of the damper pack valves.

4.2 Experimental concepts

It is well known that one cannot measure something without affecting the phenomena being measured. This is very much so in measuring large and fast-changing flow rates. (For the valve in question: 400 LPM with 40 ms switch time typically.) With the imposed budget constraints several concepts had to be evaluated in order to meet the required performance.

The ideal test setup to conduct these experiments on would be a hydraulic power pack capable of the necessary flow rate (> 400 LPM) and pressure (300 Bar = 30 MPa). For dynamic tests it should also be capable of step-response inputs and/or varying sinusoidal flow or pressure changes. Very fast servo-valves are available that can switch large flows within a few milliseconds. This can be considered as a step input to many systems with slower dynamics. Typical concepts evaluated to achieve the necessary test capabilities included:

- Accumulator arrays charged to the required pressure will provide a relatively constant input pressure for a short duration.
- The use of larger available power packs and discarding or recycling the used and contaminated oil.
- A pressure intensifier could be used in reverse to give large flows when activated with high pressure. This arrangement would only partly satisfy the pressure / flow requirements.
- Mounting of a hydraulic cylinder in series with a Hydropuls type servo actuator. Controlling the speed and force of the Hydropuls, and therefore that of the cylinder, would provide a short burst of flow. Since the valve assembly being studied opens and closes within typically 100ms, one second of flow would suffice to obtain data.
- A smaller test bench with dual hydraulic pumps capable of 90 LPM at 30 MPa was available, but in need of repair. It was decided to repair and use this facility.
- A concept for measuring the flow force induced on the logic element poppet that might prove feasible in future work is as follows: The logic element control chamber may be filled with oil and slowly bled off through an external orifice (quasi-steady state) thereby allowing the poppet to raise slowly. Measurement of the control chamber pressure and poppet displacement may be translated into flow force versus poppet height data.

The availability of instrumentation should also be taken into account when planning experimental

work. It is difficult to measure flow rates that change very fast. A positive displacement flowmeter available for this study has a large inertia that would completely alter any dynamic response being measured. This could be mitigated by including a model of the flowmeter in the simulation process, but adds several additional unknown parameters to the model. Flowmeters with a 1 ms response time are available on the market. (Senso Control SCQ flow transducer from Parker Hannifin [Cataloge (d)].) Pressure transducers (25 and 40 MPa range respectively) were obtained. Their use and calibration discussed in annexure A4.1.

4.3 90 LPM Test bench

The 90 LPM test bench has two 30 kW electric motors with variable flow radial piston pumps. Both are capable of delivering 45 LPM at 30 MPa maximum. These pumps are controlled individually for flow and pressure by proportional solenoid valves. The valves have PID controllers applying a pulse width modulated signal to the solenoid coils. LVDT sensors are used for feedback.

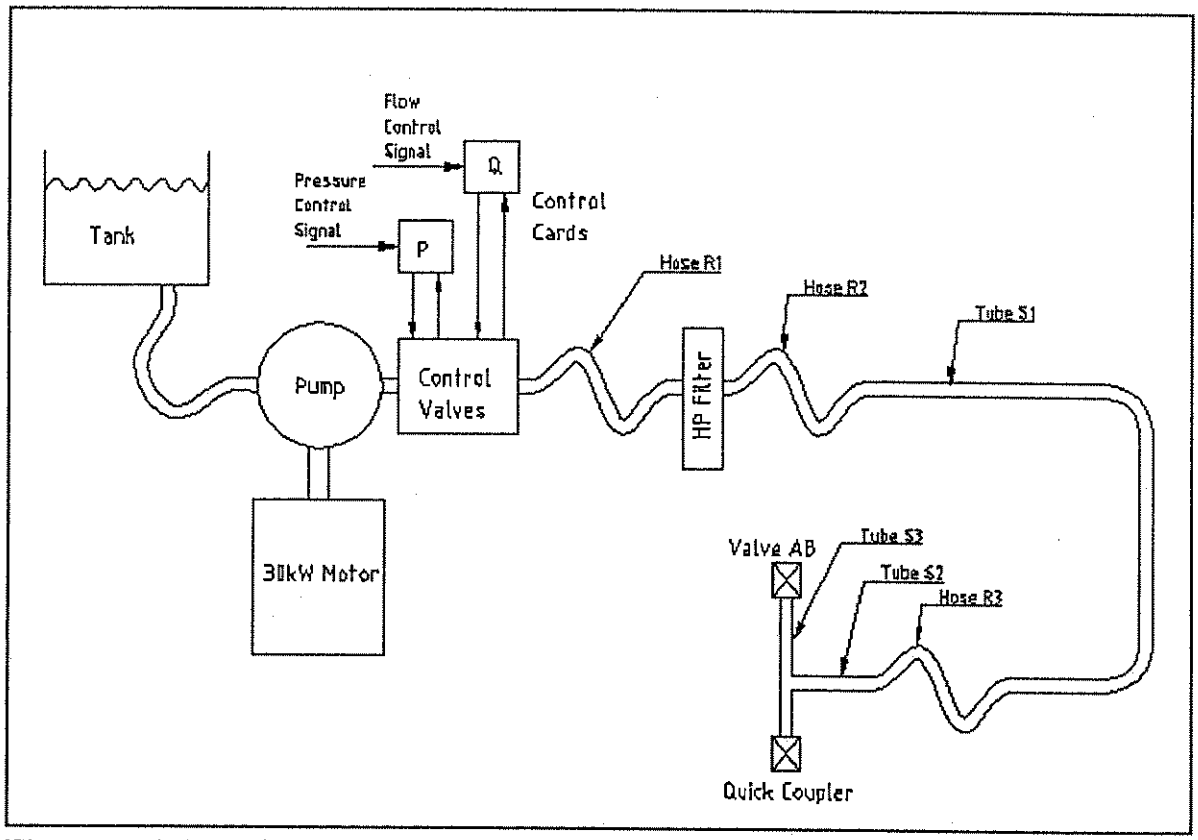

Figure 4.1 Schematic layout of one test-bench pump and supply hoses

The test bench principle of operation is simply that the maximum flow and pressure delivered by the pumps can be set from the front console. These two functions operate independently. This means that either the flow or pressure will be limited, depending on the characteristics of the load. The pumps are connected to the user interface via rubber hoses and steel pipes (layout indicated in figure 4.1). At the user interface, a valve (indicated by valve AB in figure 4.1) can be used to allow separate or combined flow rates from pumps A and B. The large supply line volume and compressibility together with the test bench control valve dynamics have a marked effect on the dynamic behaviour of the test bench. In this study the effect of test bench control valves and pump stroke control was not taken into account. The supply line approximate lengths and volumes are indicated in annexure A4.2.4.

The test bench was in dire need of repair and upgrading in order to fulfill the tasks required and to provide future usefulness. Cleaning, repairing, upgrading and testing work done on the test bench is listed in annexure A4.2.1.

4.4 Drain line steady state pressure drop experiment

4.4.1 Purpose

After some initial experimentation it was found that the test bench drain line and quick coupler used to return oil to the tank, causes a high flow resistance. This impaired the valves' dynamic performance, since the actual pressure drop was now less than that required and also varied with flowrate. Furthermore, the long pipe length introduces a large oil mass that has to be accelerated. The drain line resistance was measured for future reference.

4.4.2 Experimental setup and method

The drain line (marked T1 on the test bench console) steady state resistance was measured by connecting the test bench supply line via a pressure transducer (annexure A4.1.1) to the return line. It is assumed that the drain line vents to atmospheric pressure in the reservoir tank. The test bench turbine flow meters (annexure A4.1.2.2) was used to measure the flow rate.

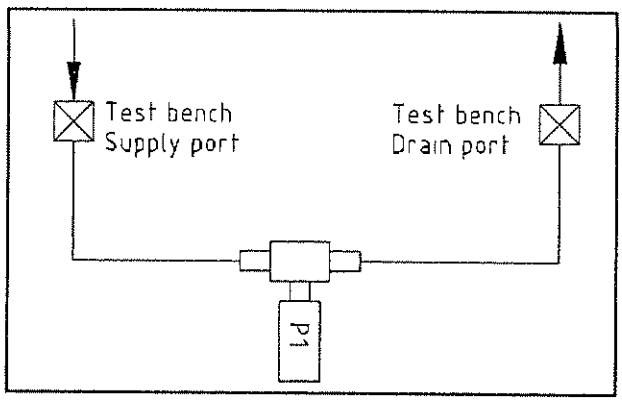

Figure 4.2 Experimental setup: Determining drain line resistance

4.4.3 Result and conclusion

The drain line resistance is shown in annexure A4.2.3, figure A4.2.2.

To overcome the problem of a high drain line resistance in subsequent experiments, a short, large diameter (0.5m long, 25 mm diameter) drain line was used to dump used oil directly into a 210 *l* drum placed next to the experimental setup (pumped back to the tank by a separate circulation pump, see photograph 7). This drastically reduced drain line resistance. The flow resistance due to the short drain line is visible in the measured and simulated results but the effect thereof on the valve dynamic performance is negligible. One uncertainty evolving from this setup is the possible buildup of air into the oil whereby the effective bulk modulus is drastically reduced. With the used oil dumping into the 210 *l* drum, and then being pumped back to the power pack reservoir separately, it is uncertain if the air would have been fully removed when it reaches the valve after passing through the test-bench. [Viersema n.d.]

4.5 Pilot valve (WSE3) steady state pressure drop experiment

4.5.1 Purpose

To determine the steady state pressure drop across the pilot valve thereby verifying against manufacturers data and obtaining the discharge coefficient parameters necessary in simulation work.

4.5.2 Experimental setup and method

The solenoid pilot valve is mounted in the manufactured test block named manifold-CSS (annexure A4.3.4 shows detail drawings) and connected to the test bench with the adaptor plate (annexure A4.3.6). This setup enables pressure transducers to be connected to all the pilot valve ports (X, Y and P) with flow introduced at any port and the valve switched. Note that the valve is only designed for flow from X to P and from P to Y. Pressure transducers (annexure A4.1.1) are connected to the CSS manifold block at the pressure tap points provided and the VS1 positive displacement flow meter (annexure A4.1.2.1) were used in the experiments. Fine tuning of flow rates were accomplished by the addition of a needle valve (manual adjustment).

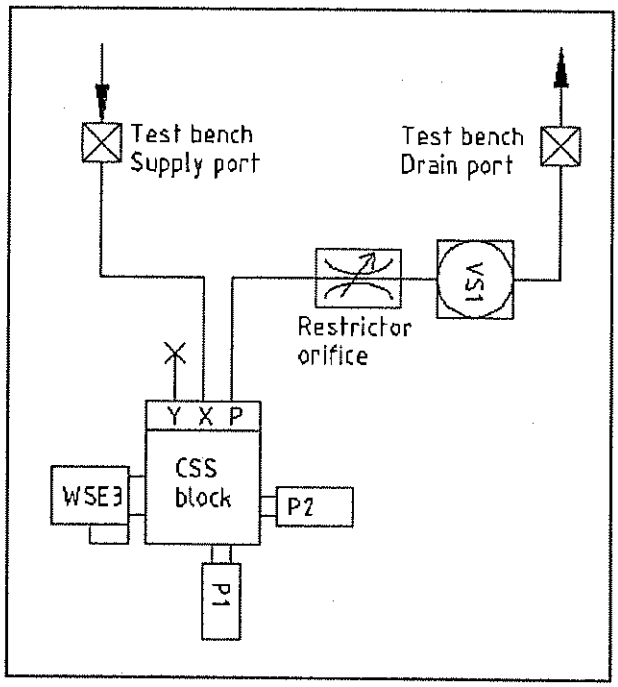

Figure 4.3 Experimental setup: Pilot valve steady state pressure drop

4.5.3 Result and conclusion

Pressure drop measurements are presented graphically in figures 4.4 And 4.5 below.

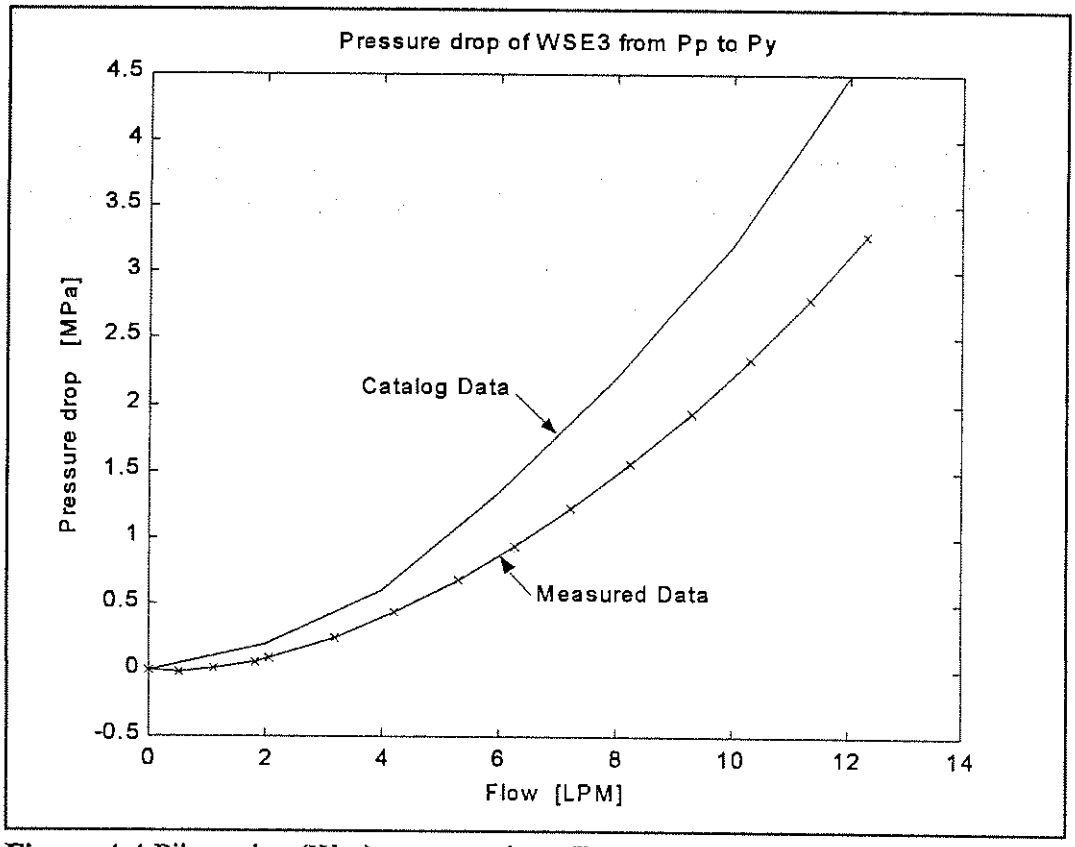

Figure 4.4 Pilot valve (Wse) pressure drop (P->Y)

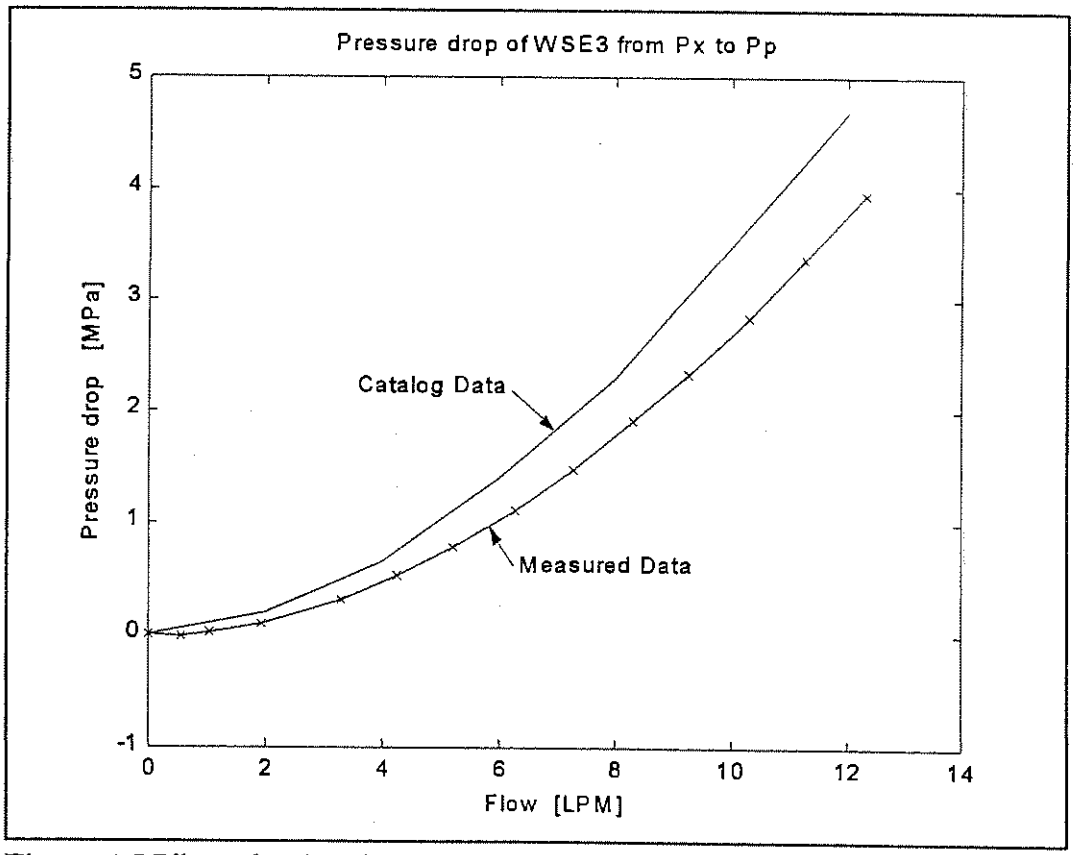

Figure 4.5 Pilot valve (Wse) pressure drop (X->P)

Since the measured pressure drop is lower than the manufacturer's curve, unaccounted flow resistance in the measuring setup does not seem likely for the error. Although the pressure transducers (250 MPa range) were calibrated, in this experiment they are used far below their total sensitivity, thereby decreasing the expected accuracy of the measurements. Venturi effects could influence the measured pressure drop since many T-junctions are present in the test-block and pressure transducer mountings. If the flow passes through non-straight passages, stagnation and recirculation zones with localised high and low pressure regions could affect the measured pressure difference. Effort was made to avoid such situations as far as possible. Different oil properties used in these experiments and the manufacturers experiments could further contribute to the error. It is accepted that the manufacturers curves are correct.

4.6 Check valve (CP108) steady state pressure drop experiment

4.6.1 Purpose

To determine the steady state pressure drop across the check valve thereby verifying against manufacturers data and obtaining the discharge coefficient parameters necessary in simulation work.

4.6.2 Experimental setup and method

A similar experimental setup were used as for determination of the pilot valve pressure drop. The CP108 valves are mounted in a custom valve block to allow easy fitment.

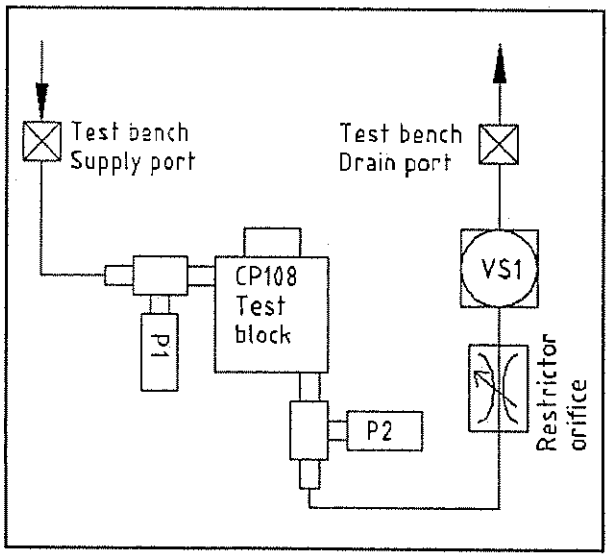

Figure 4.6 Experimental setup: Check valve steady state pressure drop

4.6.3 Result and conclusion

Figure 4.7 indicates measured results plotted against the manufacturers curve.

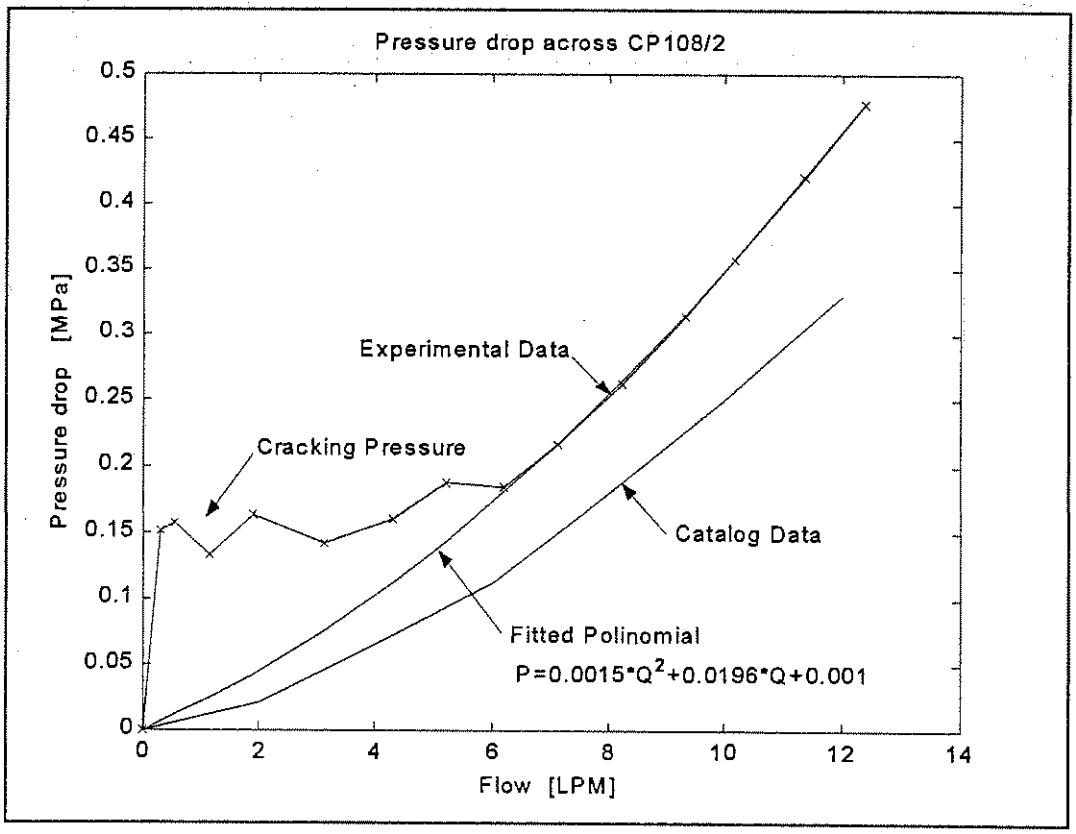

Figure 4.7 Check valve (CP108-2) pressure drop

The fact that the measured curve is higher than the manufacturer's curve suggests that some additional and unaccounted for flow resistance is present in this measurement. The experimental setup consisted of an aluminium block to house the check valves. To connect the pressure transducers, several adaptors and a T-piece on both sides was necessary (photograph 8). Since the pressure drop across the valve is very low, small additional restrictions could have a large effect on the total measured pressure drop. Another explanation could be that the manufacturers removed the spring from the check valve (since no cracking pressure is visible in their data). This could effectively lower the pressure drop. Other possibilities for the discrepancy are the same as mentioned in paragraph 4.3.1 (oil properties, venturi effects and inaccurate product data). A polynomial curve is fitted through the data. The very good correlation found, suggests that the expected physics of orifice flow are adhered to.

4.7 Logic element (LC 25) steady state pressure experiment

4.7.1 Purpose

Determination of steady state pressure drop values versus poppet height for the LC25 logic element to be used in model parameter adjustment and verification.

4.7.2 Experimental setup and method

The logic element is mounted in a valve block used for the fitment thereof parallel to the damper. Connecting plates and rubber hoses are used to connect this block to the test bench. The logic element could be controlled by the pilot valve, thereby switching flow supplied from the test bench. A stroke limiter is often used with logic elements to adjust the maximum allowable opening. A simple and inexpensive version of such a stroke limiter was manufactured using a threaded rod acting against the logic element poppet through a suitable cover plate (annexure A4.3.3). This stroke limiter was used to vary the poppet height setting in determining the pressure drop versus flow characteristics. Pressure transducers were connected to the measuring ports of the logic element valve block, with flow measured by the test bench turbine flow meters (annexure A4.1.2.2).

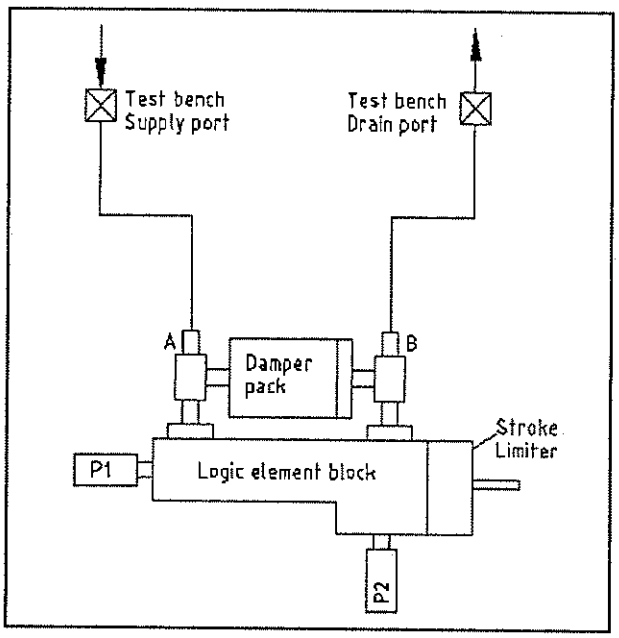

Figure 4.8 Experimental setup: Logic element steady state pressure drop versus poppet height

4.7.3 Result and conclusion

Only some data points at varying conditions were taken manually within the limited test-bench range (90 LPM). AMESim was also used for a numerical version of the same experiment. The AMESim 3D graph was correlated with the experimental data in order to calibrate the model orifice parameters. Excellent correlation was found. Attempting to show this correlation would

require many zoomed views and is therefore omitted. Figure 4.9 shows a three-dimensional view, and figure 4.10 shows a two-dimensional zoomed view with selected valve openings.

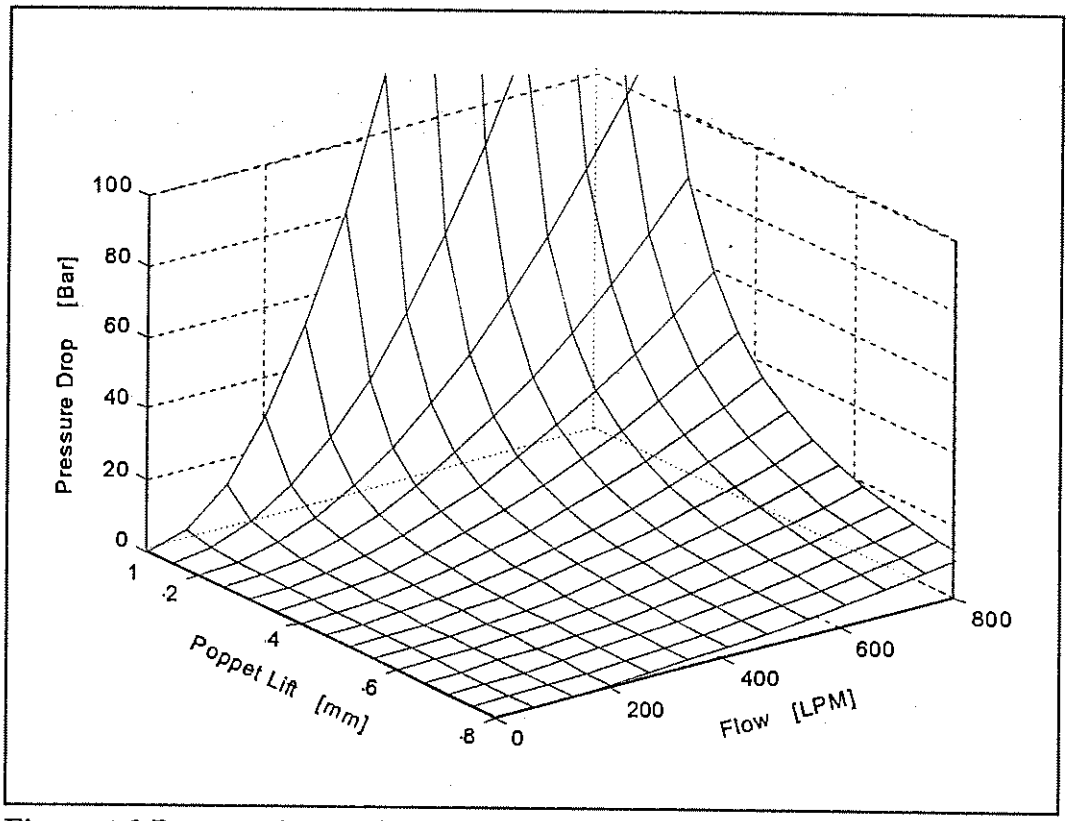

Figure 4.9 Pressure drop vs flow and poppet height for the logic element (LC 25)

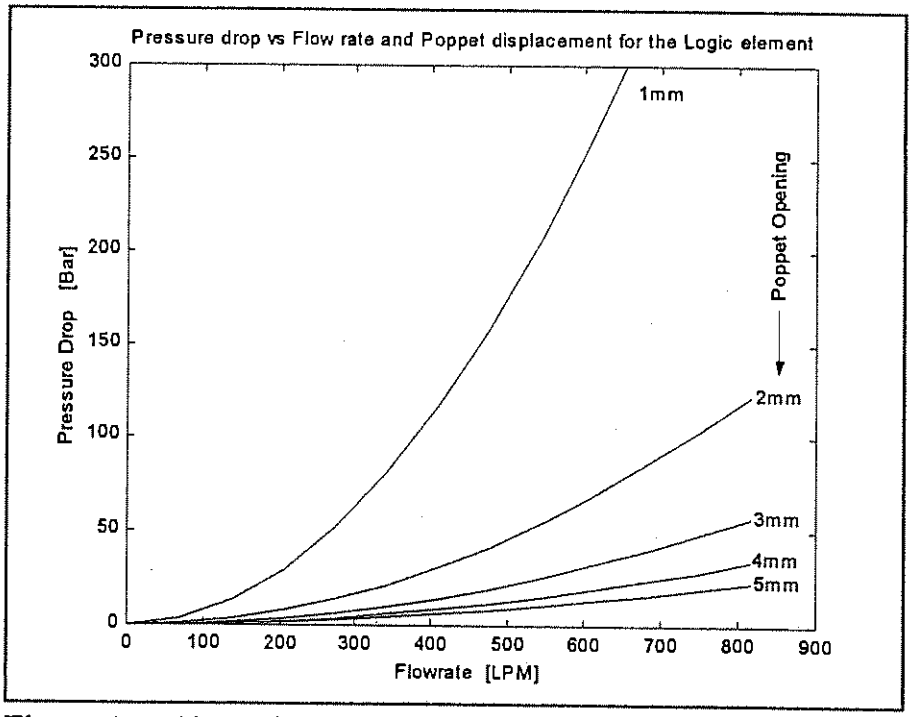

Figure 4.10 Alternative pressure drop vs flow and poppet height for the logic element (LC 25) - Created with AMESim

4.8 Damper pack steady state pressure drop experiment

4.8.1 Purpose

The damper pack was not included in the original experimental planning. Problems with the dynamic measurements prompted its use (a detailed discussion follows in paragraph 4.10). Detail knowledge of the damper pack characteristics are needed in the mathematical models.

4.8.2 Experimental setup and method

The damper pack is a standard Ratel armoured personnel carrier linear damper valve mounted in in a steel casing. This enables any oil flow through the damper pack to behave similar to oil flowing through a conventional passive damper. The damper pack was manufactured to provide damping in the Giliomee & Els (1998) hydropneumatic system. Since passive dampers have different characteristics in the two directions, care must be taken to specify the flow direction. The damper pack casing has a bolt-on cover on one side and a solid metal side at the other end. The direction is therefore specified by indicating flow as 'solid to cover' or as 'cover to solid'. Pressure drop was measured by connecting the pressure transducers to the logic element valve block, that was in turn connected in parallel to the damper pack. With the logic element closed, the pressure transducers are subject to the pressure drop across the damper pack.

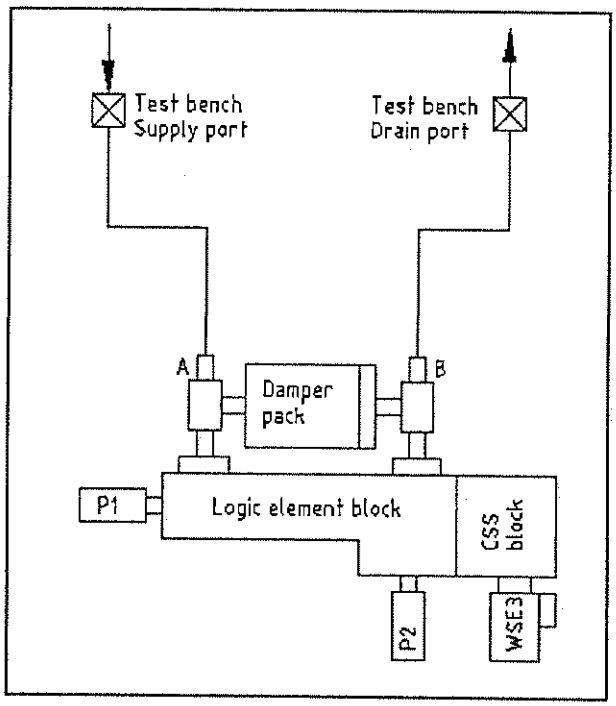

Figure 4.11 Experimental setup: Damper pack steady state pressure drop. (Logic element closed)

4.8.3 Result and conclusion

The characteristic curve of the damper pack was measured for inclusion in the mathematical models. It is shown in figure 4.12.

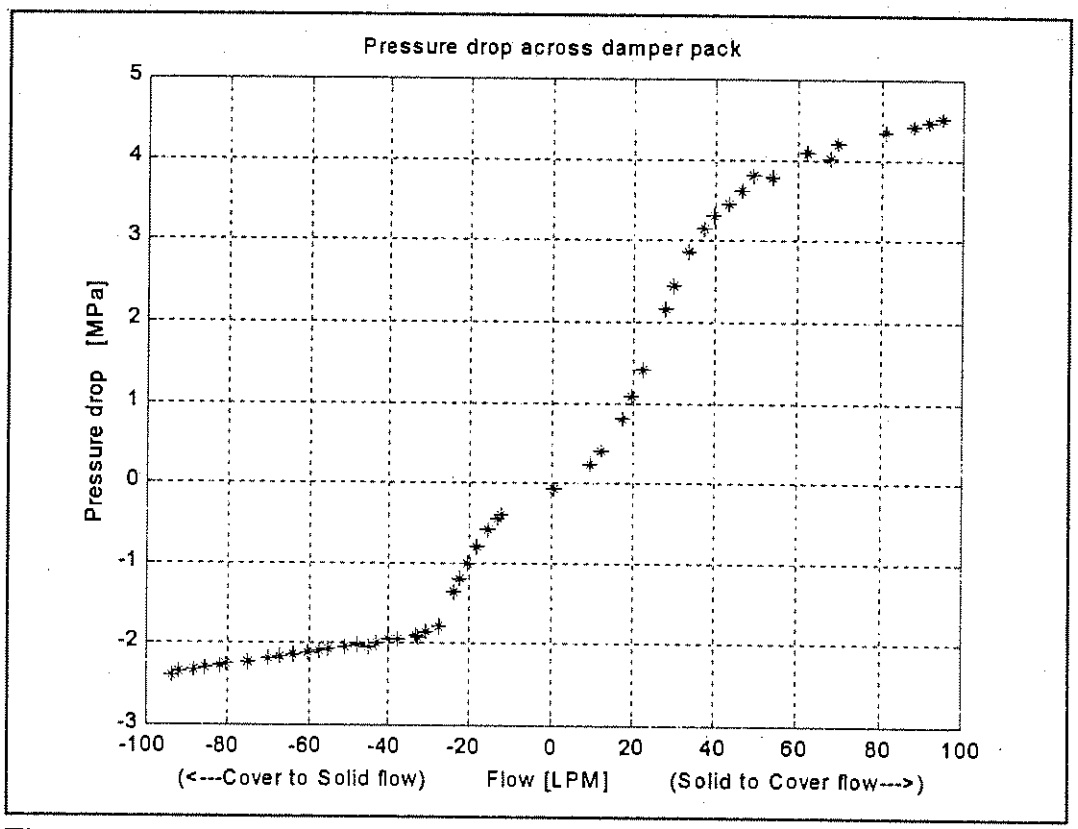

Figure 4.12 Damper pack steady state pressure drop characteristic

4.9 Pilot valve (WSE 3) dynamic response experiment

4.9.1 Purpose

In order to reduce the initial model complexity, separate models of the pilot valve and valve system were constructed. Separate experimental results were therefore required for correlating pilot valve models.

4.9.2 Experimental setup and method

Experiments were conducted by setting a maximum flowrate through the valve in accordance with the valve specification for safe operation. The system was left to obtain equilibrium and the solenoid was switched with a debounce circuit (A debounce circuit provides a sharp voltage step input by filtering out the switch dynamics. Its circuit diagram is shown in annexure A4.1.4). The pressure in front of and behind the valve was measured during the switching period at a sample rate of 1000 Hz.

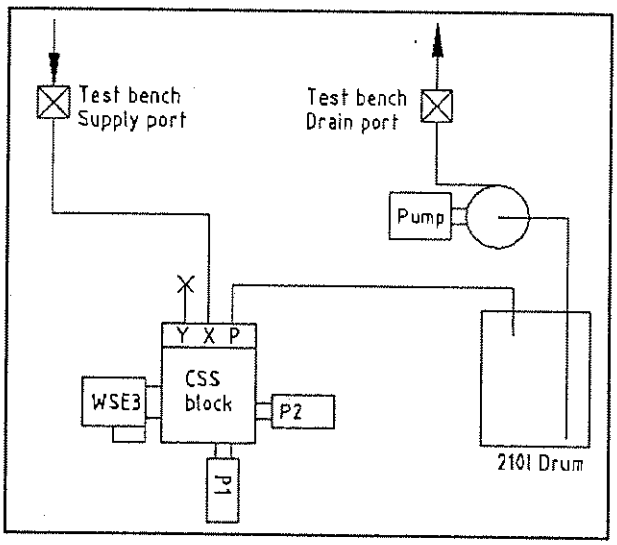

Figure 4.13 Experimental setup: Dynamic measurement of pilot valve response

4.9.3 Result and conclusion

Note (from figure 4.14 and 4.15) the apparently long time delay of 0.5 to1.5 s for a valve of this type. Many similar experimental runs were conducted, but presentation thereof would be unpractical.

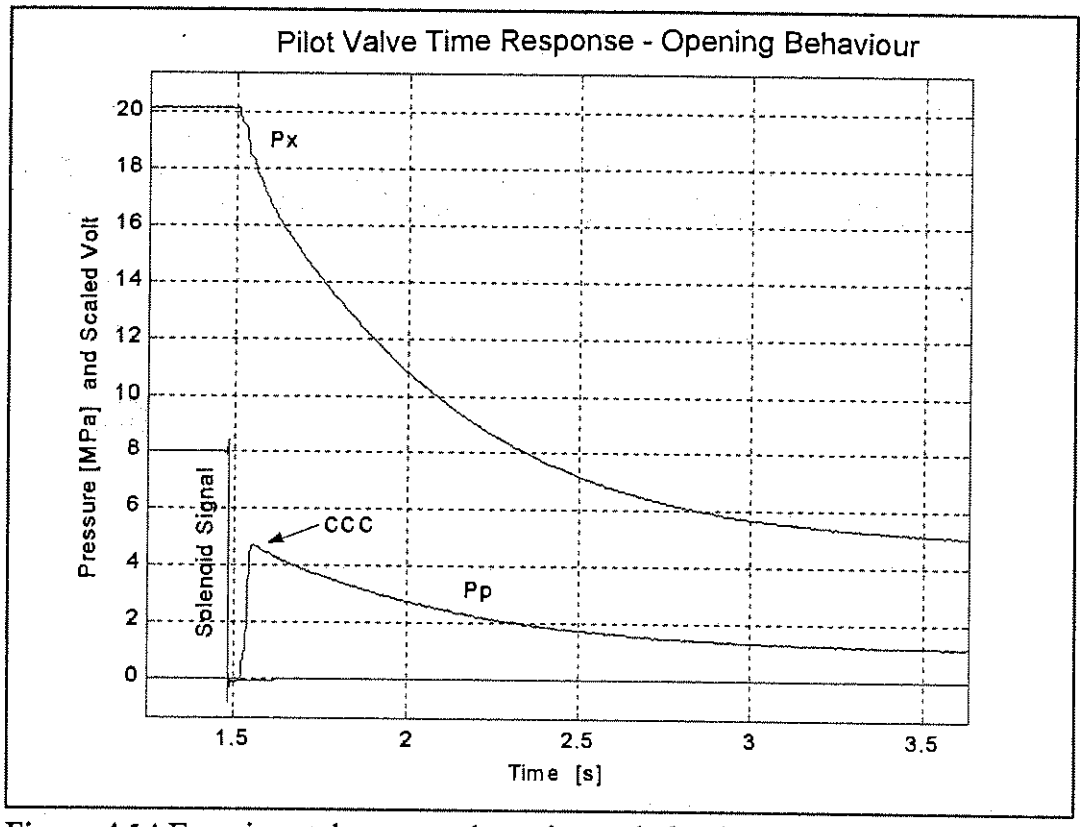

Figure 4.14 Experimental pressure dynamic trends for the pilot valve

Careful analysis of the data shows that the closing (i.e. from open to closed) behaviour measured is highly dependent on the test bench behaviour. With the valve closed the oil in the test-bench supply line leading to the valve was compressed to the maximum pressure set by the control system (the volume is calculated in annexure 4.2.4 to be approximately 13 *l*). The valve has very small ports compared to the test-bench supply line. When opened, the compressed volume of oil takes some time to drain through the pilot valve. This totally alters the measured time-delay. Similarly, when the valve closes, some time is needed to bring the supply pipe pressure up to the set value. As mentioned in chapter 3, compensation was made for this in the mathematical models by including the long test-bench supply lines.

In figure 4.15 the point marked 'AAA' indicates that the test-bench control system gradually restores the pressure in the supply line in an underdamped fashion. Data analysis shows the time taken from electrical signal input to the point where the pressure is restored (indicated as 'PBUT' in figure 4.15) versus the change in pressure required (indicated as 'pressure buildup demand' in figure 4.15) has a linear behaviour (shown in figure 4.10). This time taken to restore the pressure in the supply line is termed Pressure Build Up Time for the purposes of this study (PBUT). For the pilot valve experiments, the flow was limited to 12 LPM, thereby further extending the pressure build up time.

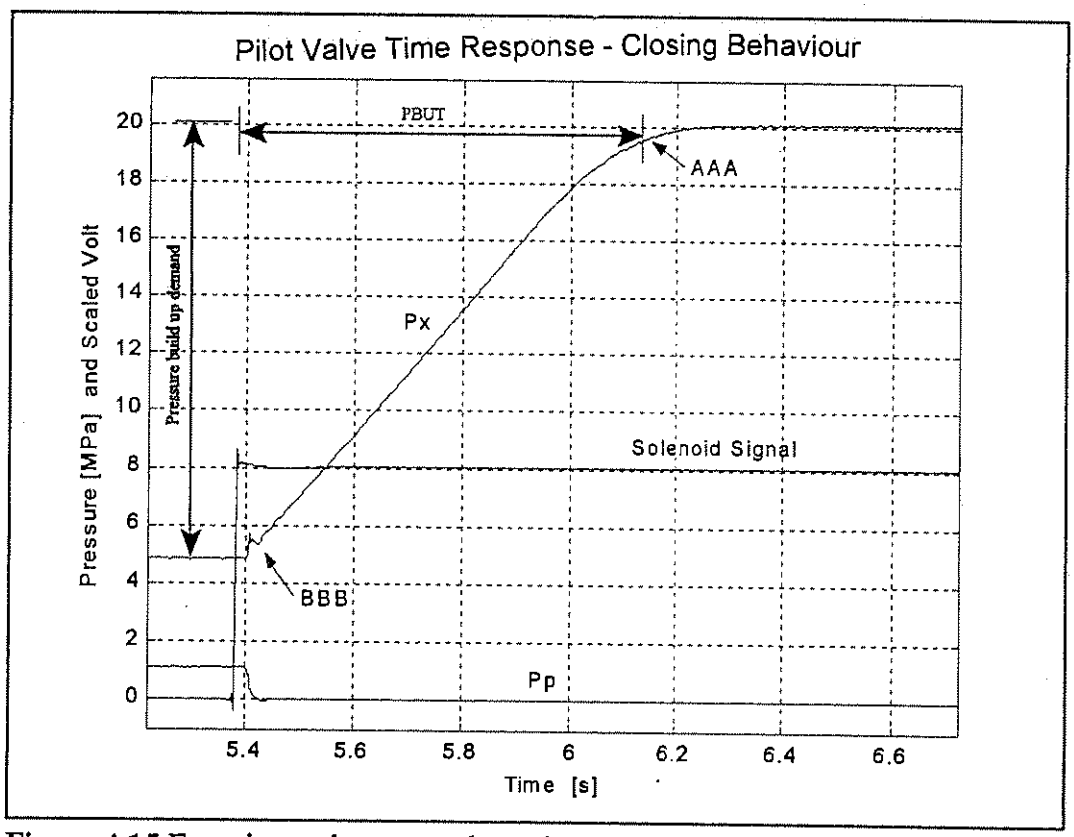

Figure 4.15 Experimental pressure dynamic trends for the pilot valve

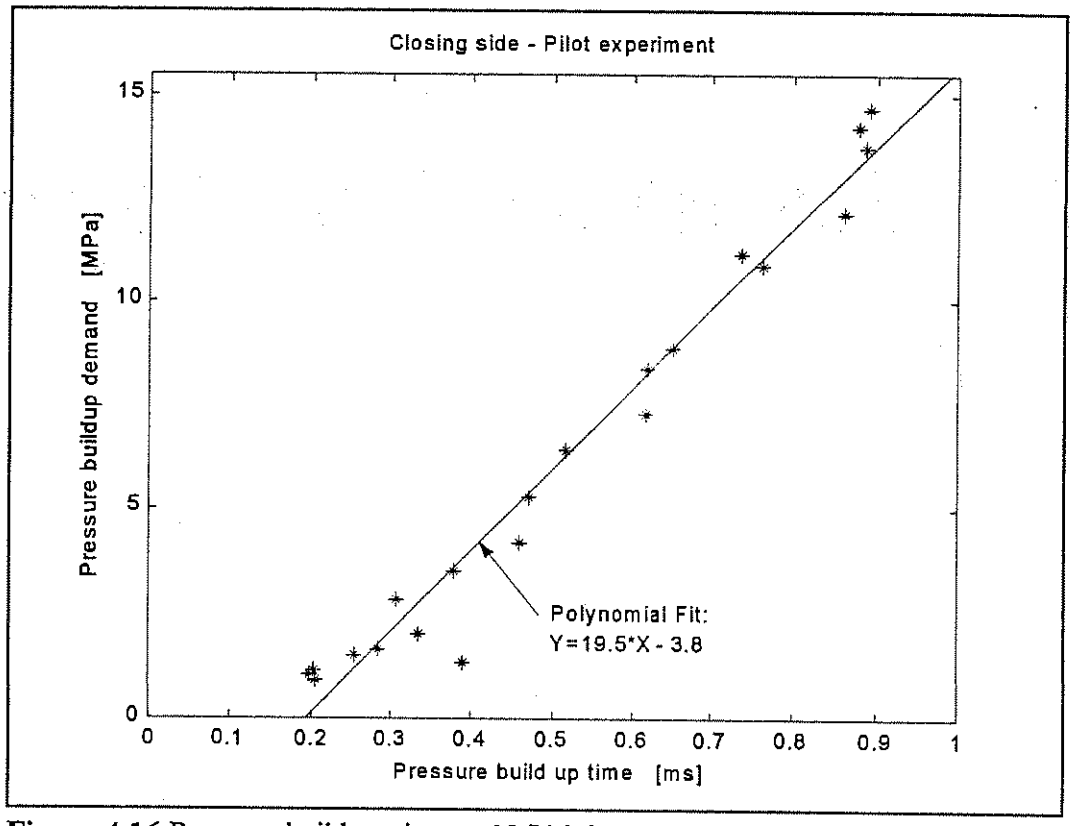

Figure 4.16 Pressure build up time at 12 LPM

Note that the pressure build up time is a function of the test bench dynamics, the test bench flow setting and the mounted valve since a certain portion of the flow required to restore the line pressure is escaping through the valve, while it closes. The curve can therefore not be used as a test bench step input characterisation.

Detailed analysis of the experimental data will be conducted in chapter 5.

4.10 Valve block assembly dynamic response experiment

4.10.1 Purpose

To obtain dynamic performance data with which to verify mathematical models.

4.10.2 Experimental setup and method

This experiment was conducted with two different manifold blocks mounted on the logic element. The original "WSE manifold" as used on the valve system in its vehicle mounted configuration and the new "CSS manifold" that contain a poppet displacement transducer for the logic element and several pressure measuring ports were used. The 'CSS' manifold block was manufactured and used in experiments to allow for the measurement of the poppet displacement and logic element control chamber pressure, providing more data for model verification. A comparison of the physical differences between the old (original manifold) and new (manifold CSS) block is given in annexure A4.3, with a detailed drawing of the block. Initially the experiments were conducted without the damper pack. The reason for its fitment will be explained in paragraph 4.10.3.

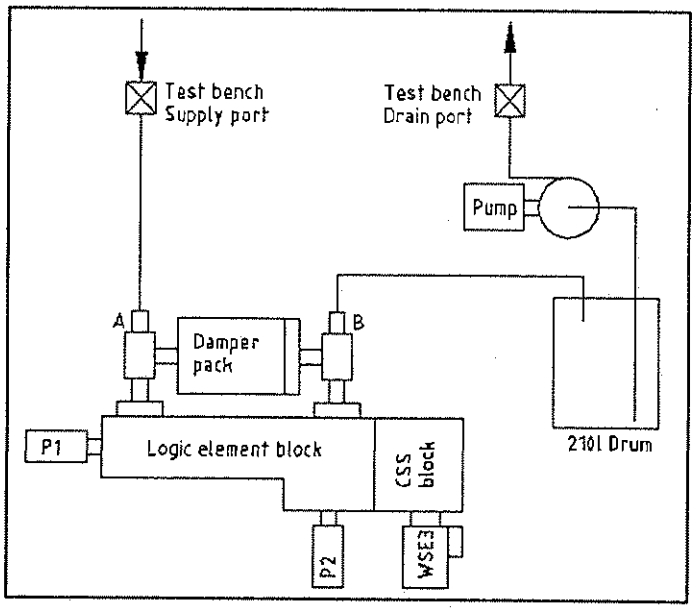

Figure 4.17 Experimental setup: dynamic measurement of valve system response

4.10.3 Result and conclusion

During testing the valve system started to oscillate due to an initially unknown reason. This entailed a relative high frequency stutter in the valve, with corresponding flow and pressure oscillations. From noise and vibration one could determine that the logic element poppet was oscillating up and down. With certain flow rates the poppet oscillated enough to touch its seat. The problem was so serious that damage to the test bench could result. What is even more inexplicable is the fact that the valve system showed the oscillatory behaviour on random occasions. (Both times with exactly the same configuration.) The Rexroth Hydraulic trainer on

logic elements [Schmitt & Lang 1998] briefly mentions a phenomenon called *fluttering*, that could be related. Many reasons for this problem were hypothesized and investigated such as mechanical damage in the experimental setup, trapped air pockets, experimental configurations, test-bench resonance and control system problems. One attempt at removing the oscillatory behaviour was the fitment of a damper pack parallel to the valve system. The damper pack construction was explained in paragraph 4.8.2. The motivation for fitting the damper pack was to allow continuous flow delivery from the test bench pumps, thereby reducing the step response requirements on the test bench. However, the additional flow only mildly reduced the oscillation amplitude. All following reference given to 'valve system' indicates the presence of the damper pack.

A frequency analysis (FFT) was conducted on the measured oscillatory displacement data. The time domain displacement trend showed violent transient behaviour before it stabilised at a frequency close to the electrical main's 50 Hz. (See figure 4.18) Investigation revealed that the solenoid signal is not affected by the 50Hz signal and had a smooth DC stabilised value. The possibility of a defective power supply causing some form of solenoid dynamics was therefore ruled out. The only other electrical influence remaining on the system was via the test-bench control cards. However, if the test-bench control system was defective, the oscillation would be visible in all the experiments, including steady state experiments. Since the oscillatory data was clearly centred around 47Hz and the electrical mains are known to be very accurately controlled around 50Hz it could be reasoned that the oscillations were not related to the electrical supply signal. A typical example of the oscillatory experimental behaviour is shown in figure 4.19.

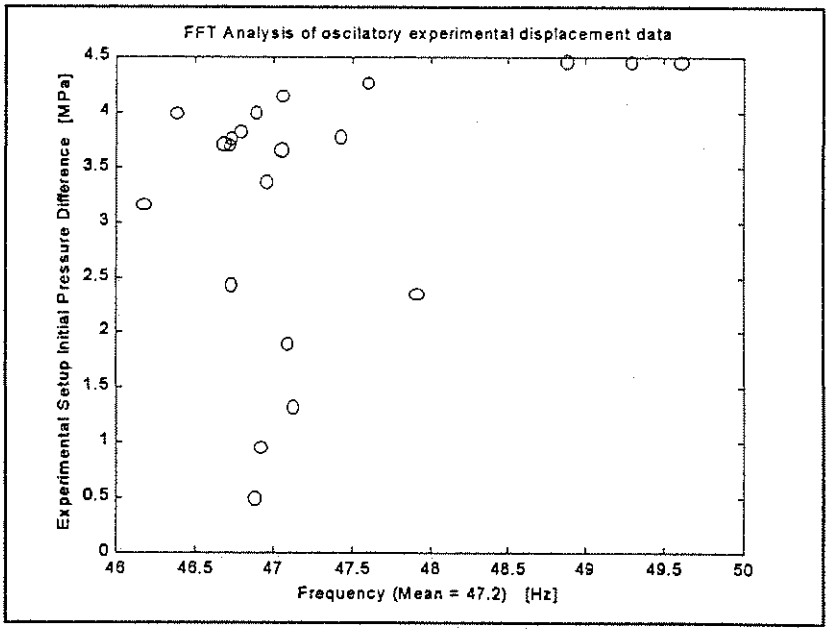

Figure 4.18 Frequency analysis of oscillatory displacement data for the valve system experiments

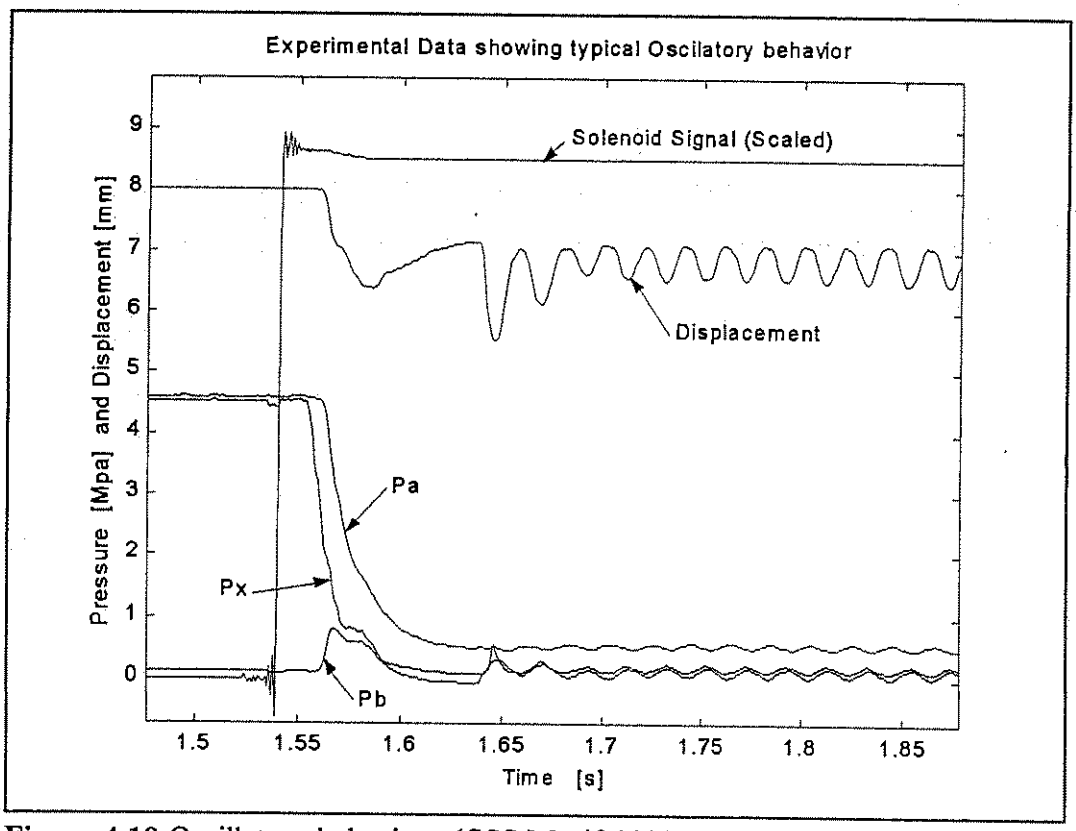

Figure 4.19 Oscillatory behaviour (CSS Manifold block)

Since the oscillations were of high magnitude (especially for the displacement), the mean steady state value thereof was used to determine the 5% and 95% values. The oscillations could, however, have the effect of changing the mean steady state values, mainly as a result of the cracking pressures in the check valves acting as a pump system. A simple experiment was conducted to verify the use of the mean steady state values with the following logic:

- The pressures in the open and closed valve positions are known.
- The total flow passes through the damper in the closed valve position.
- With the damper curve (figure 4.12), the total flow from the test-bench can therefore be calculated.
- In the open valve position, the pressure and damper curve can be used to calculate the flow through the valve by subtracting the new damper flow from the total flow.
- From simulation and experimentation, the logic element flow vs pressure drop for various poppet lifts are known (figure 4.10).
- From this graph (repeated and adapted in the figure below) it can be seen that the expected poppet position is approximately 1.2mm.
- This is close to the mean steady state value of the oscillatory displacement data of figure 4.19.

Therefore it was assumed that oscillations do not influence the valve poppet steady state position.

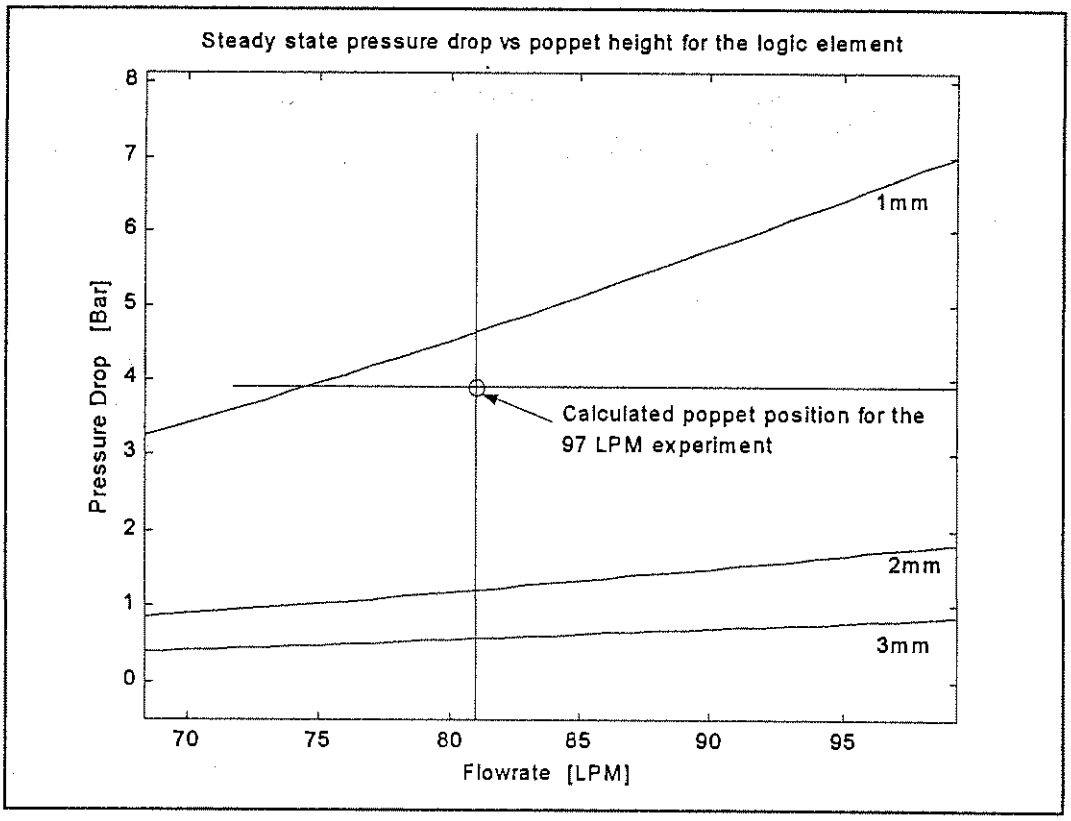

Figure 4.20 Determination of steady state displacement values for the valve system. (Zoomed view of figure 4.10)

It was also observed that the oscillation was a secondary effect and that the presence thereof did not disturb the overall response of interest in this study. Data containing oscillations was not discarded but simply treated with care. As a further indication that this was a valid conclusion, two non-oscillatory and two oscillatory data sets were compared (figure 4.21).

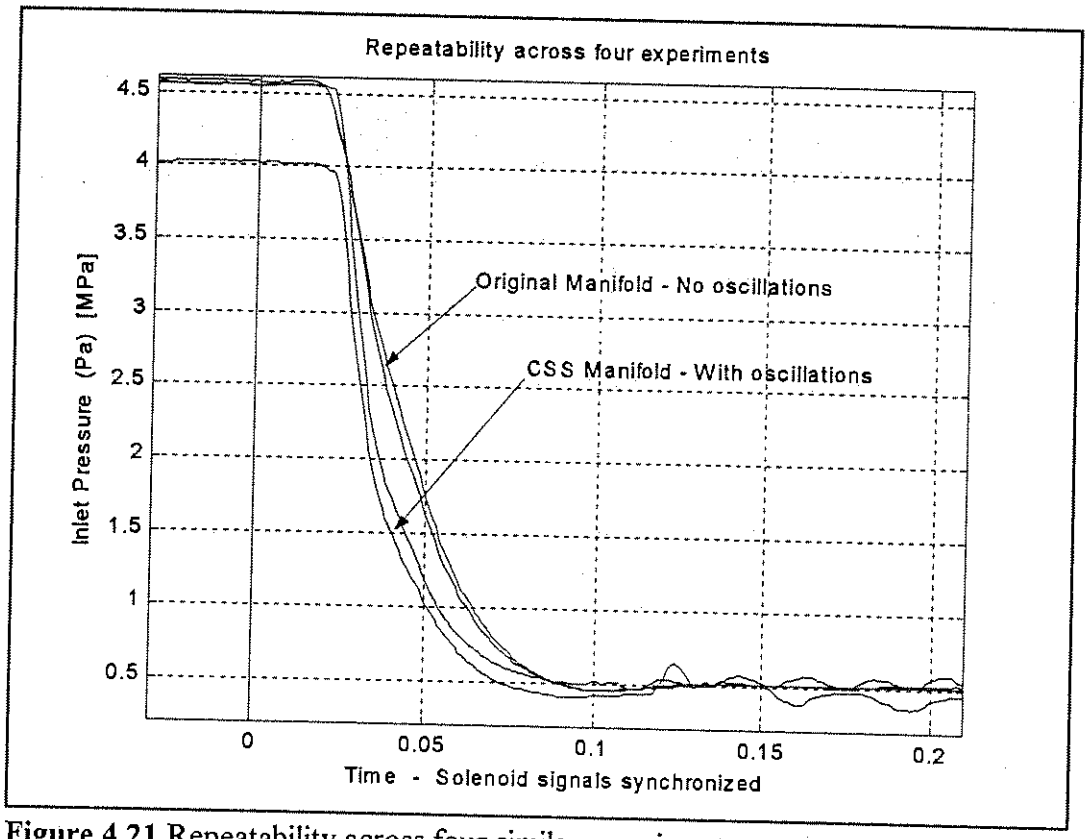

Figure 4.21 Repeatability across four similar experiments

Two important correlations can be seen from the above graph.

- There is good correlation between separate runs. Even with some slightly different initial conditions for the two oscillatory runs, correlation can still be seen.
- There is no major difference between the oscillatory and non oscillatory runs. The slight discrepancy was to be expected since two different experimental setups were used to obtain them. The non-oscillatory behaviour was measured with the original WSE manifold block that contains protection orifices and much less flow resistance than the CSS manifold block used to measure the oscillatory data in this specific figure.

The mean steady state value is a suitable parameter to use in calculating the 5% and 95% values of the displacement thereby allowing direct comparison of the model results with experimental data.

5 Results

In this chapter the results obtained from the AMESim models are evaluated against the experimental results. This allows validation of the modelling technique and adjustment of certain model parameters. Evaluation of the MATLAB system model is done in annexure A5.1.

5.1 Overview

To correlate the pilot valve and system with damper models, time domain dynamic pressure and displacement trends are superimposed. This is done for the opening and closing behaviour of the valve and at two different operating points (e.g. in figure 5.1). This ensures that the parameters affecting the dynamic performance are matched over a range of operation. It is furthermore not feasible to show all the data sets generated. With the models and experiments varied flow or pressure settings were introduced to cover the whole operating range of the valve or its subsystems to the extent of the test bench capability. Each of these settings constitute typically an 8 second time domain trend containing an opening and closure behaviour, with several variables monitored. These time domain dynamic performance graphs give an overview of the dynamic correlation of the models with experiment, but fail to show a quick overview of the time delay of the valve across the range of operating points.

To create a more elegant method of showing the time delay trend for a system, two data points of interest can be defined on the dynamic time domain trend of a state variable under consideration. After the switching signal is given, an initial (or base) delay occurs. During this period the solenoid saturates and little or no change in the value of the state variable is observed. Thereafter, the mechanical elements start activation and the state variable changes to its final value (at the final delay time). The base and final delay times are defined at 5% and 95% of the respective steady state values. When oscillatory behaviour is present, the steady state value is taken as the median of the oscillations. A problem arising was the asymptotic behaviour of some transients, creating the effect that the calculated 5% or 95% point is highly sensitive to small changes in the transient behaviour. This effect can create the illusion that two transients with similar dynamics have vastly different delay values.

Annexure A3.3.28 shows the MATLAB implementation of a function used to determine the 5% and 95% values. In the figures the abbreviations AME, MAT and EXP are used to indicate the AMESim, MATLAB and Experimental trends respectively.

Since this chapter contains many graphs it is valuable to have an overview thereof.:

- **Model:** Pilot valve (paragraph 3.7 and paragraph 4.9)
  - Figure 5.1: Opening behaviour, 10MPa
  - Figure 5.2: Closing behaviour, 10MPa
  - Figure 5.3: Zoomed view of figure 5.2
  - Figure 5.4: Opening behaviour, 20MPa
  - Figure 5.5: Closing behaviour, 20MPa
  - Figure 5.6: Correlation: Exp peak, and model trends
  - Figure 5.7: Delay trends: Opening
  - Figure 5.8: Delay trends: Closing
- **Model:** System with damper (paragraph 3.9 and paragraph 4.10)
  - Figure 5.9: Opening behaviour, 22LPM - Pa & x
  - Figure 5.10: Closing behaviour, 22LPM - Pp
  - Figure 5.11: Opening behaviour, 97LPM - Pa & x
  - Figure 5.12: Closing behaviour, 97LPM - Pp
  - Figure 5.13: Delay trends: Displacement
  - Figure 5.14: Delay trends: Pressure

5.2 Model validation: Pilot valve

As was explained in chapter one, the pilot valve uses a solenoid to activate a spherical poppet which in turn allows oil flow to switch between two possible paths. The valve contains a pressure compensating chamber aiming to reduce the effects of a high inlet pressure on the force required from the solenoid to accelerate the poppet.

The valve is investigated separately from the main valve system in order to reduce initial model complexity. Unfortunately the test bench dynamics obscured the pilot valve dynamics and it was difficult to extract the necessary data for use in correlation. The AMESim model shows acceptable correlation with experiment, although the delay trends obtained from the response data do not correlate well with the corresponding experimental values. In this regard it should be remembered that the models use approximations for some of the physics involved (e.g. solenoid magnetic circuit, flow force calculation and effective flow area) and therefore a better correlation is unforeseeable.

The layout of this paragraph consists of matching the AMESim, MATLAB and experimental work on the basis of four figures containing time trends. The experimental and AMESim trends are used to extract delay trends for the valve in question. MATLAB results are not used for this purpose.

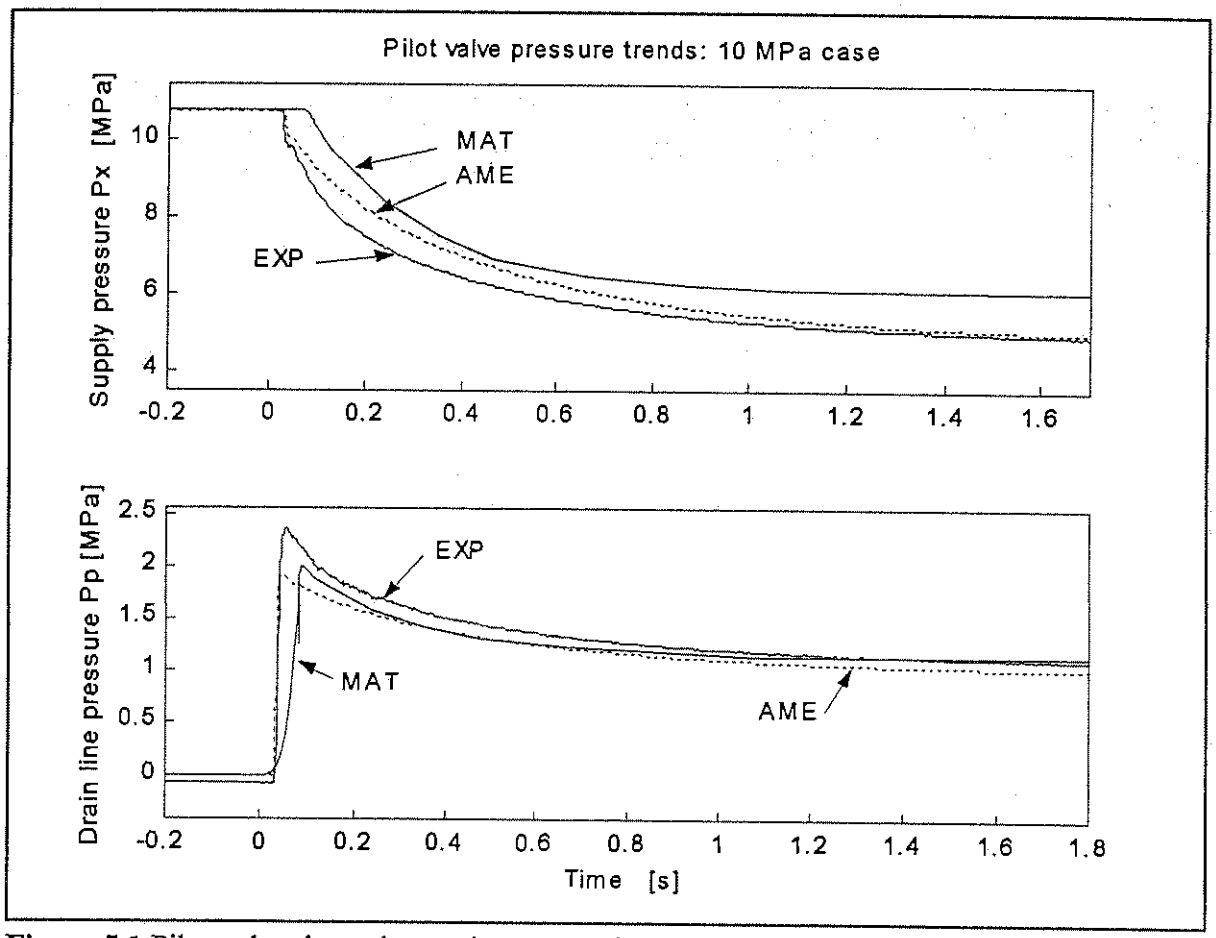

Figure 5.1 Pilot valve dynamic transients: experiment, AMESim and MATLAB results - Opening behaviour

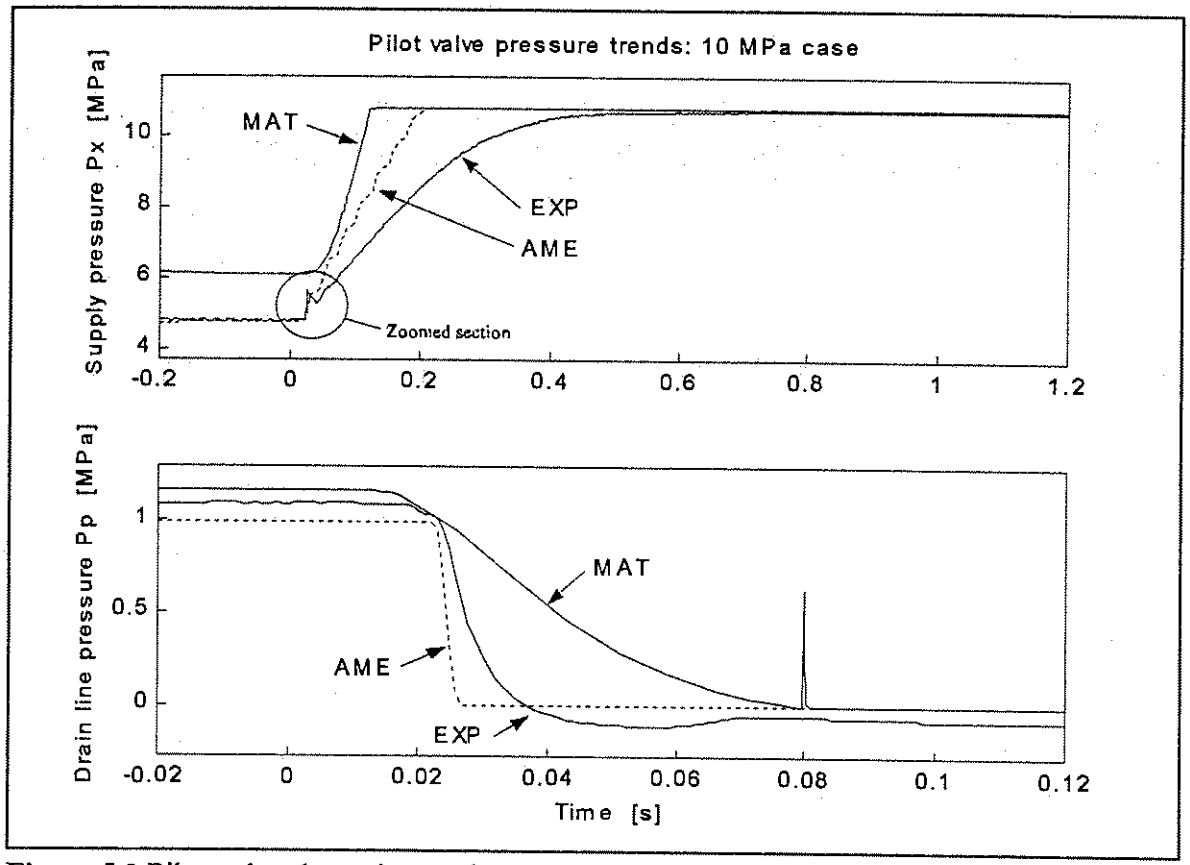

Figure 5.2 Pilot valve dynamic transients: experiment, AMESim and MATLAB results - Closing behaviour. Zoomed section indicated in figure 5.3.

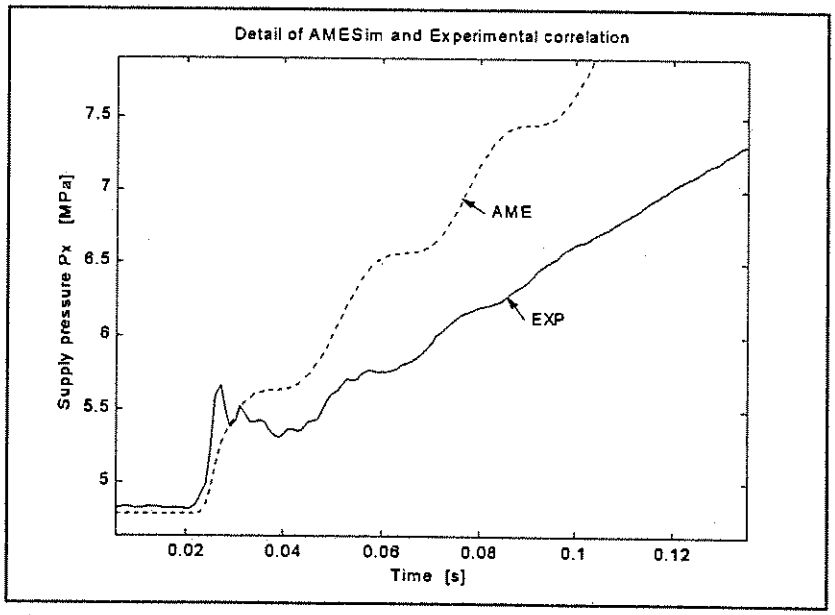

Figure 5.3 Zoomed view of figure 5.2

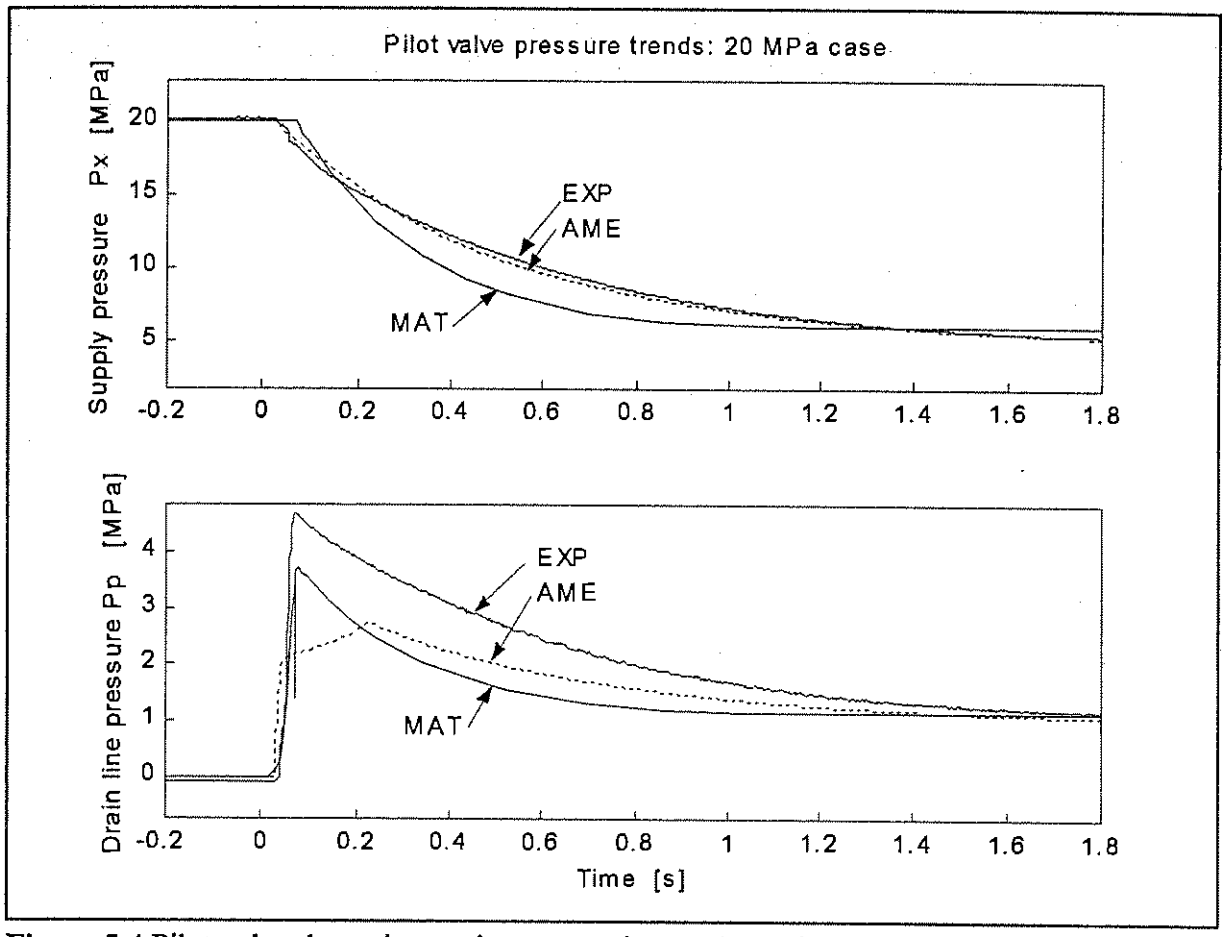

Figure 5.4 Pilot valve dynamic transients: experiment, AMESim and MATLAB results - Opening behaviour

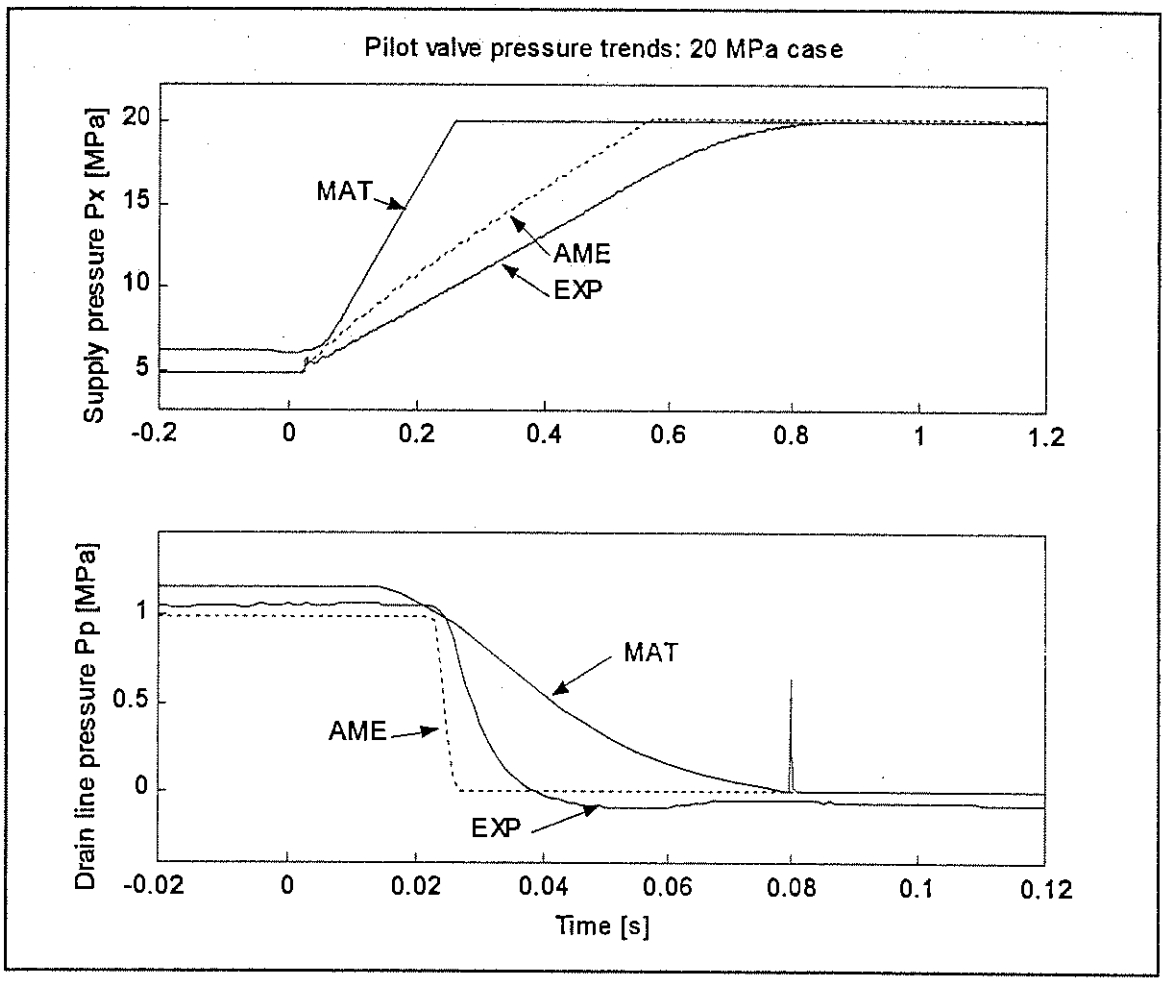

Figure 5.5 Pilot valve dynamic transients: experiment, AMESim and MATLAB results - Closing behaviour

5.2.1 Model correlation with experiment

As explained in chapter 3, the valve model consists of a force balance equation from which poppet acceleration is calculated. In the AMESim model attempts are made to separate the flow losses (orifices) and fluid volumes according to their real physical layout. This adds many parameters and state variables (27 in total) to the set of equations. In the MATLAB model, these orifices and volumes are lumped in order to reduce the number of state variables to 5. Most of these fluid volumes are only necessary to model the test-bench supply line accurately.

In both the AMESim and MATLAB models, obtaining the right steady state values requires the correct balance in lumped flow resistance in front of, through and behind the valve and the correct pressure sensor position. This requires the adjustment of C_d and Re_{tr} values of several orifices. The adjustment of both C_d and Re_{tr} values creates the possibility that the steady state correlation can be reached at a certain flow rate, but differ at another flow rate. It should be noted that once it was discovered that the MATLAB model solver was inadequate, less attention was spent to obtain the right parameters for the model. With detailed experimental determination of the orifice parameters of each component in the experimental chain unfeasible, many hours and even days were spent to obtain improved parameters for the AMESim model. Measures such as two-dimensional optimisation fields were investigated to speed up the process, but were found to be unsuccessful, since many more dimensions are needed, in order for an optimisation process to be successful.

Governing equations with similar complexity as the AMESim model would easily be programable in MATLAB, but the numerical method used would be unable to solve them. The MATLAB results are shown only to indicate that the MATLAB model created does fall in the right region of dynamic response, even with the knowledge that the MATLAB model is highly simplified. The MATLAB solver incapability starts to show with a peak in the supply pressure (Pp) trend at 0.08s (figure 5.4). This is caused by numerical integration problems. Many attempts were made to enhance the MATLAB model by including more detailed sub-models and assumptions. Unfortunately, the current model seems to be on the limit of solver stability.

Another problem is the accumulation of experimental inaccuracies. The pressure sensors were used at a fraction of their total sensitivity. Flow induced phenomena such as stagnation and recirculation points may influence the measured values. This would be especially relevant in the steady state region, where close matches between model and experiment are expected.

The influence of the test-bench is clearly visible from the time domain dynamic response graphs. The trend suggests that the pilot valve takes about 0.5 to 1 s to close fully. As discussed in chapter 4, the test bench has a long and compliant supply line. This pipe is under pressure when the pilot valve is closed, causing additional oil to accumulate in it. This accumulation of oil takes a certain time, depending on the maximum pressure that the test bench must reach (especially since the flow is limited to 12 LPM). This is shown in the pressure build up graph in figure 4.16. Similarly, the valve has an apparent opening time of 0.5 to 1 s. When the valve opens, the oil accumulated in the supply pipe must drain through the small pilot valve orifice while oil is continuously being added to the supply line by the test bench.

In order to extract useful data from the experimental time domain dynamic response data, the

drain line pressure transient is used. The drain line vents to atmosphere, and provides only minor flow resistance. This resistance causes a pressure signal to be measured only if flow is present in the drain line. Other evidence indicating that the drain line pressure transient offers an accurate method of determining the valve response is the small peak in the supply pressure transient (Px) at around 0.03s (figure 5.3). This indicates the physical closure of the valve poppet since it correlates with zero flow in the drain line trend but does not provide a suitable method of determining the valve behaviour. In figure 5.6 this is clearly visible where scaled views of the experimental supply pressure Px, AMESim drain pressure Pp and AMESim poppet displacement trends are shown.

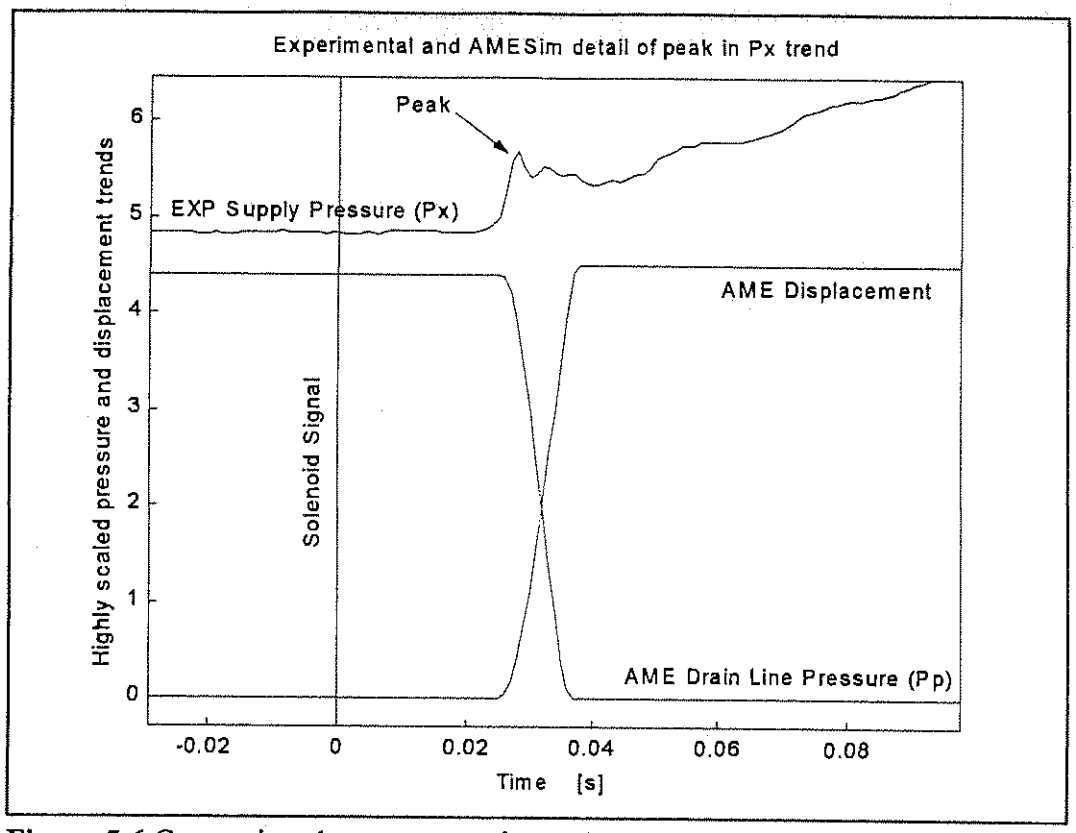

Figure 5.6 Comparison between experimental and AMESim trends

In AMESim the test bench is modelled as an ideal flow source and ideal relief valve coupled to a segmented supply pipe model. With this model it is not possible to account for test bench dynamics such as pump flow rate variation and the proportional throttle valve or relief valve dynamics. This can be seen from the comparison between model and experiment in figures 5.1 (opening behaviour) and 5.2 (closing behaviour). From these figures, the model and experimental supply pressure transients are matched for the opening case, but the experimental pressure lags slightly in the closing case (compared to the AMESim result). This indicates that the supply line model used can account only for some of the test-bench phenomena. By altering the supply line compliance, the model's response can be matched to the experimental opening or closing transient seperately. Ideally, the test bench dynamics should be incorporated into the model. An alternative

and more appropriate test setup might also be considered.

When the valve opens, a surge of oil causing a peak in the drain line pressure transient is visible. This is caused by the accumulated oil in the supply pipe escaping through the pilot valve, while at the same time the test bench attempts to re-establish the 12 LPM flow rate through the valve. This raises the question of how much the pressure forces acting on the valve poppet are affected by the test bench. To obtain an answer to this question would be to experiment with an ideal test bench or with accurate models of the valve and real test bench. In such a model the real test bench could be substituted with an ideal source and the difference observed.

Despite the inaccuracies of the models, it is encouraging that the AMESim model demonstrates the same oscillatory behaviour or high frequency dynamics as measured (figure 5.3). (Specifically the small peak in the pressure Px closing transient, at 0.03s)

5.2.2 Time delay data extracted

The 5% base delay and 95% final time delay data extracted from the experimental and AMESim model data is shown in figure 5.7 and 5.8 following.

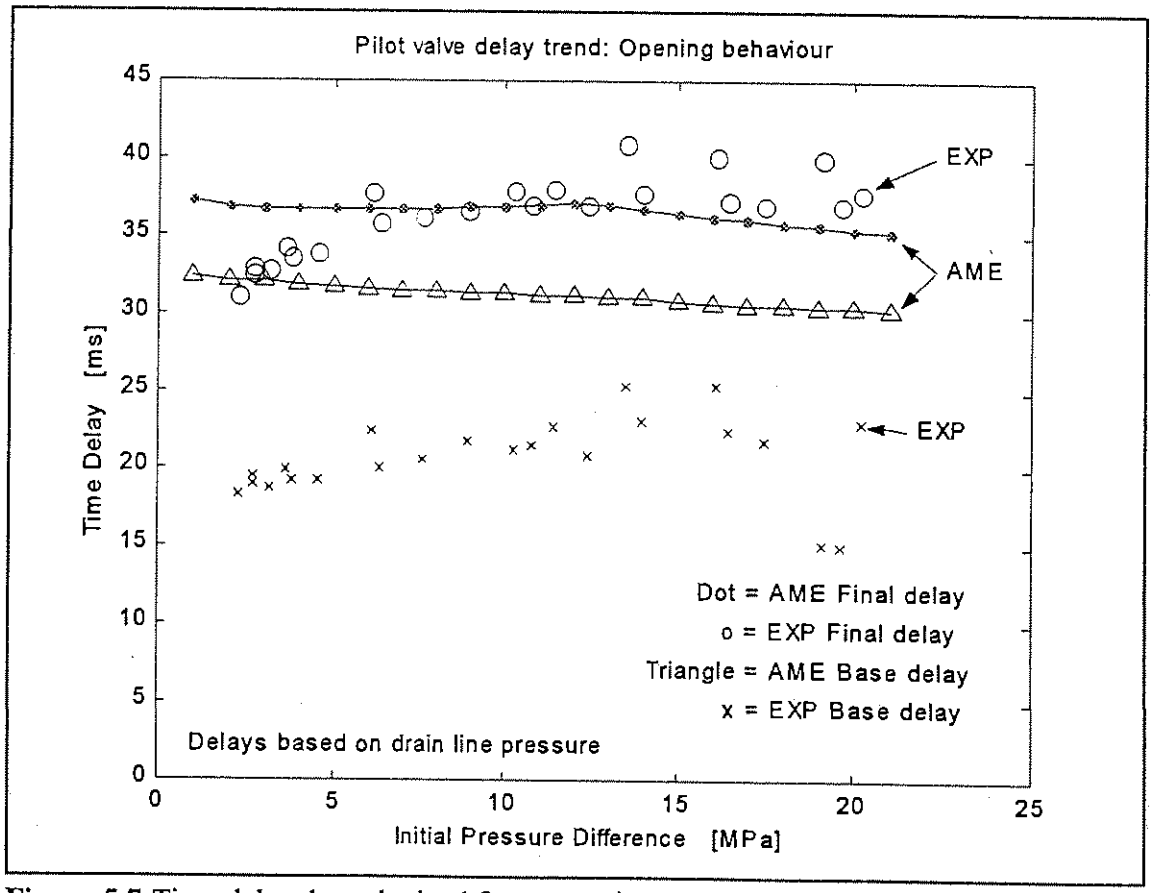

Figure 5.7 Time delay data obtained from experiments and the AMESim model

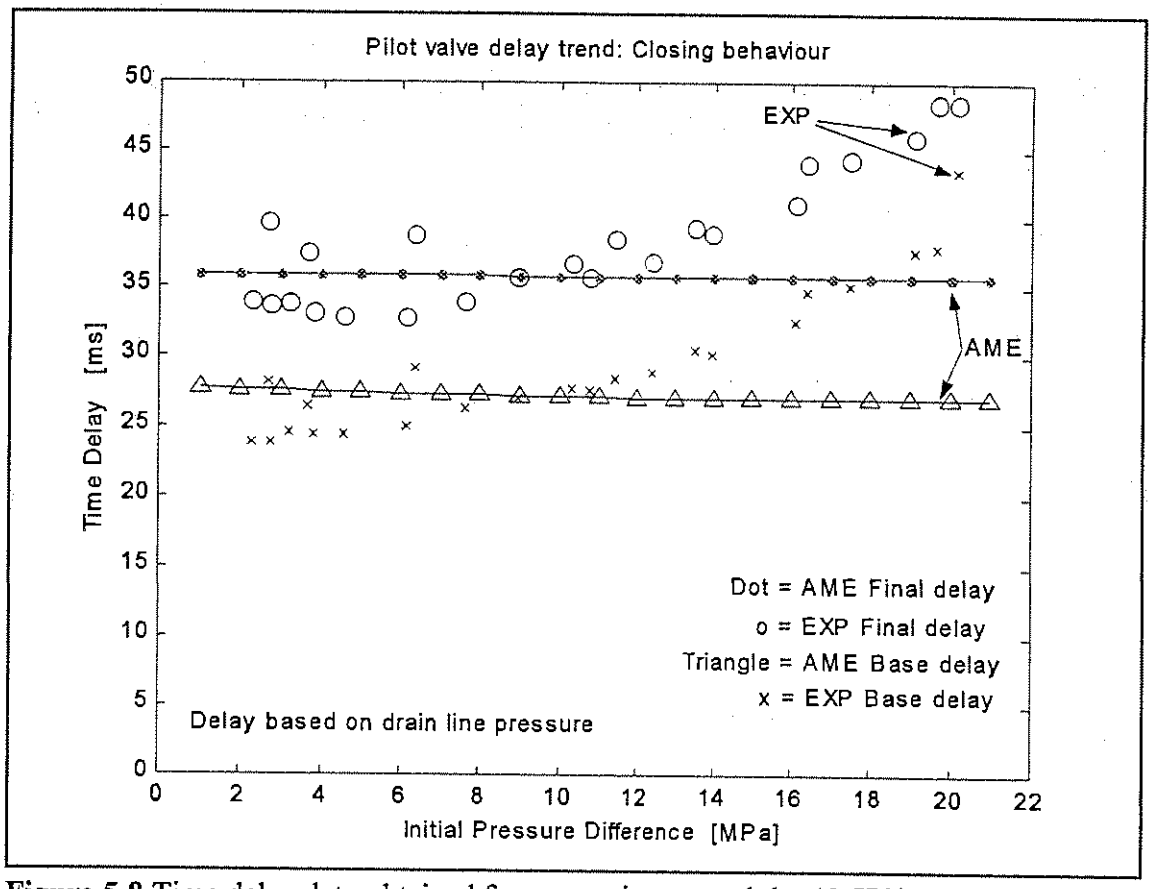

Figure 5.8 Time delay data obtained from experiments and the AMESim model

Despite the apparently constant time delay behaviour of the AMESim delay trends in figure 5.8, a nonlinear behaviour is visible on a closer scale (not shown). As mentioned, the solenoid model used is a approximation of a typical solenoid force trend and exact matching of the trends is not to be expected.

During valve opening, the magnetic field in the solenoid coil collapses and the poppet lifts off its seat. Until this point in time, the force resulting from the supply pressure acting on the ball poppet has been balanced by the same pressure in the compensation chamber acting on the compensation piston (it has the same diameter as the seat). From the time delay graph (figure 5.7) the opening behaviour base delay is relatively constant across the valve operating range (approximately 21 ms) indicating the similar solenoid functioning across the valve operating range.

When the valve is open, however, the poppet has more area exposed to the supply pressure and the compensating chamber cannot balance the force completely. When the solenoid is energised in order to close the poppet against the supply pressure, a larger force is thus needed at higher pressures. It takes a longer time for the solenoid magnetic circuit to build up the higher force needed, as indicated by the increasing base delay times in figure 5.8. Once this force has been reached, and the poppet starts to move, the time domain transient has a similar dynamic behaviour for the high and low pressure cases. This is visible from the parallel curvature of the base and final delay trends in the closing behaviour (fig 5.8). As mentioned this larger force necessary for activation, takes longer to build up in the magnetic circuit and therefore the time delay trends move outwards for higher initial pressure values. This also points to some maximum operating pressure where the solenoid will not be strong enough to close the valve.

5.3 Model validation: Valve system with parallel damper

From chapter one: The valve system uses the pilot valve (as discussed in paragraph 5.2) to alter the hydraulic pressure in the logic element chamber. This alteration of pressure is converted into logic element poppet motion that controls the amount of oil bypassing the damper valve. The bypassing of oil alters the characteristics of the damper, thereby offering the possibility of improving the ride quality and handling of a vehicle.

Although the system modelled represents the complete valve system as fitted to the vehicle, translation of measured and simulated delay values into existing damper valve delay trends should be done with care if it is to be attempted since the test bench has a substantial influence on the measured and simulated values.

The layout of this paragraph is similar to paragraph 5.2 and consists of the matching of AMESim and experimental data on the basis of time domain transient figures and a discussion thereof. The delay data extracted from the AMESim and experimental work is shown on the basis of opening and closing delay trend graphs. The valve system model incorporates the pilot valve model in the state of development as described in paragraph 5.2.

As mentioned, the valve system and damper model time domain dynamic response will only be discussed for the AMESim case, since the MATLAB version proved highly unstable. Although the MATLAB model does occasionally solve and provide results, obtaining them required adjustment of parameters for every specific simulation run until a stable solution is found. This is clearly not a feasible modelling method. Discussion of the MATLAB model is deferred to annexure A5.1.

In the experiments conducted, both test-bench pumps were used to obtain the high flow rates required. This means that two test bench supply pipes has to be modelled thus increasing the number of compliant fluid volumes and lumped orifices drastically. In this model finding suitable values for the Re_{tr} and C_d values for the orifices and compliance of the fluid volumes requires adjustment of at least 100 parameters (complete list of parameters in annexure A3.2). This is clearly not a task to be attempted manually, and unless detailed experimental values of each individual element in the experimental setup is known, the process would require some automated method such as optimisation. This was not attempted in this study.

5.3.1 Model correlation with Experiment

In the following four figures experimental and model time domain transients are presented to facilitate the discussion of the correlation between them.

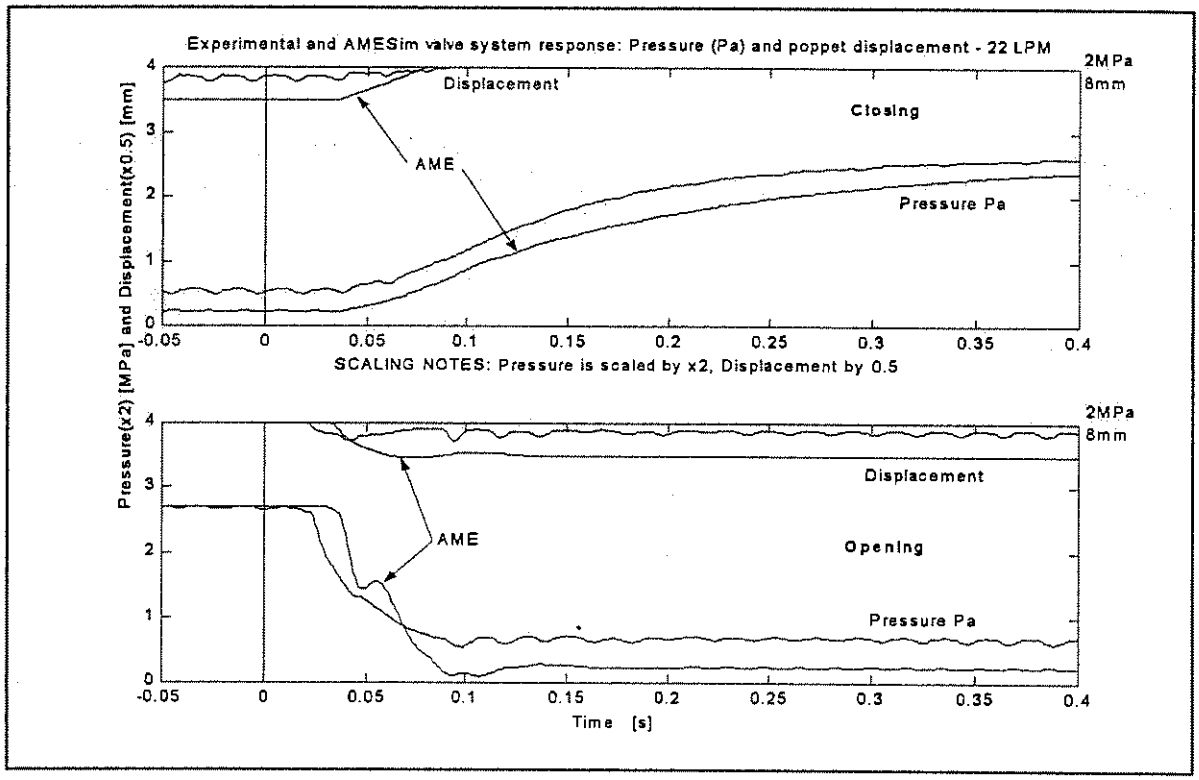

Figure 5.9 Valve system response: Pressure (Pa) and displacement - 22 LPM case

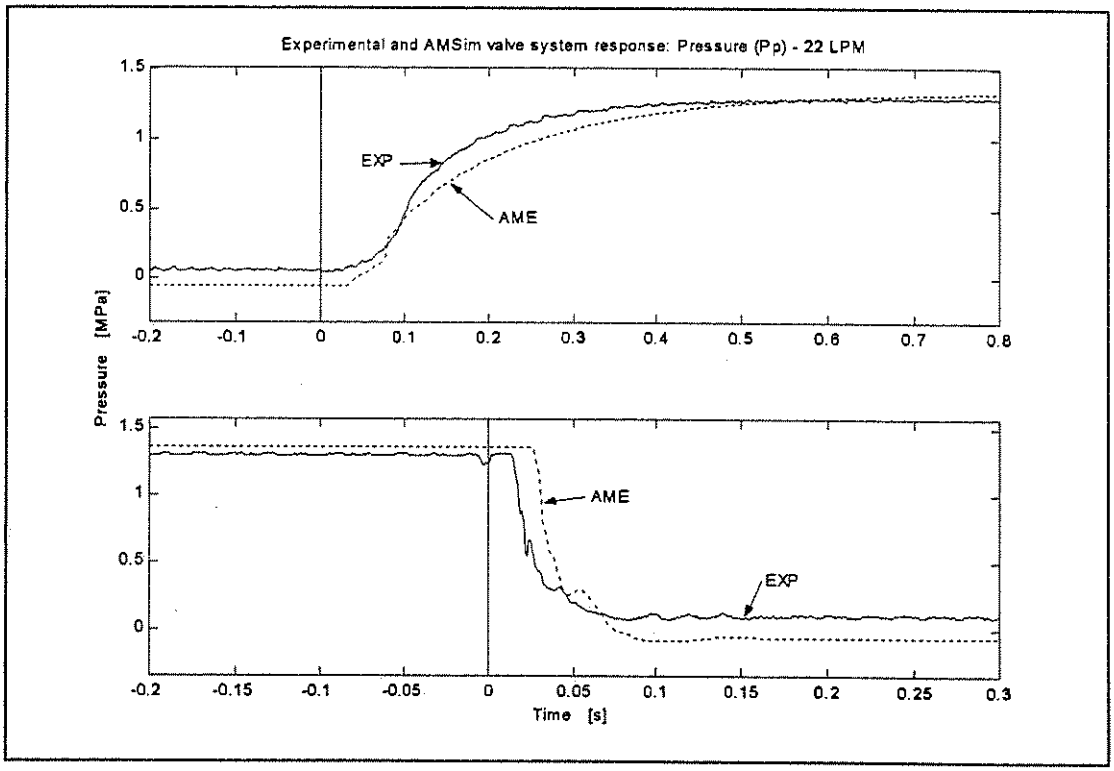

Figure 5.10 Valve system response: Pressure (Pp) - 22 LPM case

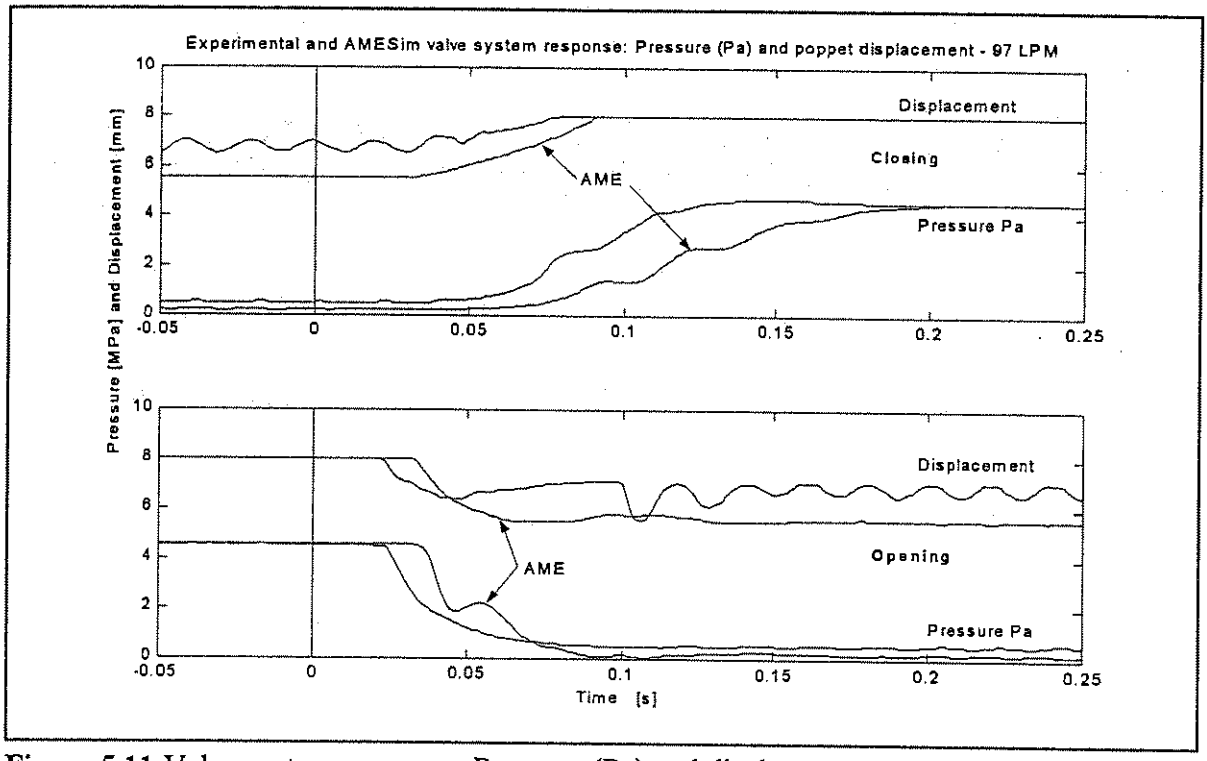

Figure 5.11 Valve system response: Pressure (Pa) and displacement - 97 LPM case

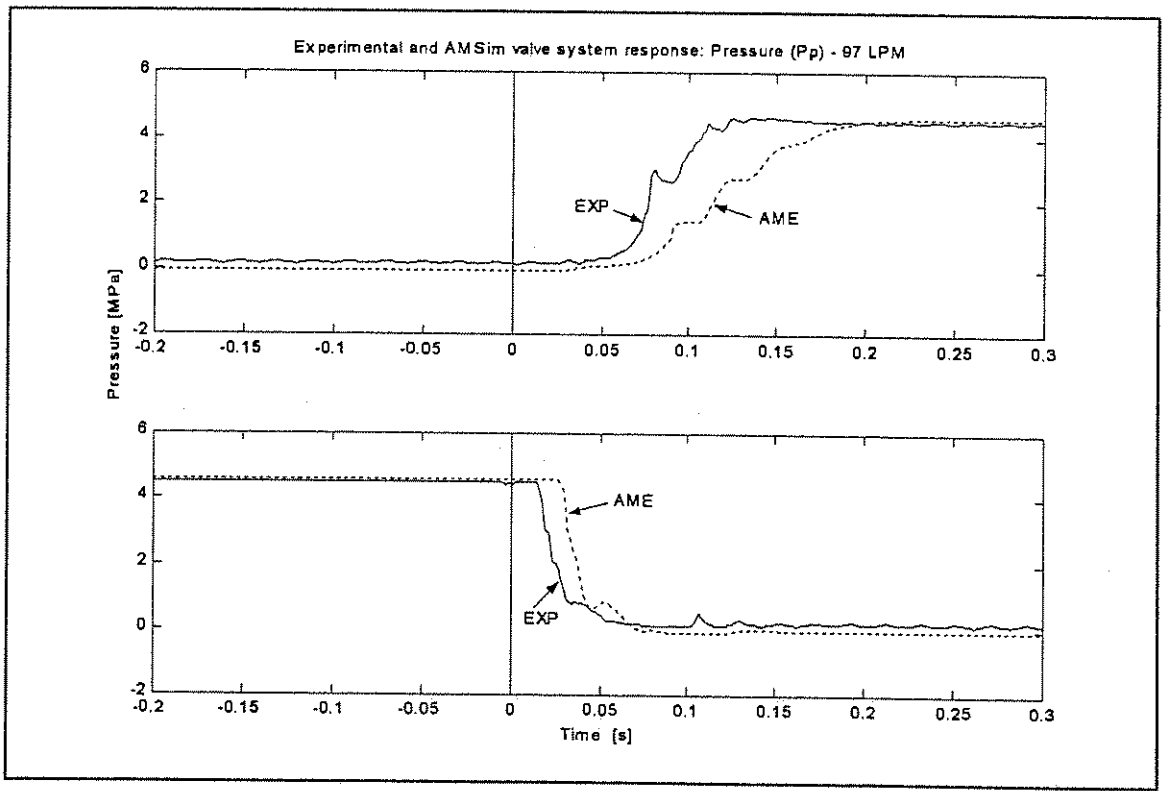

Figure 5.12 Valve system response: Pressure (Pp) - 97 LPM case

As with the pilot valve experiments, the test bench supply pipe again has to be pressurised and depressurised after valve closing and opening. This causes the problem of finding a suitable transient for use in determining the model and experimental correlation and for extraction of time delay values. As discussed in chapter 4, the logic element was fitted with a linear displacement transducer for this purpose. The poppet displacement is influenced by several factors such as the distribution of orifice elements in front of and behind the logic element. This causes higher or lower pressure forces on the poppet than in the experimental setup, again indicating that accurate knowledge of the large number of parameters employed in the model is a great influence on the model accuracy. The drain line trend (as used to correlate the pilot valve of paragraph 5.2) did not provide an accurate method of correlating the model and experiments due to low pressure signals. Since the valve behaviour is obscured by the test bench interference, using the supply pressure will only result in examining the test bench behaviour.

As discussed, high amplitude oscillations of unknown origin were experienced during the experimental work. The AMESim model provided an explanation for these oscillations. The test-bench supply pipe compliance was modelled as steel and rubber hose sections with approximately correct dimensions. Initially, low amplitude damped oscillations were visible in the AMESim results. Increasing the rubber hose compliancy reduced the oscillation frequency and increased its amplitude thereby matching the measured oscillations more accurately. Unfortunately no exact value for the hose compliancy is known. Other parameters with unknown exact values such as the oil bulk modulus, air content and viscosity also affect the oscillatory behaviour further increasing the difficulty of matching simulated results to experimental results (AMESim default values for these parameters were used in most cases).

With the AMESim model complexity in its current state of development and parameter accuracy, it is encouraging to see that the logic element chamber pressure (Pp) shows some of the same high order response as measured (figure 5.11). Considering that the pilot valve model is only approximate, the relatively close match obtained suggests that the logic element dynamics obscures the pilot valve dynamics.

As with the pilot valve model many efforts were made to improve the steady state error between the simulated and experimental time transients. It should be noted that some parameter changes alter the shape of the time domain dynamic response. Further complications in adjustment of parameters is that changes to parameters improve the correlation at a certain flow rate, but worsen the correlation at other flow rates. This indicates that two or more parameters must be changed simultaneously in order to achieve correlation throughout the valve's operating range. Other possibilities for this behaviour is the effect of simplifying assumptions made in the model.

5.3.2 Delay data extracted

Extracting the delay trends for the system can be done on the displacement or pressure transients for the valve. As discussed, the pressure transients were drastically influenced by the test-bench. The AMESim delay trends follow the correct general dynamic behaviour but do not have the correct absolute values. Several reasons for this can be given. It is possible that the experimental measurements are not entirely correct. Steady state errors in the displacement or pressure sensors could affect the 5% and 95% calculated time delay values due to the asymptotic behaviour of the time domain transients. The oscillations encountered introduced noise to the data rendering the automatic delay calculation algorithm developed useless. This necessitated manual extraction of delay trends from the data, adding further inaccuracies. The high level of data spread in the experimental delay trends can be attributed to the damper valve Belleville springs used, since these springs are known to behave randomly.

The error in the delay trend based on displacement for the opening behaviour case (figure 5.13) could be explained as follows: In the time domain transients, the simulated displacement steady state value did not mach the experimental steady state value (figure 5.9 and 5.11). Because the simulated transient steady state values are larger, the 95% delay value occurs at a later stage. (In calculating the 95% point, the transients own steady state value is used.) It is argued that if the steady-state value of the simulated results had matched the experimental values, the extracted delay trends would show better correlation.

Since the MATLAB model proved unstable, none of its results are shown. Furthermore, since the base delay values are not crucial in correlating the models, the data is not extracted from the AMESim model to improve legibility of the graphs.

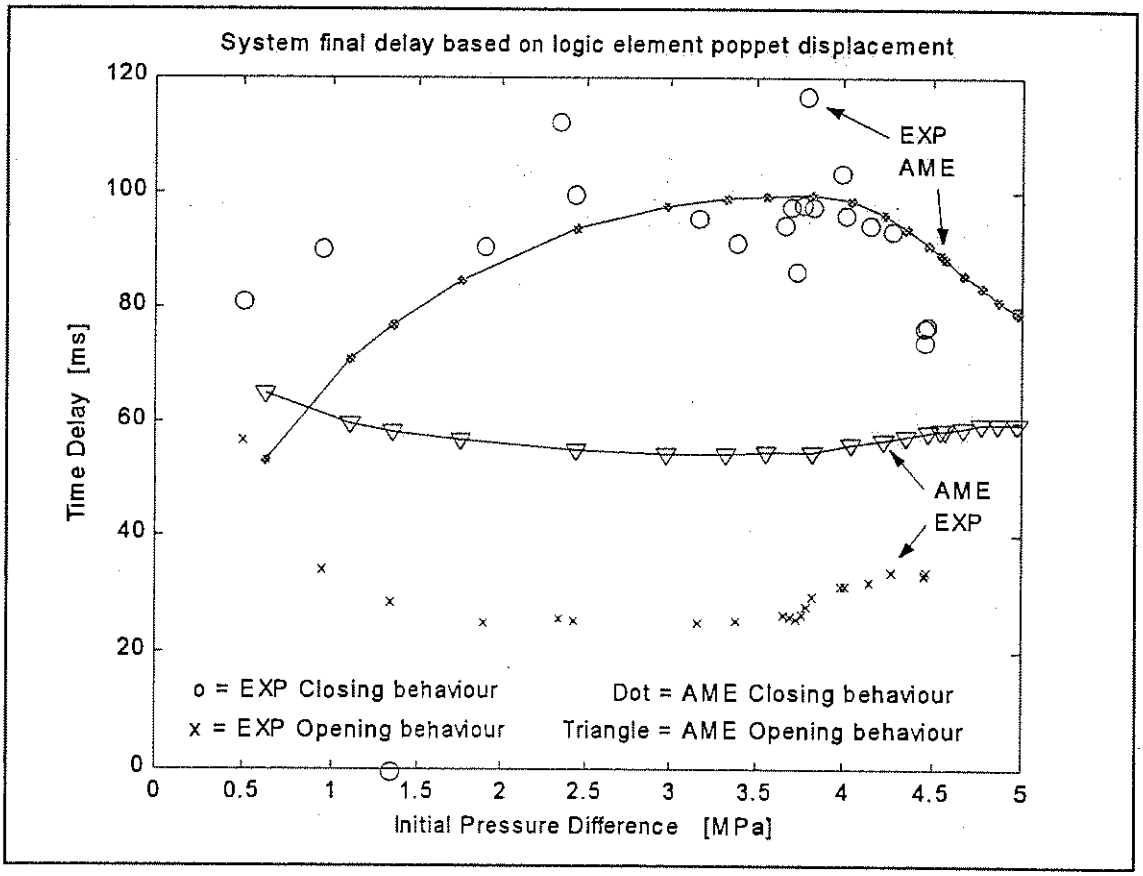

Figure 5.13 System delay trends based on displacement

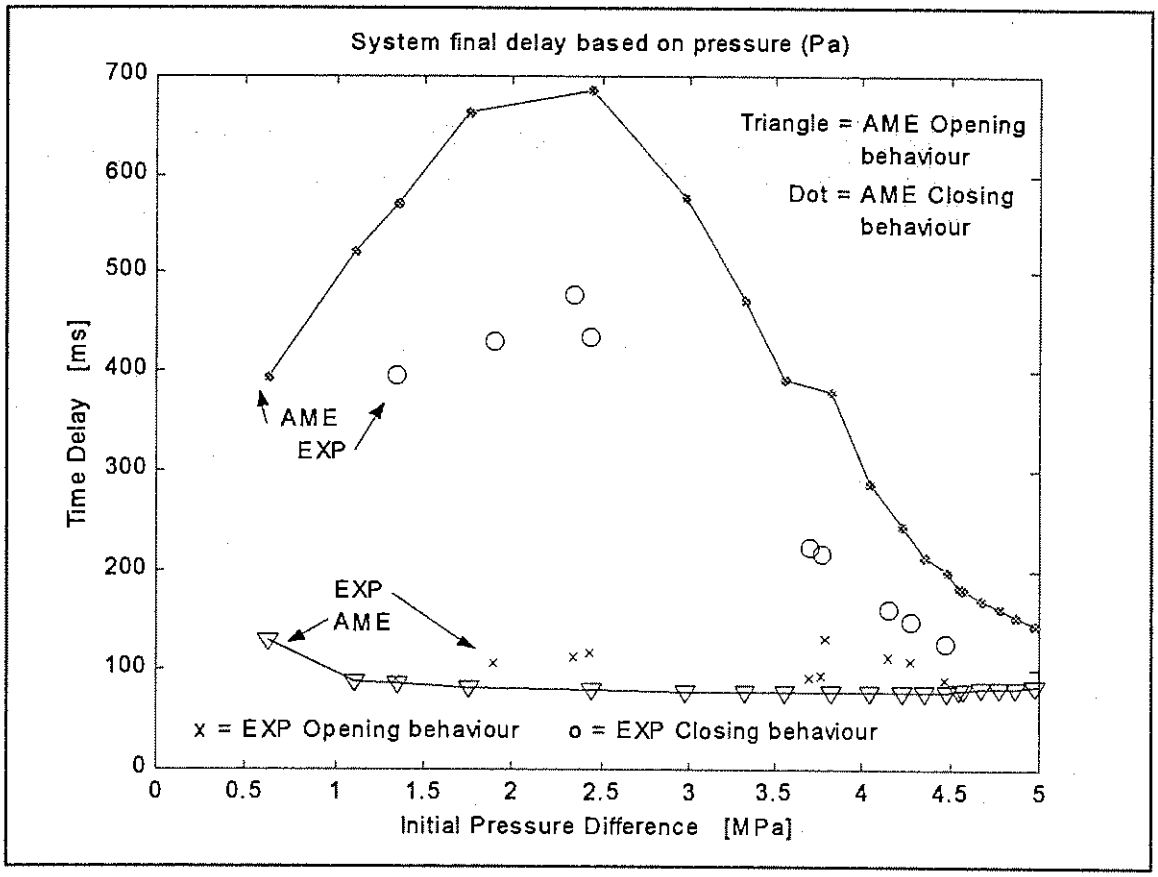

Figure 5.14 System delay trends based on pressure

In both figures 5.13 and 5.14 the AMESim delay trends follow the general shape of the experimental delay trend but differ substantially in terms of time delay magnitude. This suggests that the model contains enough detail of the physical system to reproduce the overall dynamic behaviour, but lacks in parameter adjustment.

#

6 Conclusion

From the work done during this study, the following conclusions can be drawn.

6.1 The system as modelled in this study contains fast acting subsystems. The models of these subsystems are sensitive to the physical parameter values of their components. The nature of hydraulic systems makes it difficult to obtain accurate values for the parameters (either by experimental or analytical methods) for use in the model. This lack of accurate parameters values and the subsequent need for manual parameter adjustment caused slow model development and errors in the simulated results.

6.2 AMESim has demonstrated its ability to construct valid and detailed models of an hydraulic system and it has the ability to solve the mathematical equations efficiently and with very high numerical stability.

6.3 The pre-programmed MATLAB ODE suite (mainly ODE15s in this study) is not capable of solving the stiff equations describing the particular valve system in question. This is exacerbated by the fast acting nature of the valve in question and the long pipe lengths of the test-bench. It is foreseeable that governing equations of the same complexity as that of the AMESim model would easily be programmable in MATLAB, but the proper numerical solution thereof with standard MATLAB solvers seems improbable.

6.4 The simple assumptions made in the component models give a quick first round indication of the expected system performance. Some of the assumptions made in this study (such as constant pressure and flow distributions and exponential solenoid behaviour) may however have a very large effect on the simulated response. CFD analysis can be used to create lookup tables to enhance the model's accuracy in predicting flow forces and pressure distributions acting on the poppet elements. Similarly FEM for the magnetic circuit analysis of the solenoid would aid in obtaining accurate models. This kind of analysis would, however, only be justified where the model is to be used in design studies.

6.5 In order to obtain useful experimental data, the systems used to obtain these data sets must be known accurately. In the case of this study, the test-bench posed substantial and unforeseeable interference with the measured data. Firstly, the lack of a detailed test bench model complicated the extraction of valid valve characteristics. Secondly, the magnitude

of the test bench dynamic behaviour overshadowed the valve characteristics to a large extent.

6.6 The lack of a user interface with automatic model creation in MATLAB results in tremendous effort and time needed to hard-code the system governing equations. The use of SIMULINK was only partially investigated, but from preliminary investigations proved slow in solving the stiff equations. It can further be said that hard-coded models would suffice if a model is to be included in a larger model, but fall short in design studies.

6.7 For slower acting hydraulic systems with less stiffness (such as earth moving equipment hydraulic systems), it is foreseeable that highly accurate solutions using the methods of this study should be obtainable.

Suggestions for future work

- In this study the coupling of the AMESim or MATLAB models with other simulation environments (such as DADS) was not investigated. In order to obtain full value of the models developed in this study, the interfacing of the hydraulic system with a mechanical environment has to be investigated.
- A detailed and isolated model of the pilot valve solenoid will greatly enhance model performance. A solenoid model of suitable complexity should also be included as a standard component in AMESim.
- A detailed model of the test bench and it's associated dynamics will prove invaluable in any future work conducted where dynamic system performance is of importance.
- Alternative configurations for the experimental setup should be considered and carefully investigated.
- Should the creation of models be attempted without the use of dedicated fluid power software, a programming language such as Fortran is recommended. Preprogrammed mathematical libraries are considered essential, but the user should have enough program control to implement fundamental routines such as discontinuity handling.
- The use of differential algebraic equations in the set of fluid power differential equations should be considered, since large reductions in stiffness can be made. This should be weighed and considered against the cost of more complicated solver routines.
- Several suggestions concerning the test bench are listed in annexure A4.2.2.